Final Technical Report

Project Title: Integrated Manufacturing for Advanced MEAs

Award Number: DE-FC36-02AL67606 / DE-FC04-02AL67606

Project Period: December 1, 2001 to December 31, 2006 (extended due to re-scope)

Contact: Emory S. De Castro, +1-732-545-5100, ext. 114,
e.decastro@etek-inc.com (P.I.)
Yu-Min Tsou, +1-732-545-5100, ext 145,
ym.tsou@etek-inc.com (Author)
Mr. Bruce Blaisdell, 1-732-545-5100, ext. 133,
b.blaisdell@etek-inc.com (Contracts Administrator)

Recipient: PEMEAS U.S.A., E-TEK Division, (formerly De Nora North America, Inc., E-TEK Division), 39 Veronica Avenue, Somerset, New Jersey, 08873

Team Partners: Du Pont Fuel Cells, Nuvera Fuel Cells, Northeastern University, Spire Biomedical, Inc. and Case Western Reserve University (CAPI)

Acknowledgment:

This report is based upon work supported by the U. S. Department of Energy under Award No. DE-FC36-02AL67606 / DE-FC04-02AL67606

Proprietary Data Notice:

No proprietary data

Table of Contents

Figures and Tables

Executive Summary

This program addressed a two-pronged goal for developing fuel cell components: lowering of precious metal content in membrane electrode assemblies (MEAs), thereby reducing the fuel cell cost, and creating MEAs that can operate at 120^{o}C and 25% RH whereby the system efficiency and effectiveness is greatly improved. In completing this program, we have demonstrated a significant reduction in precious metal while at the same time increasing the power output (achieved 2005 goal of 0.6g/Kw). We have also identified a technology that allows for one step fabrication of MEAs and appears to be a feasible path toward achieving DOE's 2010 targets for precious metal and power (approaches 0.2g/Kw). Our team partner Du Pont invented a new class of polymer electrolyte membrane that has sufficient stability and conductivity to demonstrate feasibility for operation at 120 ^{o}C and low relative humidity. Through the course of this project, the public has benefited greatly from numerous presentations and publications on the technical understanding necessary to achieve these goals.

Introduction/Background

A continuing challenge for PEMFC technology is precious metal thrift and creating new ion exchange membranes that are capable of stable operation at temperatures exceeding 120^{o}C and preferably 150^{o}C. The greatest barrier to reduction of platinum metal in the MEA is due to the cathode half reaction, which can be addressed through both improved catalysts and the electrode structure around the catalyst. In addition, there is a significant incentive to increase the operating temperature, the advantages being: a) smaller radiators in transportation applications, b) more efficient use of by-product heat in stationary applications (e.g. hot water generation), c) potential for faster oxygen reduction kinetics at the cathode, d) increased tolerance to CO in reformed-hydrogen feed streams, and e) better kinetics for methanol oxidation in DMFC's. For higher temperature operation, the need to limit the total stack pressure to 1 to 1.5 bar places a limit of ~0.5 bar on the water partial pressure, which corresponds to only 25% RH at 120^{o}C – a significant challenge in designing new membrane materials.
Objectives for sub-projects:
Topic 1A1: Improved Cathode and Catalysts. Create PEMFC cathodes capable of achieving 0.85 V @ 0.1A/cm^2 and 0.8V @ 0.4A/cm^2 with a total (anode and cathode) precious metal loading of 0.3mg/cm^2 under DOE specified conditions
Topic 1A2: High Temperature Membranes. Create PEMFC MEAs capable of operating at 120 ^{o}C, %RH<25, and lifetime > 5k hours with a cost less than commercially available membranes (ended Sept 30, 2005).
Topic 1A3: Advanced MEA fabrication. Develop advanced MEA fabrication technologies using advances from (1A1) or (1A2) by: a) Determining conditions to produce highly active alloys with Ion-Beam technology; b) Creating advanced ink coating application technology: determine if competitive with Ion beam; and c)Creating a (catalyst) application technology that can produce flexible form factors with low waste. As part of a re-scoping of this program, the final deliverable for 1A3 is to assemble and test 4-10 element stacks comprised of these high and low temperature materials fabricated on a pilot production line and evaluate performance and durability.

During the period of Topic 1A1, E-TEK developed a new catalyst preparation method that reduces the crystallite size of supported platinum catalysts. The resulting new catalysts led to fuel cell performance improvement. This new catalyst synthetic method is particularly useful for making finely dispersed Pt catalysts with loading higher than 40% on a carbon support such as vulcan-XC 72, where almost all commercial catalyst manufacturers find very difficult to achieve. Another area which significantly improved the cost/performance is the reduction of anode loading. By adjusting the formulation and roll coating in addition to employing the new E-TEK catalyst, it was demonstrated that 0.05 mg/cm2 of Pt can be achieved consistently on a large scale machine coating of > 10 m2. The MEAs with low loading anode of 0.05 mg/cm2 of Pt were demonstrated in Nuvera 225 cm2 cell stack to have the same performance as MEAs with standard anode of 0.5 mg/cm2 Pt.

Pt alloy preparation represented another significant step at E-TEK to improve performance for this program. The first alloy showing performance very close to the program target was platinum chromium alloy catalysts. Later on platinum cobalt alloy catalysts also showed similar performance. Both alloy catalysts were prepared with a procedure combining the new synthetic method described above for finely disperse Pt catalysts and unique cobalt and chromium chemistry. Besides alloy synthetic chemistry E-TEK also found an innovative approach in gas diffusion electrode structure. This is the fine-gradient approach where a gradually changing gradient in porosity and hydrophobicity is built in the structure of gas diffusion electrode. Along the progress of this program, this approach has been found to be effective in achieving optimized performance at a wide range of current densities; the fine gradient approach was also found to be crucial for achieving long-term durability due to its water handling capability. For MEAs with Pt catalysts, the voltage degradation rate was significantly reduced by incorporating the fine-gradient electrode structure. For MEAs with Pt alloy cathode, the fine gradient structure has been found to be particularly important because of catalyst surface property.

IBAD (ion-beam assisted deposition) is another method that E-TEK developed for using in advanced MEAs. Much advancement in this approach has been made. The most important one was the discovery of deposition of Pt layer on GDL (gas-diffusion-layer) by IBAD can result in much enhanced performance than the original concept of depositing on membrane. The porous surface of the GDL provides a nearly ideal substrate for porous Pt deposition. The IBAD layer exhibited excellent oxygen kinetic activity because of its unique structure. IBDA layer functions well in pure oxygen and its low porosity limits its effective use as an air cathode. On the other hand, IBAD serves very well as a hydrogen anode without any incorporated ionomer. This makes IBAD as a great anode candidate for long-term applications where ionomer might be the weakest link. As described below IBAD GDEs were demonstrated in 500cm2 Nuvera cell stack.

Scaling up of MEAs for stack operation was another important goal for this program. During the program, a number of stack testing longer than 1000 hours were conducted at Nuvera with MEAs of 225 cm2, 250 cm2, and 500 cm2. In earlier 225 cm2 Nuvera

cell stack low loading anode mentioned above and PtxCr cathode was successfully demonstrated. In September 2005, a 4-cell 250 cm2 stack equipped with MEAs with E-TEK machine-coated fine-gradient PtxCr cathode and low loading anode were tested at Nuvera. The total precious metal was around 0.38 mg/cm2 for each cell. 1300 hour of operation was demonstrated with degradation rates in the range of 1-14 uv/hour. In the final 500 cm2 MEA stack installed at Nuvera in February, 2006, tested GDEs included: standard MEAs, fine-gradient Pt MEAs (gradual change of porosity and hydrophobicity along membrane-GDL), two MEAs with PtxCo (0.29-0.3 mg/cm2) cathode and low loading anode (0.04 mg/cm2 Pt), and two MEAs with IBAD (ion beam assisted deposition) anode (0.1-0.19 mg/cm2) and low loading cathode. In this test, the MEAs with PtxCo cathode had about 40% of the precious loading of a standard MEA, but showed essentially the same performance.

Durability and low RH% applications are future focus of DOE fuel cell program. In the final period of this program E-TEK demonstrated that unsupported Pt catalysts showed excellent stability toward frequent shutdowns and near-OCP operations, whereas in the same condition, supported catalysts showed rapid degradation in performance. . E-TEK also identified corrosion resistant carbon for making corrosion resistant supported Pt or Pt alloy catalysts and demonstrated very good preliminary results. In the area of low RH% MEAs, E-TEK had advancement in electrode structure and rolled out new products.

Comparison of the Actual Accomplishments with the Goals and Objectives of the Project

Table 1A: Progress Toward Meeting DOE Membrane and Electrocatalyst Targets for Transportation Applications

Characteristic	Units	2005 goal	2010 goal	Cell status	Stack Status[1]
MEA Electrode for Transport [2] (<100°C)					
PGM specific power	g/kW rated	2.7	0.3	0.6	0.7
PGM total loading	mg/cm^2	0.3	0.1	0.39	0.35
Electrocatalyst for Transport [3]					
PGM total loading	mg/cm^2	0.3	0.1	0.16	(4)
Kinetic Activity	A/mg Pt at 900mV	0.3	0.44	.748	---
Kinetic Activity	uA/cm^2 at 900mV	600	720	2946	---
MEA (high temperature, status at 30%RH)					
Operating Temp.	°C	≤120	≤120	120	---
PGM specific power	g/kW	2.7	.3	3.13	---
Performance at 0.8V (1/4 power)	mA/cm^2	250	400	400	---
	mW/cm^2	200	320	320	---
Degradation[5]	%	10	10	20	---
Membrane for high temperature (DuPont)					
Conductivity @ 100 °C & 25 kPa water	S/cm	0.10		0.025	---

vapor					
Conductivity –20 ^{o}C	S/cm	0.01		0.023	---
Survivability	^{o}C	-40		recovers	---
Durability with cycling 120 ^{o}C	hours	N/A		200 hr, total of 20 cycles of RH & current	---

Notes: (1) Tested at 250kPa A, H_2 dead-end, Cathode stoichiometry 2-2.5, 70^{o}C; (2) MEA based on fine gradient ELAT® methodology; (3) MEA based on dual Ion Beam Assisted Deposition methodology ; (4) Demonstrated dual IBAD anodes at 500 cm^2 stack element, 0.08mg/cm^2 w/o loss of power (5) 1,000 hr accelerated under %RH and open circuit potential/high current cycling

1. Achieved 0.85V at 0.1A/cm^2 and 0.80V at 0.4A/cm^2 with 0.39mg/cm^2 platinum total loading.
2. Achieved stack durability decay rate <1 uV/hr (1000 hrs, constant current) with under 0.39 mg Pt/cm^2 total using coating technology suitable for mass manufacturing
3. The fine gradient approach has led to successes in lowering PM without a loss in power, greater ability for water elimination in the GDL, and with the proper design, greater water retention in the electrode for operation in dry conditions
4. Roll-to-roll ion beam deposition demonstrated that the technology is ready for use in commercial anode structures. There is a further cost savings in the elimination of ionomer. Preliminary data for IBAD cathodes indicates greater stability compared to supported catalyst.
5. DuPont has developed several new classes of polyelectrolytes that exceed the benchmark Nafion® in conductivity at low RH and high temperature: these materials represent a significant advance and justify DuPont's further pursuit of membranes with these materials beyond the term of this project

(1) Overview of Alloy Progress: Polarization Curves

In lab cell testing using a PtxCo cathode GDEs (Pt loading =0.24 mg/cm2) and low loading anode (0.04 mg/cm2), i.e., total loading 0.28 mg/cm2, the following performance was achieved : 0.870 volts at 0.1 A/cm2 and 0.79 volts at 0.4 A/cm2. This is essentially similar to DOE goals. The MEA employed a 2 mil per-fluorocarbon membrane. The cathode used a fine-gradient structure for optimum performance and durability.

Figure 1 MEA performance of an MEA with PtxCo cathode (Pt=0.24 mg/cm2) and Pt anode (0.04 mg/cm2) at DOE condition of 80 deg C and C/A 2.5 bara

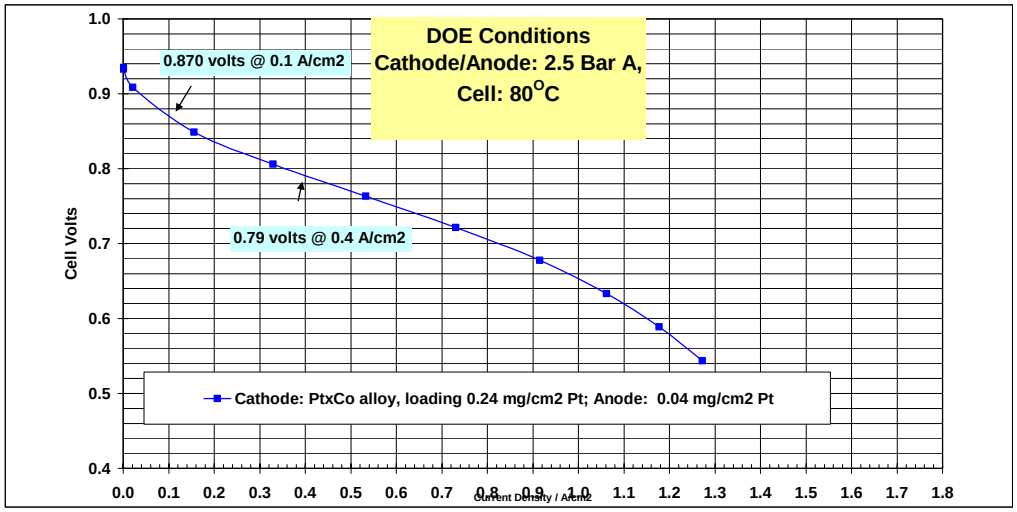

(2) Oxygen Kinetic Current of PtxCo Gas Diffusion Cathodes at 900 mv vs. NHE
From Tafel Plots one can calculate the important DOE parameters: IR free oxygen kinetic current at 900 mv vs. NHE at 80 deg C, 2.5 bar a. Two E-TEK PtxCo cathode GDEs and one E-TEK Pt GDE were evaluated, but only the PtxCo GDE with 0.25 mg/cm2 was evaluated at the aforementioned DOE condition, the other two was evaluated at lower pressure and temperature. The complete Tafel plots will be discussed in the Results and Discussion Session. As Table 1 shows, the kinetics of PtxCo GDE with 0.25 mg/cm2 matches DOE current single cell status. At high loading of 0.45 mg/cm2 PtxCo catalyst utilization apparently decreased to lead to lower O2 kinetic current. At the same loading, PtxCo/C showed significantly higher kinetic current than Pt/C.

Table 1B. Oxygen Reduction Kinetic Current at 900mv (IR Free) for Various E-TEK Pt GDEs.

Cathode	Pt Loading mg/cm2	Temperature deg C	O2 Pressure bar a	Current Density@ 900mv (IR free), A/mg
Pt/C	0.52	70	1.5	0.11
PtxCo/C	0.45	70	1.5	0.18
PtxCo/C	0.25	80	2.5	0.27
DOE single cell status		80		0.28
DOE stack status		80		0.11

PtxCr cathode GDE also showed better performance than standard Pt GDE, the details

of comparison of PtxCo, PtxCr , and Pt cathodes will be presented in Results and Discussion Session. Generally, the advantage of Pt alloy over Pt is about 20-30 mv.

Catalyst Development and Electrode Structure: Results and Discussion (Program 1A1)

Catalyst Activity Improvement

There are two ways to improve the cathode catalyst performance. They are increasing the surface area and improving the intrinsic catalytic activity. To increase the surface area one needs to find a synthetic method to disperse the catalyst well on the support. Before the start of this program E-TEK employed a method based on Pt sulfite complex (1). The sulfite complex is oxidized by H_2O_2 to form PtO2 which is then adsorbed on the surface of the carbon support. One of the drawbacks of this method is the lack of crystallite size control when Pt loading is high. It becomes very severe when loading is higher than 40%. It is believed that the major cause is the nature of reaction between H_2O_2 and Pt complex. E-TEK decided to develop a new chemistry and was very successful.

(1) E-TEK Pt catalysts from new synthetic method. The new method resulted in Pt catalysts with crystallite size increasing very modestly with the loading. With the new Pt chemistry, E-TEK catalysts not only surpassed its old catalyst easily but also are superior to industrial standards. Figure 2 illustrates the XRD crystallite size for E-TEK new Pt catalyst technology as compared with old technology. Note that the advancement of E-TEK Pt catalysts took two stages, the first was fundamental chemistry change and the second step was the process improvement. With the new Pt chemistry, E-TEK can make Pt black (unsupported) under 6 nm.

Typical crystallite diameters of commercially available platinum black range from 6.5-12 nm resulting in a BET surface area in the range of 20-27 m^2/g. However, by adapting this new synthetic method we have been able to reduce the size to ~ 5.3 nm and BET of 34 m^2/g. Recently, in small batches, we have shown proof-of-principle of platinum blacks with size in the range of 3.5-4.7 nm and BET of 40-55 m^2/g. The XRD sizes of E-TEK Pt black along with those of two commercially available blacks are summarized in Table 2. For comparison, crystallites of 3.5 nm are typically the range of the commonly observed diameters of *supported* Pt catalysts, 2.0-4.0 nm. One of the reasons that the catalyst utilization for Pt black-based electrodes is not as good as that for supported catalysts is the particle size of the catalysts is so large that most metal atoms are embedded inside the particle and could not be used. This is certainly the case in the past when Pt black had sizes larger than 100 A or even 200 A 20-30 years ago. The situation has been changed when E-TEK is able to produce Pt black with 3.5 nm XRD size.

Figure 2A. The XRD Crystallite Sizes of Three Generations of E-TEK Pt Catalysts

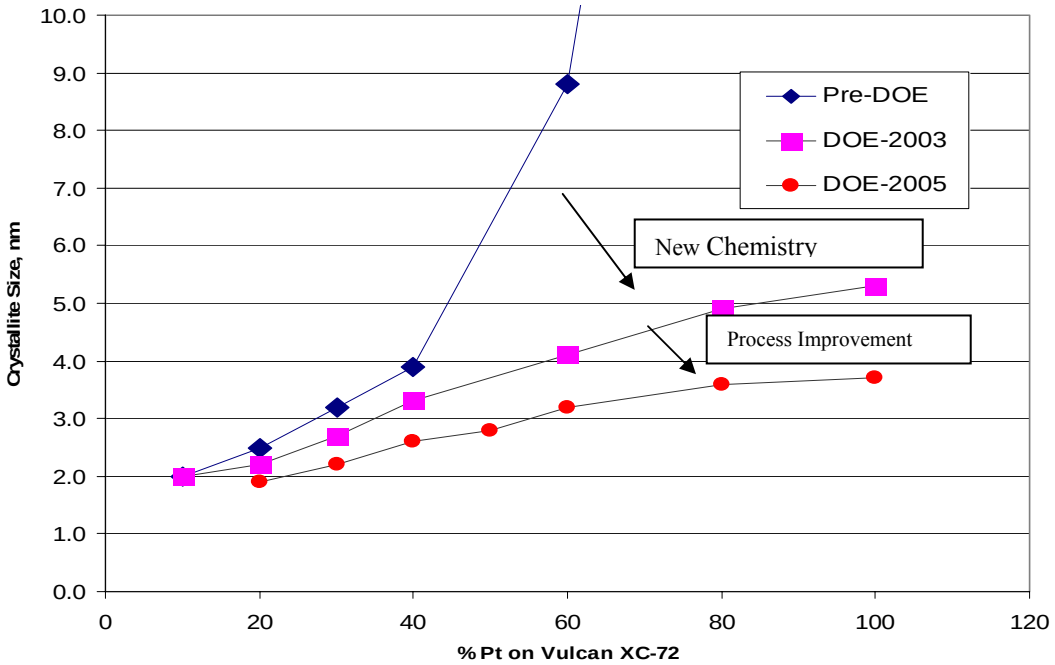

Table 2. XRD Sizes and B.E.T. Surface Areas of Pt Black Catalysts

	2005 HP Gen II	2004 HP Gen I	Company 2	Company 1
XRD, nm	3.5-4.7	5.3	10	6.4
B.E.T. surface area, m2/g	40-55	34	20	27

(2) Fuel Cell Performance Improvement for Supported Catalysts

The smaller crystalline size and more uniform spatial distribution on the support of the HP 2005 30% Pt/C catalysts (pink square) as compared to HP 2002 (red circles) also carries a performance improvement as shown in Figure 2B. The improvement can be attributed to surface area increase and more even current distribution through the catalyst layer.

Figure 2B Comparison of fuel cell performance for E-TEK HP 2002 and HP 2005 30% Pt/C catalyst 70 Deg C, H2/air: 0.5 bar g

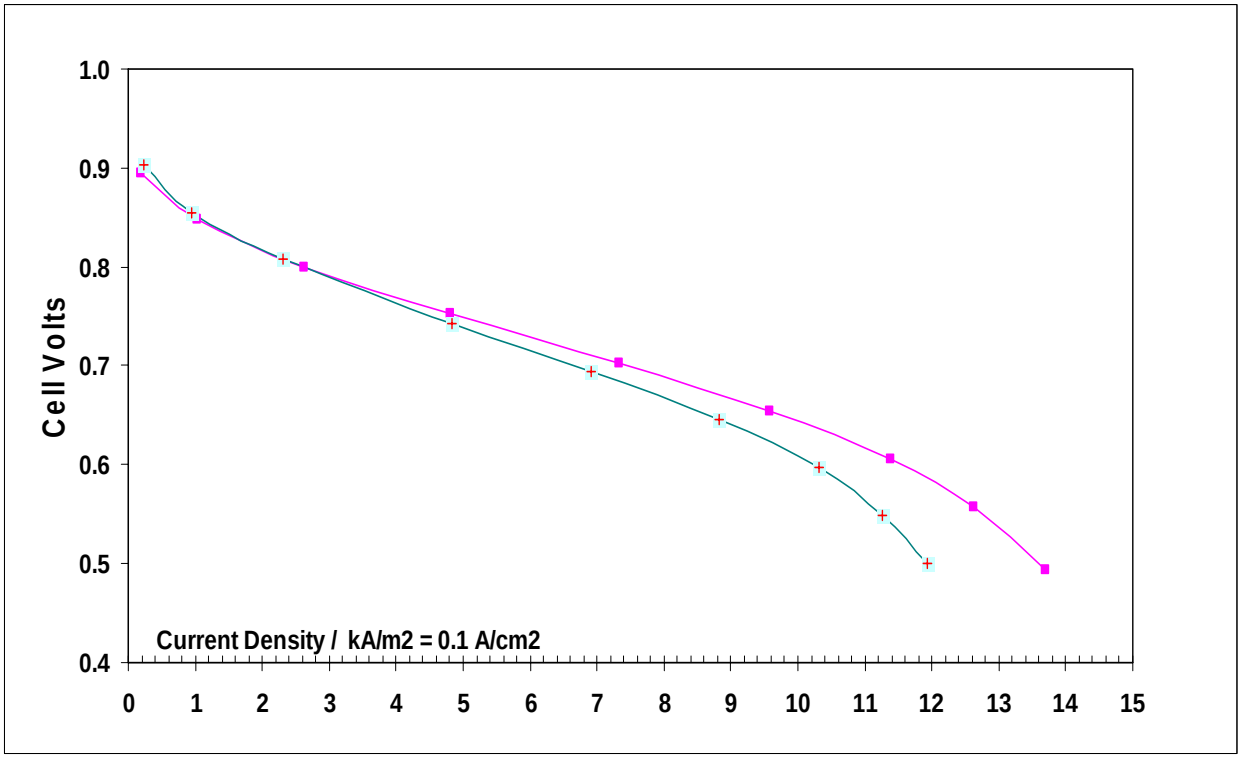

(2) Capability of Unsupported Pt -- Performance in H_2/Air Operation
Figure 3 compares the single-cell performance of a MEA with E-TEK Pt black (BET 34 m2/g) cathode to a cathode with 60% Pt/C, a cathode with the industrial standard (3rd party) Pt black cathode, and a third party leading commercial MEA with supported catalysts (presumably with 0.4-0.5 mg/cm^2 in the cathode).. All MEAs used standard anodes except the commercial MEA for which anode is unknown.

Figure 3 – Comparison of MEA Performance with Various Pt Catalyst Cathodes and Standard Anode;
Nafion 112 Membrane, Cell 70 deg C, H_2/air 0.5 bar g

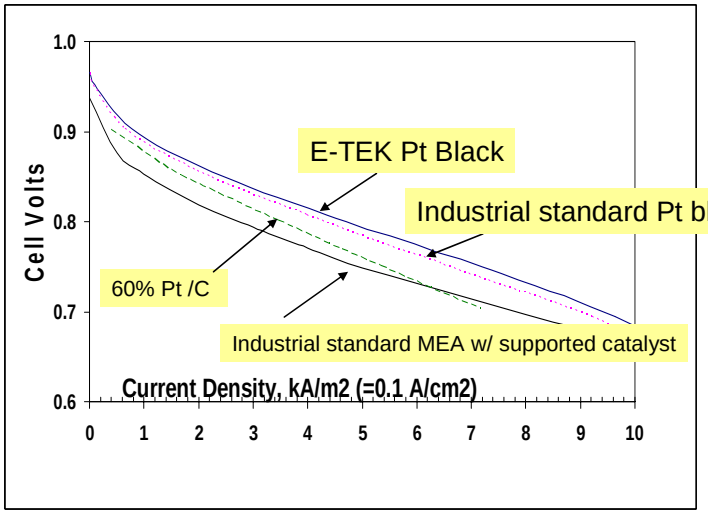

The performance advantage of Pt black catalyst is obvious from Figure 3. Although the MEA with platinum black cathode has significant higher loading of platinum as shown, but it was found supported catalysts is not capable to match the performance even the loading is increased to a value where either no performance change above it or the electrode thickness

becomes so high so de-lamination can occur. The superior performance of Pt black originates from its high utilization because there is no carbon to block the catalyst access by reactants.

Pt Alloy Advantage

(i) Completely Machine-made PtxCo Cathode GDE and O2 Kinetics Study

a) Performance/polarization curves of PtxCr/C, PtxCo/C vs. Pt/C and comparison with DOE goals.

In earlier development period of this program we described preparation of PtxCo and PtxCr cathode GDEs and corresponding MEAs which showed performance better than Pt cathode GDEs by about 20 mv. Typical performances are shown in Figure 4. In Figure 4, the PtxCo and PtxCr cathode used fine gradient structure to compensate for the different surface property. Without the fine-gradient structure high current densities will be impacted as shown in Figure 5. The cathode GDEs in Figure 4 and 5 were prepared by methods requiring rather sophisticated procedure and has limited production rate at commercial scale. The limitation was related to the thermal stability of Pt alloys. In the later stage of this program E-TEK developed a novel process which allows E-TEK to make PtxCo cathode GDE at the same rate as Pt GDE. Figure 6 shows the performance of an MEA with N112 and PtxCo cathode (cathode 0.45 mg/cm2) prepared with this new process with an anode of 0.5 mg/cm2 Pt anode. Previously we showed that if the anode is replaced with one with 0.05-0.08 mg/cm2 Pt, no performance was lost below 0.8 A/cm2. The operating condition is the standard DOE protocol

Figure 4. Performance Comparison of fine-gradient PtxCr and fine-gradient PtxCo cathodes and standard Pt cathodes

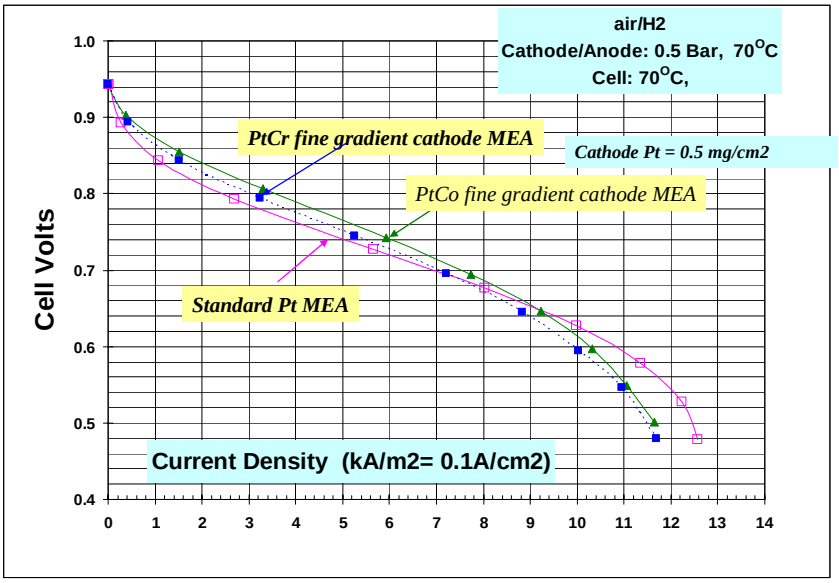

The advantage of Pt alloy cathode over the standard Pt cathode is clearly seen.

Moreover, it exceeds the DOE performance goal at both 0.1 A/cm2 (0.88 volts vs. 0.85 volts) and 0.4 A/cm2) 0.805 volts vs. 0.80 volts, although with higher catalyst loading. When the cathode loading of PtxCo is reduced to .0.25 mg/cm2 and the anode loading is reduced to 0.05 mg/cm2 – total Pt loading at 0.3 mg/cm2, the goal at 0.1 A/cm2 is still made (0.87 volts vs. 0.85 volts), but the performance at 0.4 A/cm2 is slight below the DOE goal (0.79 volts vs. 0.80 volts).

Figure 5. Effect of Fine-Gradient Structure on the Performance of PtxCr Cathode

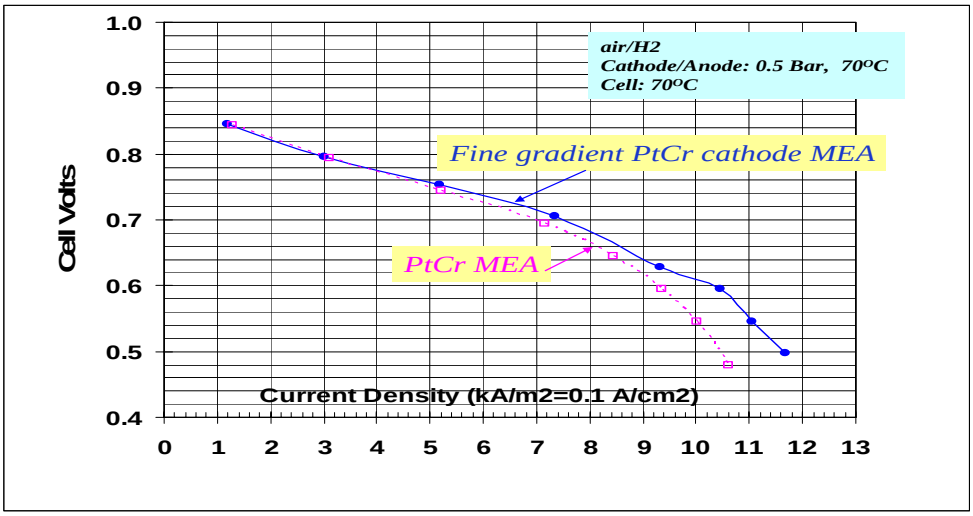

Figure 6 Polarization curves of MEA with 2 mil membrane and (A) PtxCo cathode (0.45 mg/cm2) and standard Pt anode (0.5 mg/cm2), (B) PtxCo cathode (0.25 mg/cm2) and low loading Pt anode (0.05 mg/cm2), ; Cathode/Anode: 2.5 Bar A, 80^{O}C;

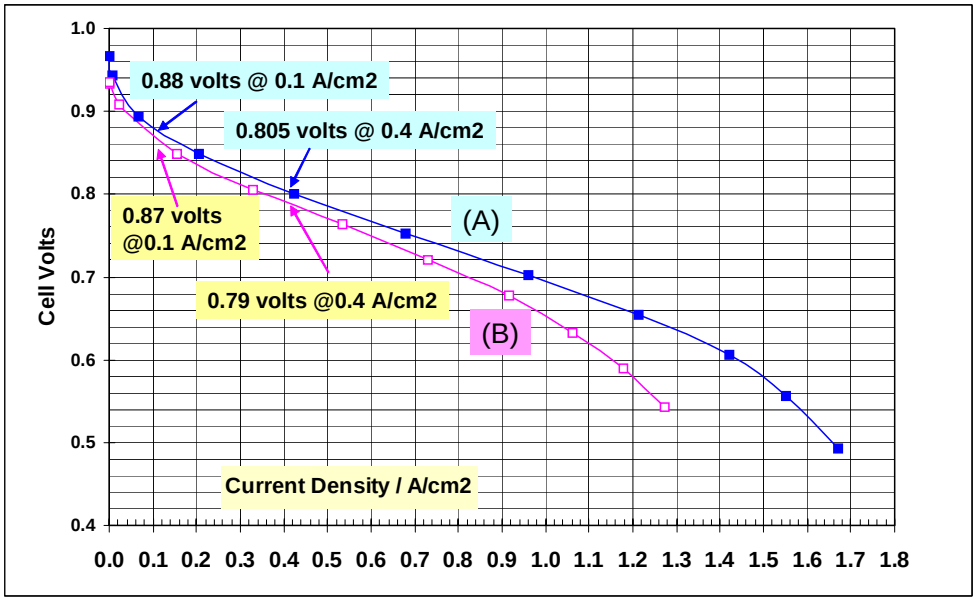

The PtxCo cathode showed significant better activity as shown in the polarization curves in Figure 7 where an MEA with standard anodes and Pt cathode (0.5 mg/cm2) is compared with the MEA with PtxCo (0.45 mg/cm2) cathode in Figure 1, at 70 deg C, 1.5 Bar A, H_2/air. The IR corrected polarization curves are also shown each catalyst. 20 mv advantage is clearly realized by comparison the two IR corrected curves. To further understand the fundamental forces behind the enhancement of reduction activity for PtxCo cathode we conducted performance evaluation in O2/H2.

Figure 7. Comparison of Performance of MEAs with PtxCo/C cathode and Pt/C cathodes (0.45 to 0.5 mg/cm2). Both have standard anode and standard 2 mil membrane. Condition: 70 deg C, 1.5 bar

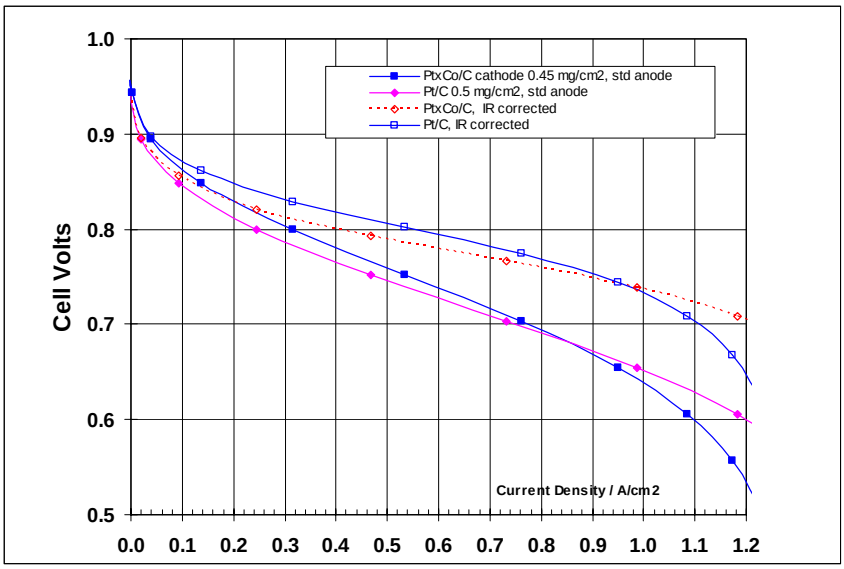

(b) O2 Reduction Kinetics Study.

Figure 8 shows the IR corrected Tafel plots PtxCo/C cathode in O2/H2 operations. Also included is the Tafel curve for Pt/C in O2/H2.

The Tafel slope for PtxCo/C is 87 mv/decade in air/H2, deviation from linearity was observed at current density above 0.25 A/cm2, indicating a significant mass transport component appears above this current density. For Pt/C, the Tafel slope is around 75 mv/decade, about 12-13 mv/decade less than that of PtxCo/C. This difference in Tafel slope leads to gradual decrease in performance difference between the two cathodes. The almost equivalent performance for the two cathodes in the Tafel plots of Figure 8 at 1 A/cm2 is also reflected in the polarization curves shown in Figure 7. However, careful analysis of the IR corrected polarization curves and Tafel plots indicated the PtxCo cathode benefits from a somewhat better hydrogen ion or oxygen diffusion property. Because of the rather small performance difference (~20 mv), more detailed experiments are needed to further disentangle these factors.

Figure 8. IR corrected Tafel plots PtxCo/C cathode in O2/H2 operations. Also included is the Tafel curve for Pt/C in O2/H2.

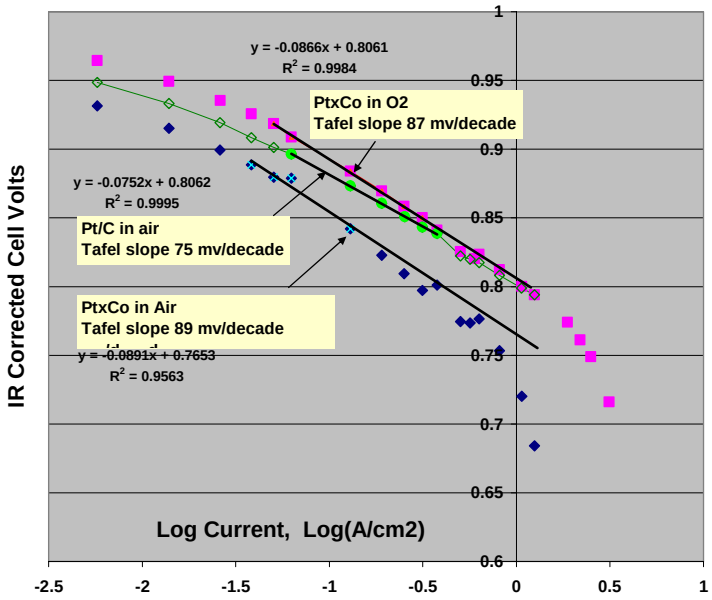

(c) Pressure Dependence

When the operating gas pressure is increased to Air/H2, 4 Bar A/3.5 Bar A, the advantage of PtxCo cathode can maintain above 1.2 A/cm2, the higher pressure dependence seems to indicate the O2 diffusion property is worse for PtxCo cathode. From this observation and the observation above that PtxCo has an overall better diffusion property, one can conclude that PtxCo catalyst provide better proton conduction. In the future we would like to confirm this by AC impedance study.

Fine-Gradient Electrode Structure

(1) Cloth GDE/MEA

As discussed above, E-TEK used fine gradient structure in Pt alloy cathode for optimized performance over a wide current density range. The fine gradient structure was also found to be important for long-term performance stability. A gradual change in porosity and hydrophobicity should be better for managing water. In the development E-TEK MEA based on carbon cloth, the early generation showed a tendency of gradual decreasing water proofing capacity and exhibited a degradation rate of 56 uv/hour degradation rate, by adjusting the electrode structure, especially on the cathode side, we made two consecutive improvements in 2005 and 2006, reducing degradation rate to 18 uv/hour in 2005, then to almost non-detectable in 1100 hour operation. Figure 10 shows the comparison. The initial performances of these MEAs were almost the same.

Figure 9. Performance Comparison of the two MEAs in Figure 7 & 8 at Air/H2 4/3.5 Bar A

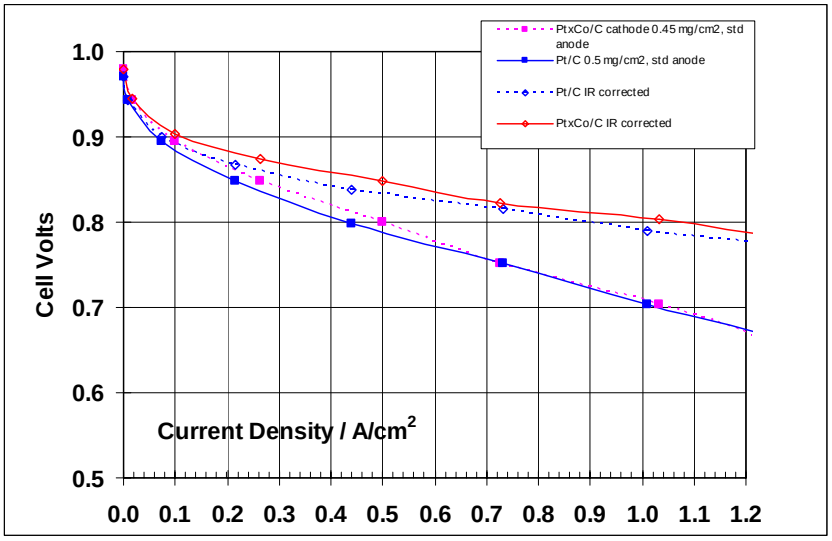

Figure 10. Comparison of performance stability of (A) 2006 E-TEK cloth MEA and (B) 2005 E-TEK cloth MEA

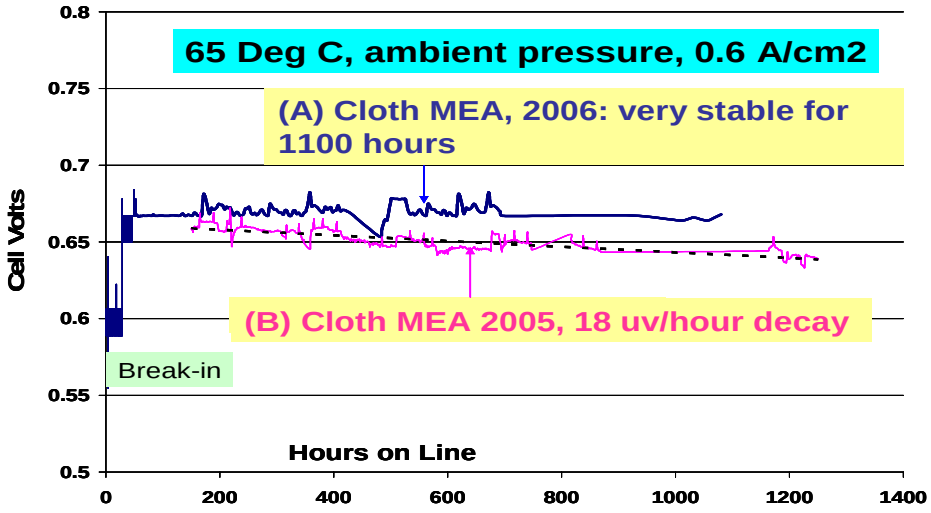

(2) Paper GDE/MEA

Development of machine-made paper GDE/MEA has been lagging cloth versions. The lack of flexible paper for roll-to-roll coating has been the main cause. Since 2005 E-TEK has identified a flexible paper which can be placed on coating machine for roll-to-roll machine coating. Following the roll-out of paper GDL in 2005, the GDE coating process has been gradually improved in performance. Initially the same technology used for cloth GDE/MEA and MEA was used to make paper GDE/MEA. However, it was discovered that paper has

quite different property from cloth. The technology used for cloth MEA frequently led to an unsatisfactory paper MEA. One of the cause is the “water buffering effect” of paper is much less for paper than cloth. This aspect was discussed in a recent conference: 13th Japan Fuel Cell Development Information Center (FCDIC) Conference, May 16-17, 2006, Tokyo. In a presentation by D. Kramer, E. Lehmann, G. Scherer, of Paul Sherrrer Institut, it was concluded: (1) Carbon cloth GDL was less influenced by the accumulation of water than carbon paper GDL; (2) larger amount of water accumulated in cloth than in paper as “buffer effect” (by neutron radiography). Early version GDE developed at E-TEK frequently showed impeded oxygen diffusion at median current density. Recently by applying fine gradient approach we are able to reduce the extent of uneven distribution of hydrophobicity. This uneven distribution frequently resulted in local area for water accumulation. One can also over correct this problem by making an electrode to be too hydrophobic for proton conduction. Figure 11 illustrates the performance of several versions of electrode structures with paper as the substrate.

Figure 11. Polarizations curves of paper MEAs with different hydrophilicity H2/air 0.5 bar, 70 deg C full humidification (optimized lab cell)

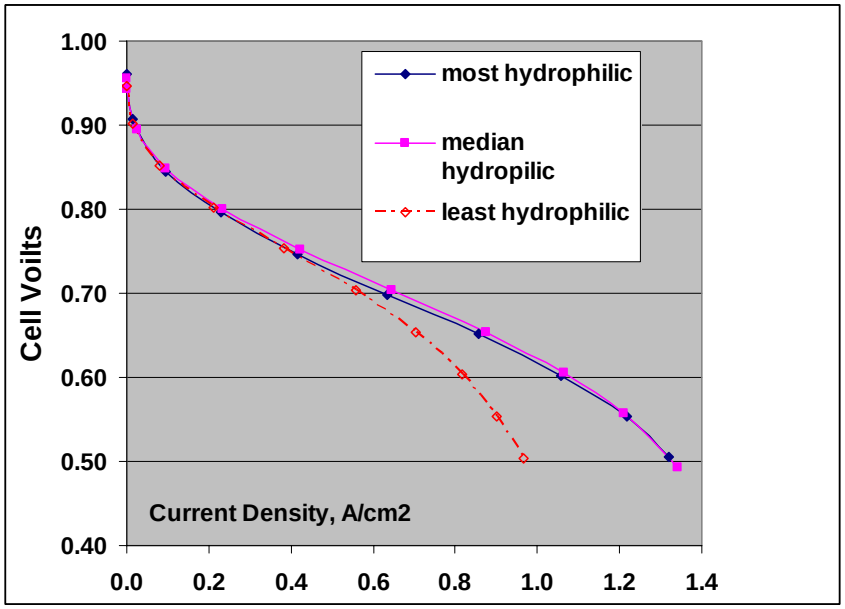

The initial version had the lowest hydrophilicity; there is not enough catalyst to sustain high current density. As we increase the hydrophilicity, the performance leveled off. The MEA with the highest hydrophilicity also showed the best performance as the cell was controlled at constant current of 0.6 A/cm2, 65 deg C , and ambient pressure (< 2psi g). However, the water management property was poor as one can see in Figure 5. Initial performance about 0.68 volts was good, but after 100 hour operation, a sudden drop in voltage by about 60 mv occurred; moreover, a large fluctuation of volts (>30 mv) periodically was observed. Many variations of conditions were then attempted to achieve a stable performance. But we were unable to either restore the initial performance or reduce the fluctuation to a reasonable extent.

The paper MEA with median hydrophilicity showed very good performance stability. Figure 12 shows the durability test at the same condition as in Figure 11.
The 7 uv/hour voltage degradation rate is comparable to what was observed for the 2006 version cloth MEA as shown in Figure 10. The paper MEA with median hydrophilicity showed just slightly lower performance than 2006 cloth MEA.

Figure 12. Volts vs. Time for the most hydrophilic paper MEA at 65 deg C, 2 psig air/H2 pressure (triple-serpentine graphite plate cell)

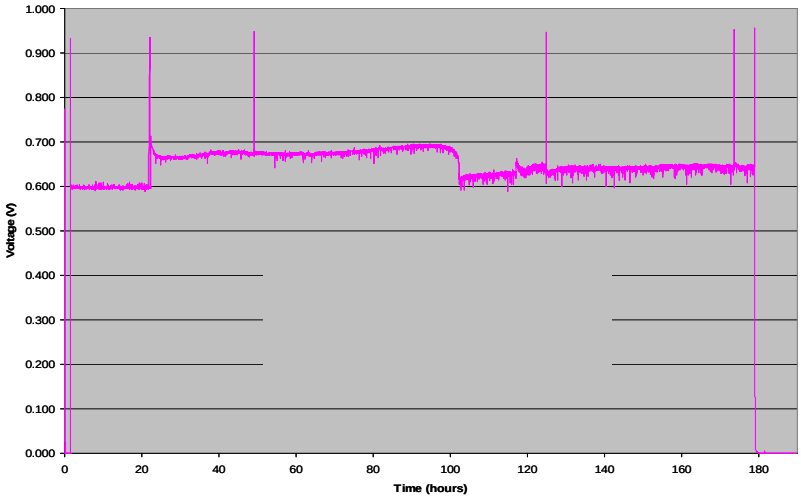

The paper MEA with median hydrophilicity showed very good performance stability. Figure 6 shows the durability test at the same condition as in Figure 5.
The 7 uv/hour voltage degradation rate is comparable to what was observed for the 2006 version cloth MEA as shown in Figure 2. The paper MEA with median hydrophilicity showed slightly lower performance than 2006 cloth MEA, about 10-15 mv.

Figure 13. Volts vs. Time for the paper MEA with median hydrodrophilicity. Condition as in Figure 12

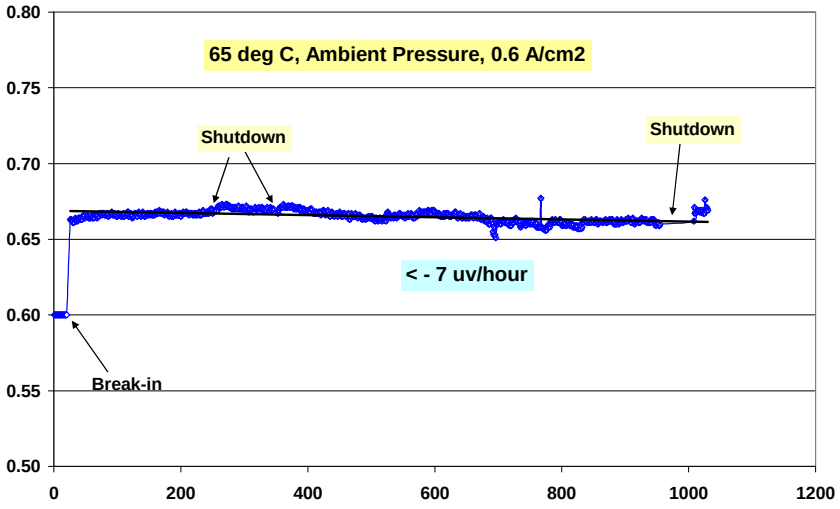

Long Term Test of Alloy Fine Gradient

With the success of the machine-coating of PtxCo cathode GDE (, fine gradient electrode), we decided to do a long-term test of the PtxCo cathode. An MEA was made with the PtxCO cathode (Pt=0.43 mg/cm2) with a standard anode and a 2 mil perfluorocarbon membrane was used. After the cell broke-in at 0.6 volts, it was operated at 0.6 A/cm2, 65 deg C, and ambient pressure (~2 psi). It then stabilized at 0.68 volts, then increased to 0.684 volts. Even after 400 hours on line it still showed slow increasing in performance. If we take 0.684 volts as the steady value, then about 16 mv advantage was observed for PtxCo/C cathode over Pt/C cathode This MEA is still being tested.

Figure14. Long-Term test of MEA with PtxCO cathode (Pt=0.43 mg/cm2), standard anode and a 2 mil perfluorocarbon membrane. 65 deg C, ambient pressure.

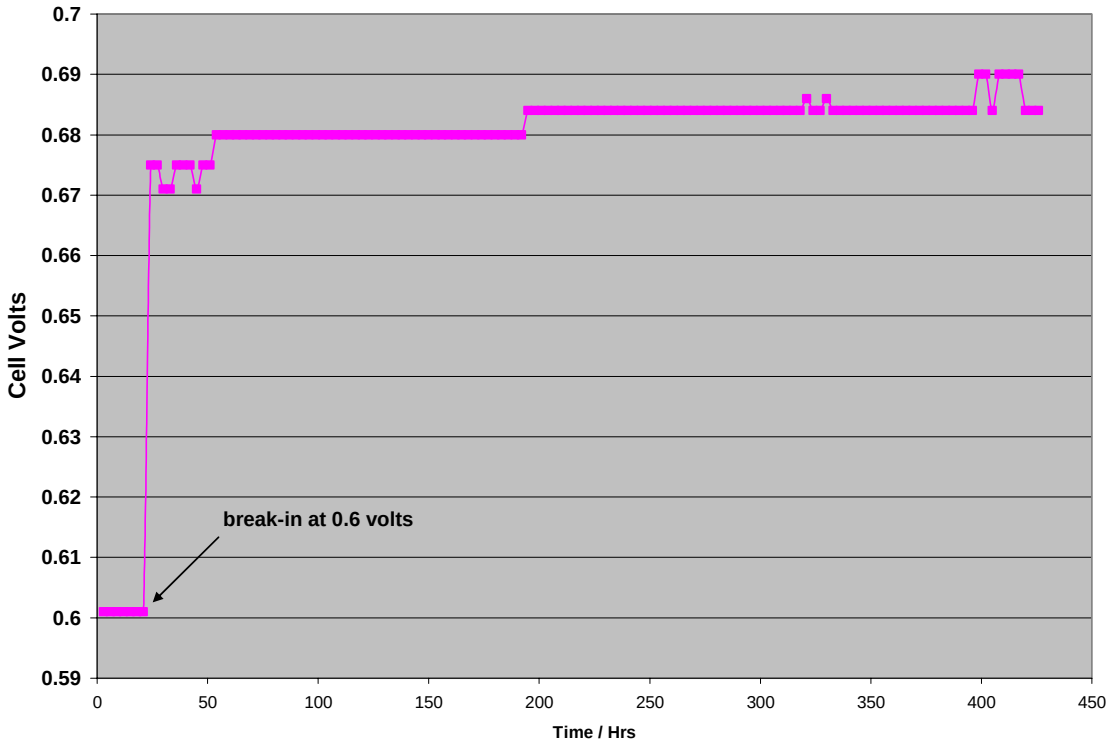

IBAD Study

(1) Scale up of IBAD MEA to 50 cm2 Cell

Ion-beam-assisted deposition is a unique method for preparing electrode. It is completely “dry” and does not require a pre-formed catalyst for electrode preparation. Besides, in the course of this program we discovered that no ionomer is required in the electrode structure for IBAD to function. The close proximity of the Pt to the membrane facilitates a very favorable proton conduction mechanism. This is very important milestone because all earlier IBAD work was conducted in lab cells smaller than 25 cm2

In 4th quarter of 2005, we were able to scale it up to 50 cm2.MEA with IBAD - 70% open pattern style A. During this program we also developed the new IBAD method by depositing Pt coating on GDL materials instead of the original process of depositing on membrane.

This 70% open pattern of style A with the method of deposition on GDL was scaled up and MEAs of 50 cm2 was tested and compared with the same MEAs of 25 cm2. Figure 1 showed the comparison. As Figure 15 shows, the performances were essentially the same up to a current density of 500 mA/cm2 in H2/air operation at 70 deg C. An analysis of gas diffusion was also conducted .by comparing the performance of O2 and air under the same condition. The resulting 20 mv and 65 mv oxygen gains observed at 100 mA/cm2 and 400 mA/cm2, respectively, fall into the range commonly observed for conventional MEAs.

Figure 15. Scale-up of MEA with IBAD as both cathode and anode
IBAD is 70% open with pattern A; 70 C, 43psig (air)/36psig (H2)

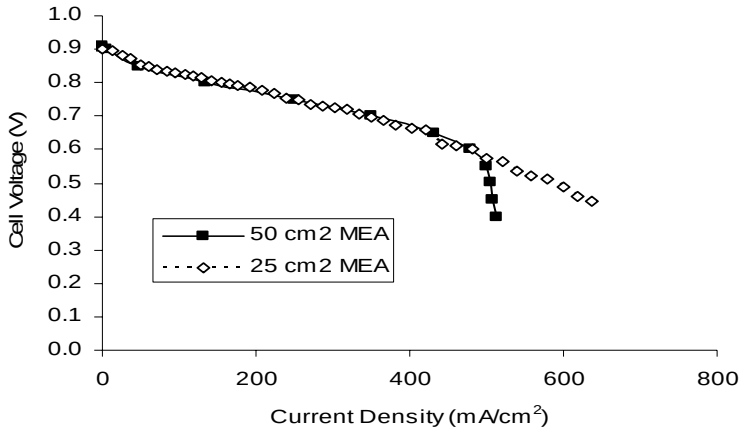

(2) Hybrid Cells- IBAD Method 1 and IBAD Method 2

Two kinds of IBADs have been developed. One kind is able to coat long roll like E-TEK's ELAT process but without liquid formulations. Data presented above was for IBAD method I. Both IBAD I and II can be used as anode with any ionomer (solubilized per-fluorocarbon ion exchange polymer) in the catalyst layer. These IBAD anodes can be combined with Pt ELAT with very low loading to form asymmetric MEAs. The performance of these MEAs can be operated at close to ambient pressure (0.5 bar) with very low total precious metal loadings. Figure 16 shows the typical performance. Because the IBAD coatings do not have carbon support, it could exhibit very good durability when carbon support corrosion is a problem under certain operating and/or start/shutdown condition. As mentioned above another advantage of IBAD is it does not need ionomer which could be the most unstable components in high temperature

operations.

Figure 16. Polarization Curves for MEAs with IBAD (method 1 and 2) as anode and ELAT as cathode. 70 deg C air/H2 0.5/0.5 bar a

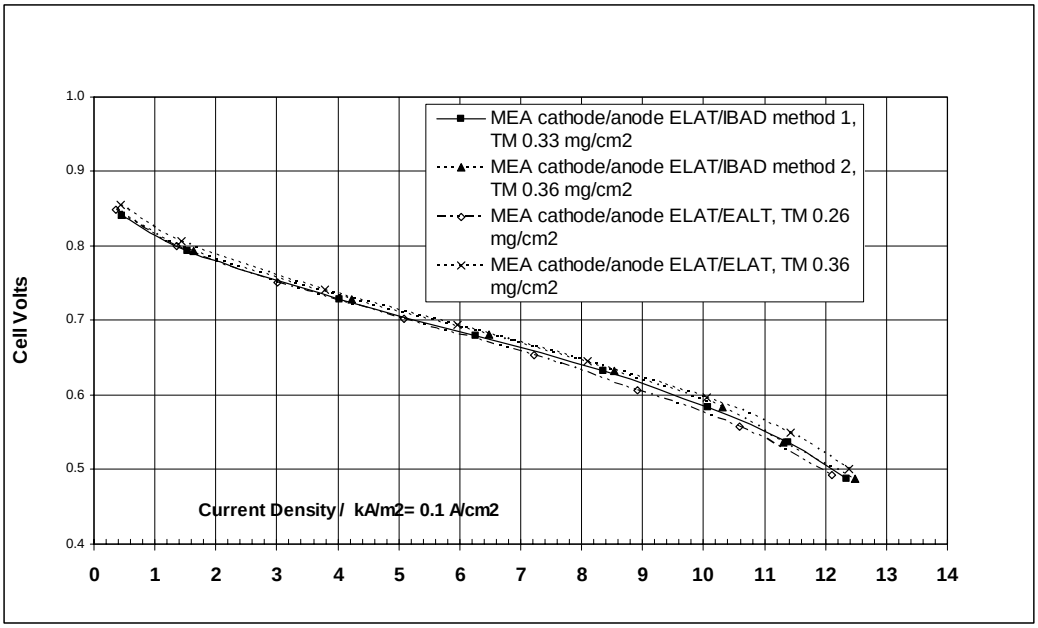

Development of a High Temperature Interface

As part of our efforts in developing high temperature MEAs, we explored the creation of a high temperature electrode interface that ultimately would be mated to the new membrane materials emanating from Du Pont's efforts on membrane development. Our initial trials were to use PFSA (perfluorosulfonic acid) ionomers and extend their high temperature capability by the addition of inorganic agents that assist in binding water, and use these in constructing the electrode layer onto the gas diffusion layer. For developing these materials, we employed standard Nafion® 112 as the membrane.

Figure 17 illustrates the results of identifying a suitable additive and optimizing the ratio of additive to ionomer, and the impact of this additive when we decrease the %RH. For 30% RH at 120 ^{o}C, at 0.1A/cm2 we obtain 0.85V and for 0.4A/cm2 we obtain 0.82V, exceeding DOE program goals (note PM content is also exceeding goals).

Figure 17: Polarization Curves for a "high temperature interface," under various %RH conditions. Gas Diffusion Electrode standard architecture, 1mg/cm^2 total PM, Nafion 112, 250kPa,120^{o}C

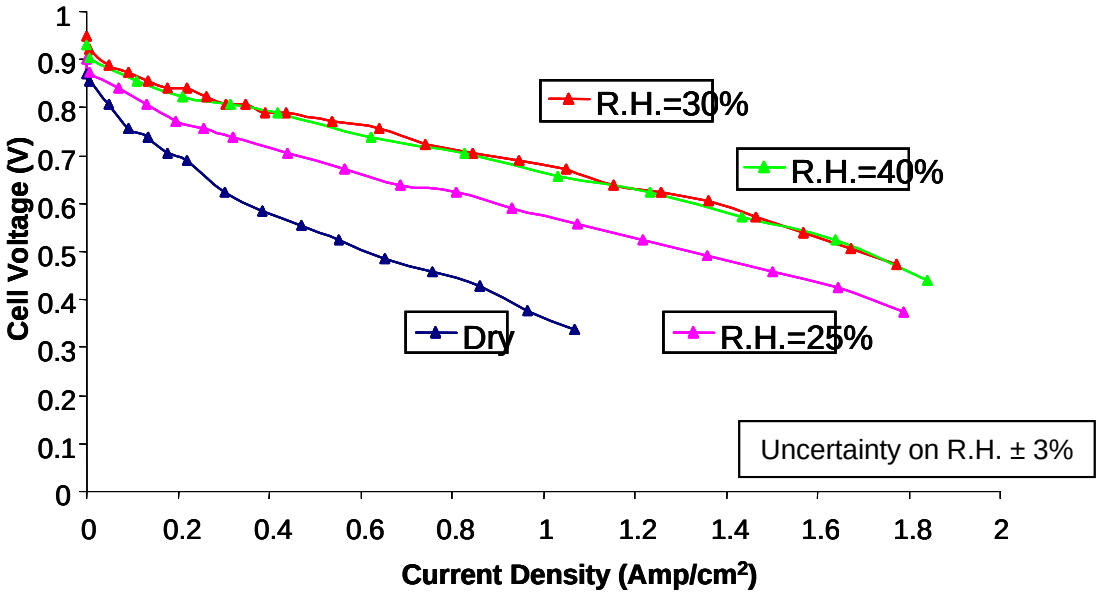

An alternative approach to developing a specialized interface for the higher temperature membranes is to employ IBAD. As previously discussed, this method does not need ionomer to extend the interface from the membrane to the electrode. The absence of ionomer would be most suited to new membranes that do not yet have ionomer development, as well as eliminate a potential failure mechanism for durability – breakdown of the ionomer interface. In Figures 18 and 19 we show the results of operating IBAD assemblies at the higher temperatures under various %RH conditions. Using Nafion 112.

Figure 18 employs a standard "method I" IBAD deposition (batch), while Figure 19 employs "method II" or continuous deposition. While neither of these assemblies approaches the DOE power targets, of interest is their relative stability across a wide range of %RH at the higher temperature. They vary little across a range of 25-45% RH except when the MEA is run "dry". We believe this behavior is due to the very thin electrode layer being in intimate contact with the membrane whereby water availability is controlled by the membrane. Figure 18 and 19 suggest this approach is viable for new high temperature membranes.

Figure 18: High Temperature MEAS using IBAD coated anode and cathode, method I IBAD, 0.32mg/cm2 total PM, Nafion 112, conditions as in Figure 17. Temperatures indicate humidifier bottle temperature.

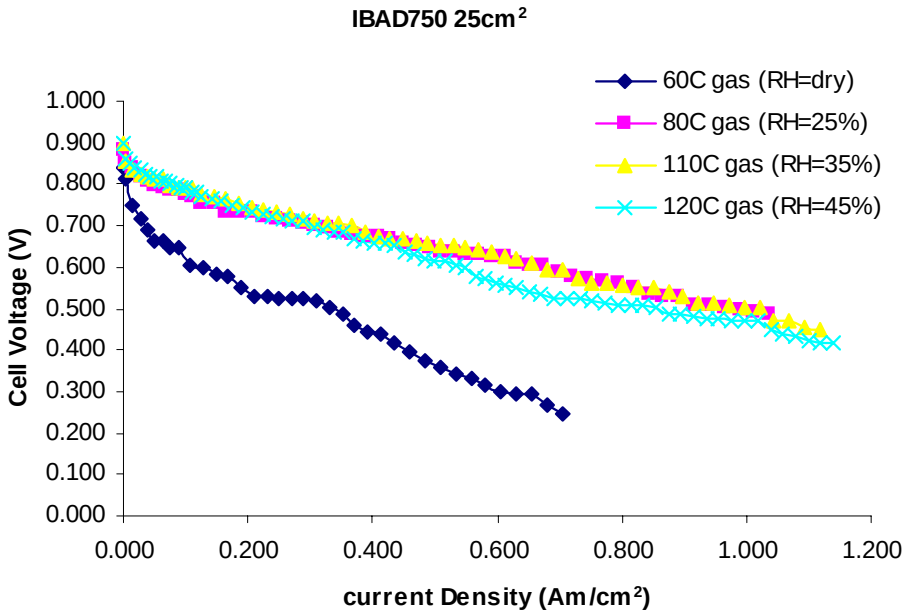

Figure 19: High Temperature MEAS using IBAD coated anode and cathode, method II IBAD, 0.16mg/cm2 total PM, Nafion 112, conditions as in Figure 17. Temperatures indicate humidifier bottle temperature.

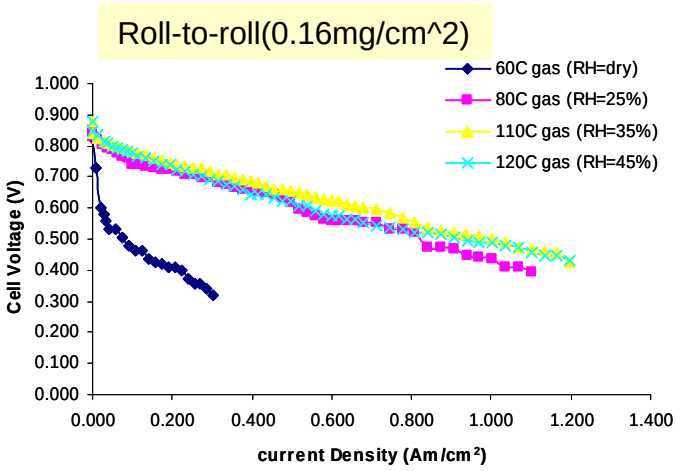

Stack Testing

(1) Low Loading Anode
In order to reach the DOE goal it is very important to reduce the anode loading to below 0.05 mg/cm2, so enough Pt, > 0.25 mg/cm2, can be used in cathode. Although many publications described using anode of loading, i.e., < 0.05 mg/cm2, without any sacrifice in performance, it is actually to carry it out in a large scale. E-TEK's machine coating is perfect to implement this. Because of the very low loading, it's crucial to be able to coat very even coating, machine-coating has the advantage of consistence so thin spot can be avoided. Another factor is that to effectively avoid the thin spot, the catalyst property needs to be modified. E-TEK successfully accomplished both. The low loading anode was made on machine and 225 cm2 MEAs were prepared along with standard cathodes. A seven cell 225 cm2 stack was assembled and tested at Nuvera, it's consistency is shown in Figure 20. The performances of the MEAs with low loading were also compared with the standard MEAs in the same cell stack (three each) in Figure 21.

Figure 20. The Performance of Seven 225 cm2 MEAs with Low Loading (0.05-007 mg/cm2 Pt) Anodes and Standard Cathodes at 70 deg C, 1.5 bar a

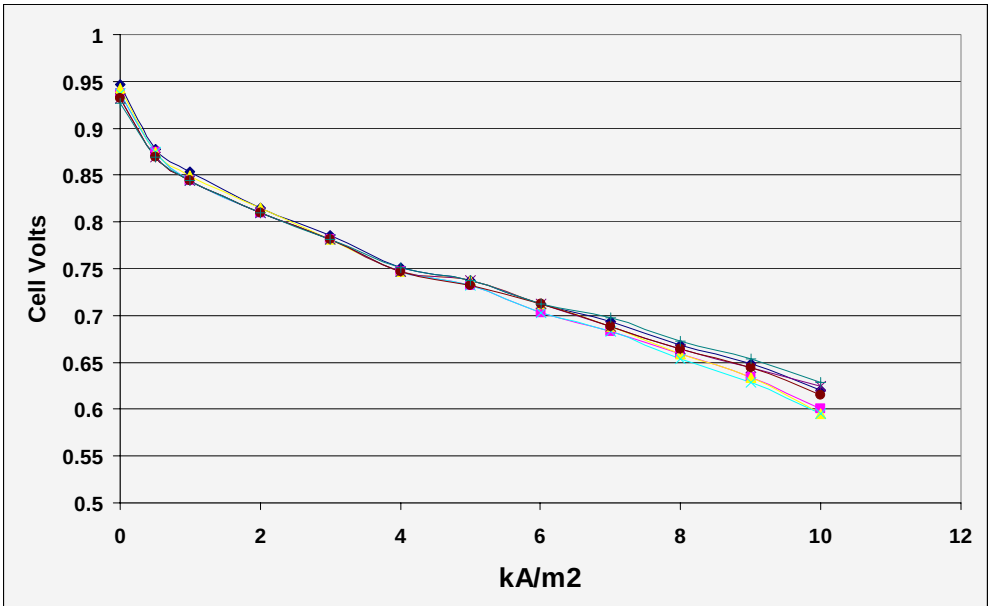

Figure 21, Average performance comparison of MEAs with standard anodes and low loading anodesas in Figure 15. All cathodes are standard (0.5 mg/cm2). Three cells each, condition as in Figure 20.

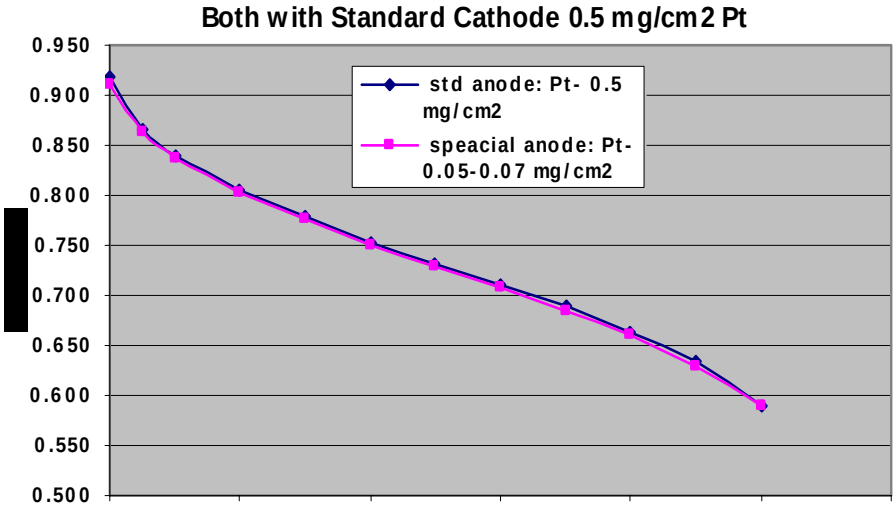

PtxCo On Corrosion Resistant Carbon Support

In 2006, we described the new development at E-TEK about the corrosion resistant carbon. In brief, E-TEK has been engaged in searching for corrosion-resistant carbon with PEMEAS Celtec Division in Frankfurt to improve the catalyst durability. Recently DOE also emphasized the importance of catalyst support in future fuel cell research. As described in 2006 1st quarter report of this program, by accelerated electrochemical test at 180 deg C, we identified a carbon support (corrosion resistant carbon 1) with 1/3-1/4 of the corrosion rate exhibited by Vulcan. From other observations, we believe the corrosion stability enhancement is most likely to be even higher than this. Pt_xCo on corrosion resistant carbon 1 was prepared and compared to presently used Pt alloy in 180 C H_2/O_2 PBI/H3PO4 cells. The initial performances of the two were very similar but the potential cycling testing between 0.85 and 0.6 volts showed Pt_xCo on corrosion resistant carbon 1 had much better stability (180 deg C, ambient pressure, H_2/O_2). The performance comparison is illustrated in Figure 22 whereby the high temperature MEA

now containing this alloy on either Vulcan X-72 or Carbon 1 is subjected to potential cycling, (1 hour at each potential), and the relative current measured at 0.6V is recorded. Although the power output is not comparable to that typically obtained in PEMFCs, the stability shown here is indicative of the importance of stable, graphitic supports.

.

Figure 22 Relative Current Density at 0.6 volts for (A) PtxCo on Corrosion Resistant Carbon 1 vs (B) 1st Generation Pt alloy on Vulcan XC-72.

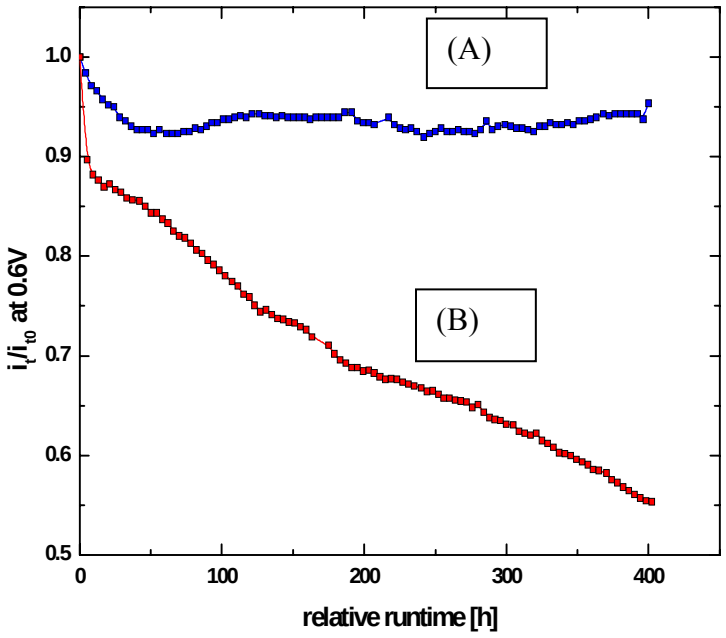

With these encouraging results, we have prepared PtCo catalysts on the corrosion resistant carbon with different ratios and the XRD graphs of these catalysts are shown in Figure 23. They have shown good performances in high temperature fuel cells and are expected to show good performances in low temperature (60-90 deg C) fuel cells. The relative strong peak at ~25 2-theta indicated higher graphitization of the carbon.

Figure 23. XRD Graphs of PtxCo, PtyCo, and PtzCo

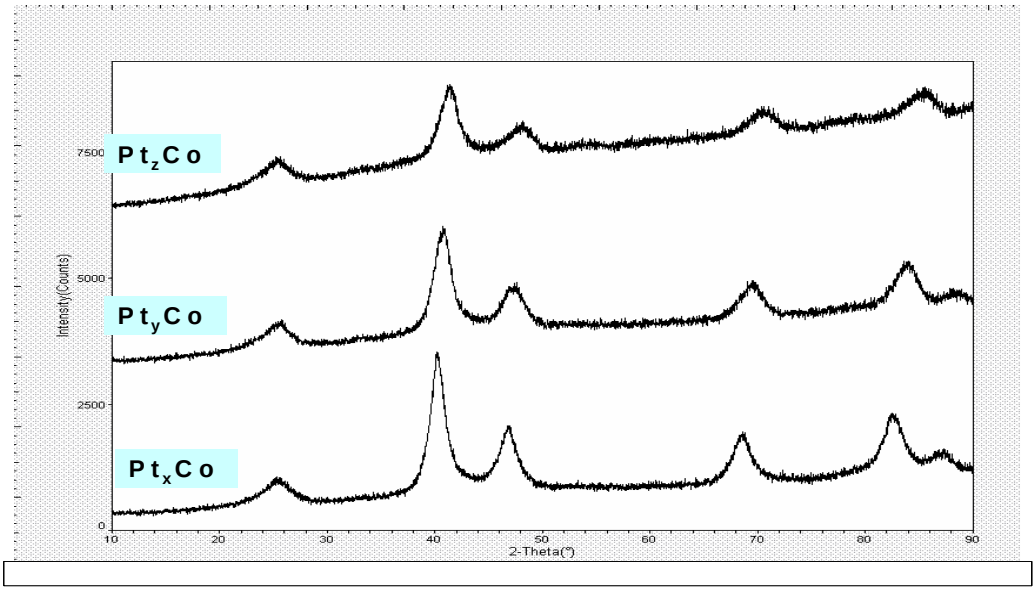

Alternative Catalyst Approach for Operating Under Strenuous Conditions.

In a recent article (Mark F. Mathias, et al., “Two Fuel Cell cars in Every Garage?” Interface, The Electrochemical Society, Vol 14, no. 3 Fall 2005, pp. 24-35) it was found that an MEA with supported catalysts will show unaccepted large performance degradation although a relatively small percentage of carbon support weight was lost. After more experimenters evaluated operation under start/stop conditions, they confirmed that a majority of the loss of performance occurs mostly during the cycling period, and that this loss is attributable to carbon corrosion.

Thorough analysis by many researchers (e.g. Carl A. Reiser, et al., Electrochemical and Solid State Letters, 8 (6) A273 (2005)) pointed to fuel starvation as the major cause. Besides improper operation or fuel distribution system problem, the situation can occur when an idled cell is brought online by feeding hydrogen to the air-filled anode. An internal discharge between areas with H_2 coverage and those with no or low H_2 coverage can drive the potential at certain areas in the cathode catalyst layer to above the carbon corrosion potential. A similar situation of “partial H_2 filled chamber” occurs when cells were shutdown and anode chamber is purged with air. Mitigation strategies were discussed but completely avoiding damage might be difficult or costly. Because of these issues many fuel cell stacks prematurely failed because of the loss of carbon. It has been found that as a percentage of carbon in the catalyst layer is oxidized and lost the cell will experience catastrophically failure. The percentage is usually in the range of 15-30%, which is most likely related to loss of catalyst layer electronic conductivity as it severely decreases the catalyst utilization.

(1) Solution to the carbon corrosion problem: eliminate carbon support

One of the approaches to avoid the carbon corrosion problem is to completely eliminate the carbon support for the catalyst at the first place. In previous section of this report we have described that unsupported Pt (Pt black) is a good solution to this carbon corrosion problem, and we have been very successful in making new Pt black catalysts with high performance. We are going to show some data below which indicates the excellent durability of Pt black catalysts under strenuous operating condition.

(2) Durability with On-Off Cycling: Comparison of MEAs with Pt black and supported catalysts

A number of 50 cm^2 E-TEK MEAs were tested in the lab cells and subjected to cycling. Prior to cycling studies *in-situ* cyclic voltammogramms were taken under N_2/H_2. The

results in Table 6 confirm the BET data; however they are more relevant as they represent electrochemical surface area. Surface charge is a direct indicator of electrochemical surface area. E-TEK Pt black catalysts showed consistently higher desorption surface charge than a commercially available industrial Pt black by ca. 66%. The catalyst surface areas calculated by using the surface charge for E-TEK Pt black catalysts are in the range of 12-15.5 m^2/g. Comparing with (BET) measured surface areas of 34 m^2/g, one obtains the low limit of catalyst utilization percentage of >35%-46% in the MEA (BET surface area is the upper limit of electrochemically active surface area). This ratio is a fairly high number, indicating a good formulation.

Table 3. Calculated surface areas for Pt black MEAs made by E-TEK and that by alternate supplier (surface charge proportional to electrochemical surface area)

Source	Cell No.	Cathode Charge mC/50cm^2	Anode Charge mC/50cm^2
E-TEK	3156	5807	4478
E-TEK	3168	6445	4945
E-TEK	3177	7109	5694
Commercial Pt black	reference	3907	3002

The Pt black MEAs were tested under a very strenuous condition by operating at 0.05 A/cm^2 65 deg C for typically 8 hours then followed by shutdown and started up again on the next day. The polarizations curve was taken at BOL and after 2000-2500 hours. The same testing was also applied to a reference MEA with supported catalysts. Figure 24 shows the dramatic difference.

Figure 24, Effect of Daily Shutdown on Performance, Comparison of E-TEK Pt Black MEA and a Pt/C MEA; 65 ^oC ambient pressure 6.0/4.0 H_2/air, 100% RH

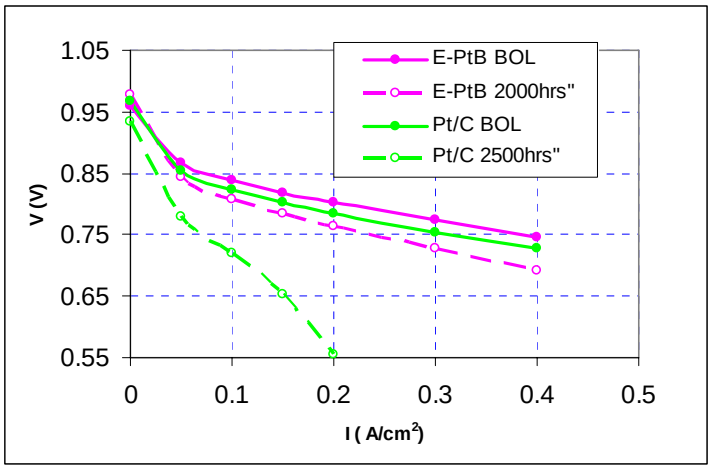

(3) Unsupported Pt Alloy Catalysts

While we have focused on eliminating or reducing the impact of carbon corrosion, there still remains catalyst sintering mechanism. Recent publications (Mark F. Mathias, from previous, and Hubert Gasteiger, Applied Catalysis B, Environmental, 56, 2005, 9-2005.) have found that Pt alloys can have much higher stability under potential cycling stability. For example in Mathias, it was reported that under voltage cycling between 0.7-0.9 volts (30 sec pulse) at 80 deg C, supported 50% Pt lost 70% surface area with a large loss of performance after 30,000 cycles. Under the same testing conditions, 30% Pt:Co alloy looses much

less surface area and it was concluded Pt:Co might be able to meet the durability requirement if there is no significant specific activity loss. In any case, Pt:Co showed much better performance durability during voltage cycling condition, if one can further eliminate the problem with carbon corrosion as stated above, a durable catalyst to reach DOE target might be possible. At E-TEK, in previous reports of this program we have developed supported Ptx:Co and Ptx:Cr which showed significantly better performance (20-30 mv) than Pt catalyst.

Although we have demonstrated Pt alloy cathodes, such as PtxCo, PtxCr can exhibit better performance than Pt, supported Pt alloy catalyst would have the same stability problem as supported Pt catalysts under start/stop or voltage cycling condition. Pt alloy black catalyst would have higher probability to avoid the stability problem. Synthesis of unsupported Pt alloy catalysts is a challenge because the growth of particle size of the alloy is difficult to avoid in traditional alloy preparation method. Recently E-TEK has developed a new method for Pt alloy preparation. With the new method we are able to control the XRD crystalline size. Figure 25 shows the XRD graphs for two potential Pt alloy catalysts, Pt2Co and Pt4Co2Ir. Addition of iridium in the cathode catalysts can improve catalyst stability. Future work will be developing formulation for these alloy catalysts to realize their full potential for performance and durability.

Figure 25. XRD graphs of Pt black and Pt alloy black catalysts with novel synthetic method

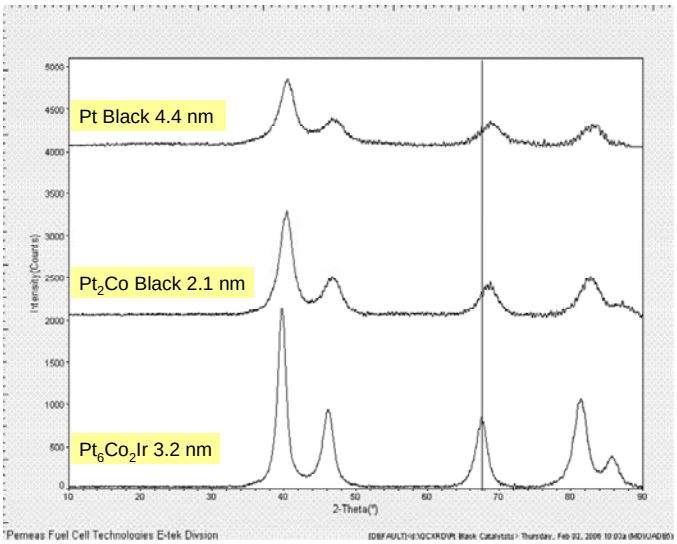

Refinement and Scale Up: Results and Discussion (Program 1A3)

Status

Program 1A3: Highlights

- E-TEK successfully developed roll-to-roll machine coated PtxCo cathode methodology. The cathode showed significant performance advantage over Pt cathode GDE. The new version employs new GDE fabrication procedure which preserves the Pt alloy electrochemical activity even after large scale coating/post treatment. It is expected to roll out a new product of Pt alloy GDE to the market in the near future. With a total Pt loading of 0.3 mg/cm2 – cathode 0.25 mg/cm2 and anode 0.05 mg/cm2, at DOE protocol, 80 deg C, 2.5 Bar A, the performance at 0.1 A/cm2 is 0.87 volts and at 0.4 A/cm2 is 0.79 volts. O2 kinetic current of a 0.25 mg/cm2 PtxCo GDE showed 0.27 A/mg Pt at DOE condition, almost equal to current DOE status, 0.28 A/mg
- PtxCo and PtyCo alloys on corrosion resistant carbon were made and the cathode GDEs prepared with them showed better performance than current high temperature (160-180 C) Pt alloy cathode in low current density range and equal performance at high current density range. They showed much better durability under potential cycling condition.
- 500 cm2 Cell stack with various E-TEK MEAs were tested in Nuvera stack for 650 hours, results are analyzed. MEA with Pt3Co fine-gradient cathode combined with low loading anode showed the best performance stability. IBAD anode showed similar performance stability.
- Two versions of fine gradient GDEs have been successfully developed for 50% RH on the cathode side. These cathodes use the fine-gradient structure approach and catalyst of higher hydrophilicity for easy of retaining water but also avoiding excessive water accumulation. The new versions showed outstanding voltage stability under constant load with a fluctuation in the range of 10 mv for the best version.
- Testing of Pt black MEA at a partner's lab indicated outstanding stability under frequent shutdown condition. Analysis after 2000 hour on line indicated very small increase in catalyst particle sizes. New version of MEAs with unsupported Pt catalyst with advanced structure was developed and tested.

Results

GDEs/MEAs for Low RH%

As part of the program re-direction, the focus changed from developing MEAS that operate at 120 degres C to those that can operate at under 25% RH with occasional excursions to 120 degrees C. This is one of the goals of DOE FreedomCar program. In addition, there is growing interest in this kind of MEA in applications such as Telecom back-up systems. Our focus on this area has led to the following conclusions: (1) for an MEA, cathode can be relatively hydrophobic, but the anode needs to be able to hold water to prevent excessive loss of water from electro-osmotic drag. (2) As RH% decreases to lower level, such as 50%, it's important to have an anode with higher hydrophobicity than the cathode, so the water will be retained by the anode. 3) By increasing the hydrophilicity of both anode and cathode, but keeping a higher level of

hydrophilicity in the anode one can improve the performance even more in low RH% operation. In the current study we continued exploration along this line.

Two versions of new MEAs were made. We have designed two new electrodes with different hydrophilicity. Both of them were more hydrophilic than the electrode used previously and which showed better performance at low RH, i.e., 50% RH cathode and anode, than the standard electrode. These two versions of cathodes use fine-gradient structure approach for easy of retaining water, in addition to the fine-gradient structure approach described in the last two reports. The fine gradient structure can avoid excessive water accumulation which can impedes oxygen diffusion, but we found that using catalysts of higher hydrophilicity is the key for water retention and low RH% operation. The two new versions have the following cathode and anode hydrophilicity: (1) version 1, fine gradient, anode: highest hydrophilicity, cathode: moderate hydrophilicity; (2) version 2, fine gradient, anode: moderate hydrophilicity, cathode: high hydrophilicity. These two MEAs are compared with an MEA with both anode and cathode to have simple structures and low hydrophilicity. They were all tested in 50 cm2 graphite triple serpentine flow filed lab fuel cells. Figure 7 shows the polarization curves at 65 deg C 100% RH. The performance of version 1 MEA is slightly better than that of the one with simple structure, but version 2 is significantly better than both of them. Version 1 has highest total Pt loadings among thee three MEAs, but the high utilization of cathode catalyst is the main reason for very good performance of this version.

After beak-in these MEAs were subjected to a condition of low cathode RH% of 50% and H2/air stoich at 1.1/2.5, and constant current density of 0.35 A/cm2, cell temperature 65 deg C. As Figure 8 shows under this condition, the MEA with simple structure and low hydrophilicity could not hold steady volts, it showed periodical oscillation and spikes of lower voltages to as low as 0.3-0.4 volts. On the other hand, version 1 and version 2 showed very stable voltage, with voltage fluctuation of 10-20 mv for version 2. The same fluctuation range was observed for version 1 but with occasional oscillation to about 30-35 mv (every two hours or so). Moreover, the maximum cell voltages for version 2 and MEA with simple electrode structure now become very different-68 mv vs. 61 mv. AC impedance measurement during operation indicated that for the MEA with simple structure, the lower voltage period corresponding to membrane drying associated with high impedance reading. Presumably the dry air carries water away from cathode, which in turn “borrows water from the membrane” and the replenishment of water from anode side is not faster enough and the membrane starts to lose water. The high IR will raise the temperature and speed up the water diffusion rate and in the meantime water accumulation at the anode side will also speed up the diffusion of water through the membrane. The simplest way to mitigate the problem of membrane drying is to increase the water holding ability of the cathode- in this work version 1 and version 2 MEAs are demonstrated to be able to do this. The slightly enhanced voltage stability of version 2 relative to version 1 could be due to the higher hydrophilicity of the cathode of version 2.

Figure 26.Hydrophilicity Study: Polarization Curves of Three MEAs in Triple Serpentine Graphite Plate Cells
65 deg C, H2/Air 2.5 psi g, 1.3/1.7 stoich, 100 RH%

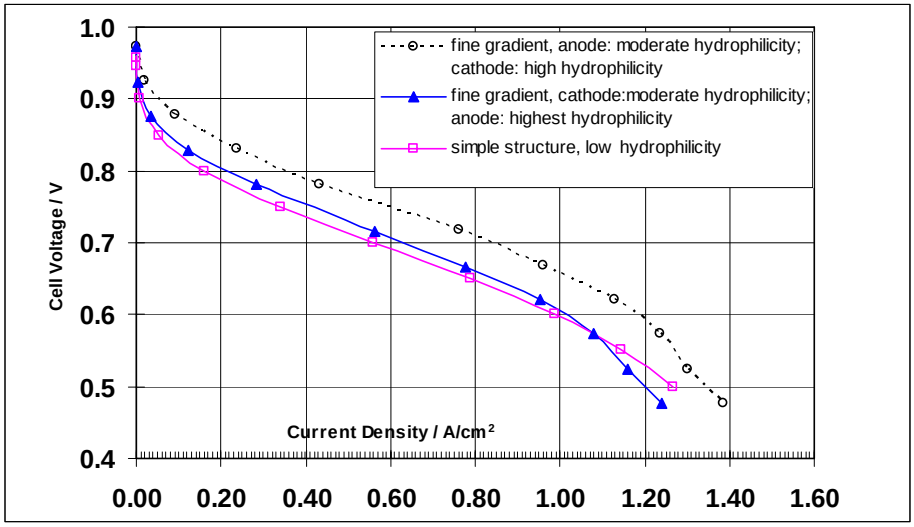

Figure 27. Cell Voltage – Time Curves for the Three MEAs in Figure 26, at 65 dg C, 0.35 A/cm2, cathode/anode RH% 50%/100%, and H2/air stoich 1.1/2.5. (A) simple structure, low hydrophilicity; (B) version1, fine gradient, cathode: moderate hydrophilicity, anode: highest hydrophilicity; (C) version 2, fine gradient, cathode: high hydrophilicity, anode: moderate hydrophilicity.

(A) MEA with simple structure and electrodes of low hydrophilicity

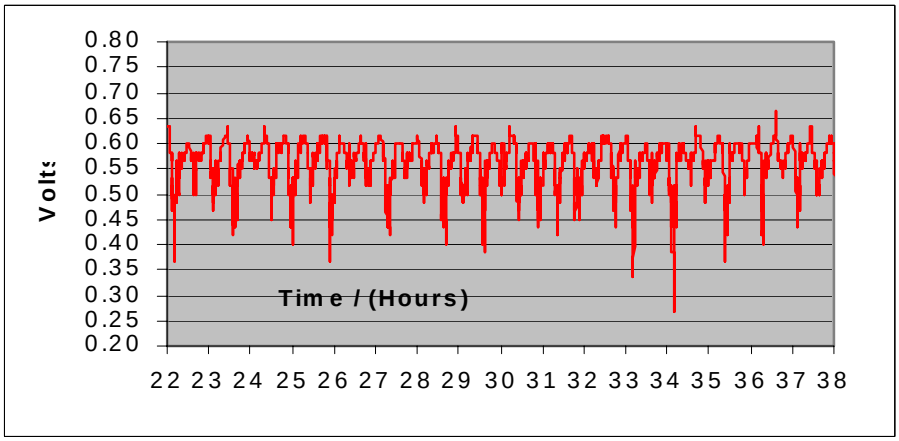

(B) Version 1 MEA

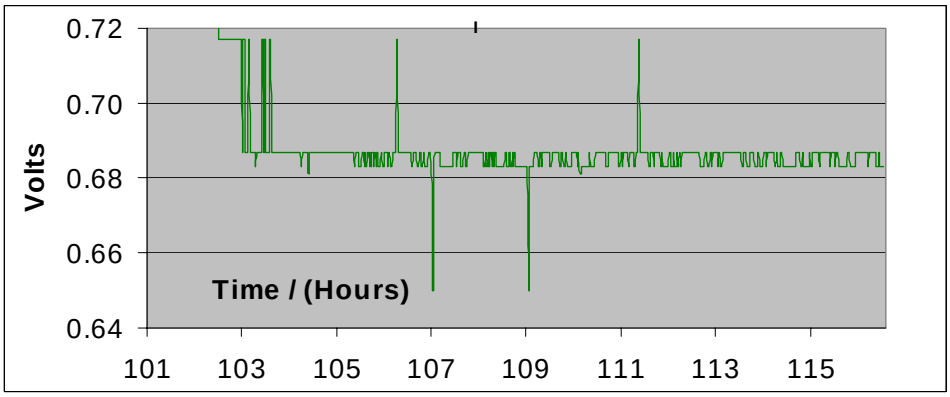

(C) Version 2 MEA

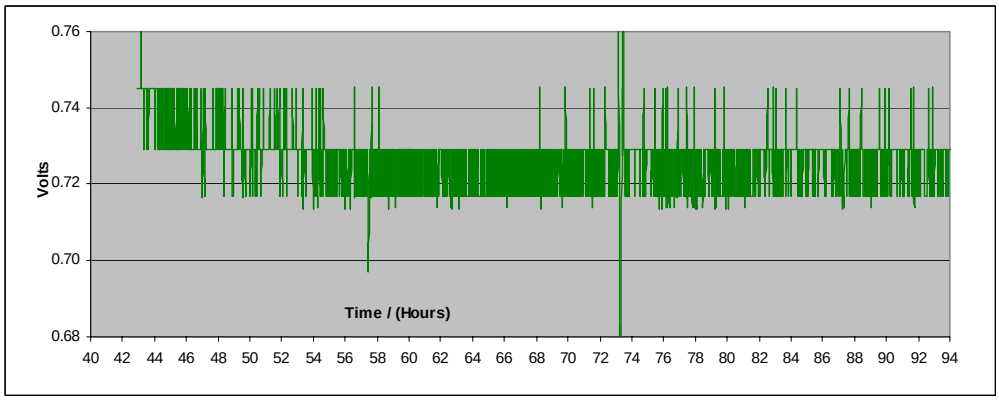

Low RH MEAs: Refinements

With the future applications of hydrogen fuel cell moving toward lower humidity, such as <50%, it is important to understand how different gas diffusion electrode (GDE) structures respond to humidity change. Since the 4th quarter of 2005 we have done a number of fundamental studies to elucidate the structure aspects on low relative humidity operations. We will summarize our observations below.

(1) Hydrophilicity Consideration

In general lower humidity operation requires the structure of GDE to retain water, so a more hydrophilic structure is desired. However, it is likely to make the structure to be too hydrophilic and results in impeding gas transport. For a start we made three MEAs with electrode structures as follows: version 1 has both anode and cathode to be most hydrophobic, version 2 has both anode and cathode to be medium hydrophilic (version 2), and version 3 has most hydrophilic anode and medium hydrophobic cathode. Figure 26 compares the performances of the three versions at 100/100 RH% and 50/50 RH%. At 60 deg C when the three MEAs were operated with 100/100 anode cathode RH%, the performances were similar with version 1 to be slightly better than the other two. However, as

RH% dropped to 50% at cathode and anode sides, the performance of version I dropped a lot. While the performance of version 2 and version 3 dropped much less. It is interesting to note that at 100/100 RH% version 3 is slightly better than version 2, but at 50/50 RH%, the difference widened. The relative performance at 100/100 RH% can be understood as that during operation, water is carried through the membrane continuously and one would like to have an anode to be more hydrophilic to balance out this electro-osmotic drag action to prevent excessive loss of water from the anode side. This requirement becomes more important at 50/50 presumably because of replenish of water at anode side at 50%RH is much slower than the case at 100%, so a more hydrophilic anode will be much more critical.

To further illustrate this anode/cathode balance, we investigate the effect of cathode RH% and anode low RH%. Figure 29 shows that for version 1, drop in cathode RH% from 100% to 50% resulted in moderate performance loss, but a drop in anode humidity caused a much large loss of performance. Combination of Figure 26 and Figure 27 reveals that cathode can be relatively hydrophobic; however, the anode needs to be able to hold water to prevent excessive loss of water from electro-osmotic drag.

Therefore, the important principle for building MEAs for low RH% operation is that (i) the hydrophilicity of anode needs to be higher than that of cathode to prevent cathode from “stealing water” from the anode side. Another principle is that (ii) a critical hydrophilicity for both cathode and anodes is needed for holding water.

(Figure 28: three MEAs with change in hydrophobicity)

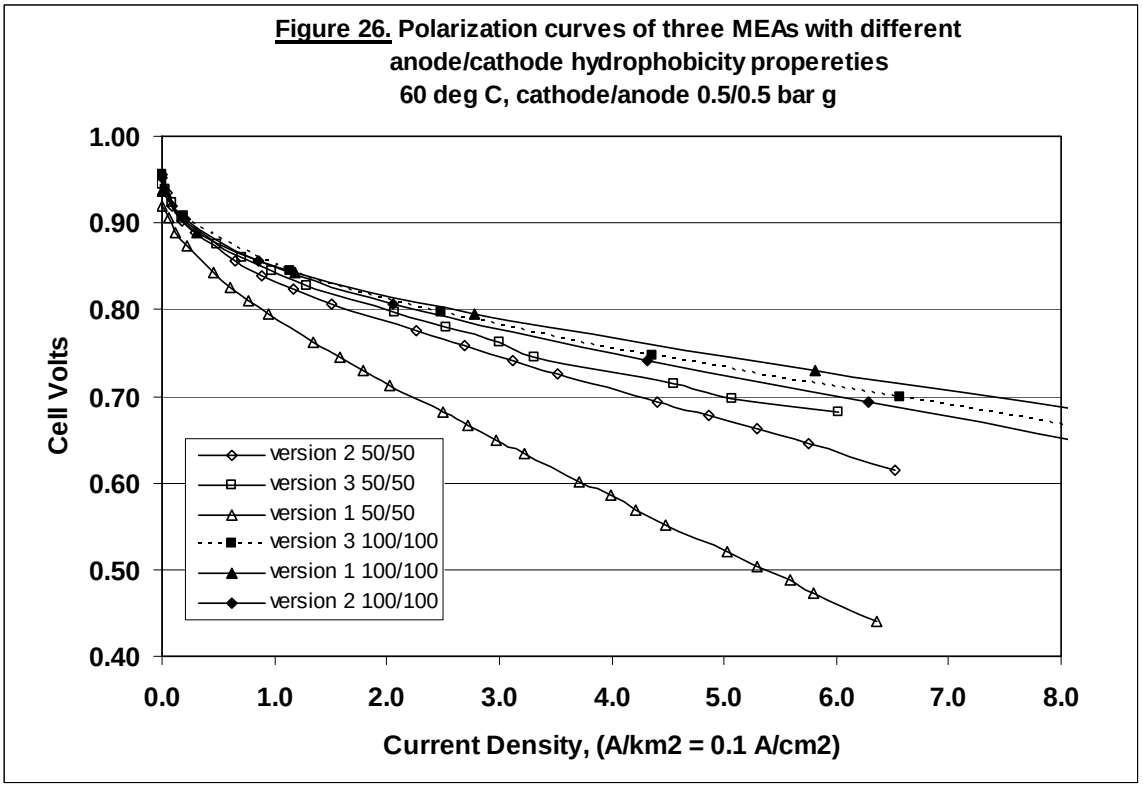

Figure 29: Polarization Curves for Version 1 MEAs vs %RH

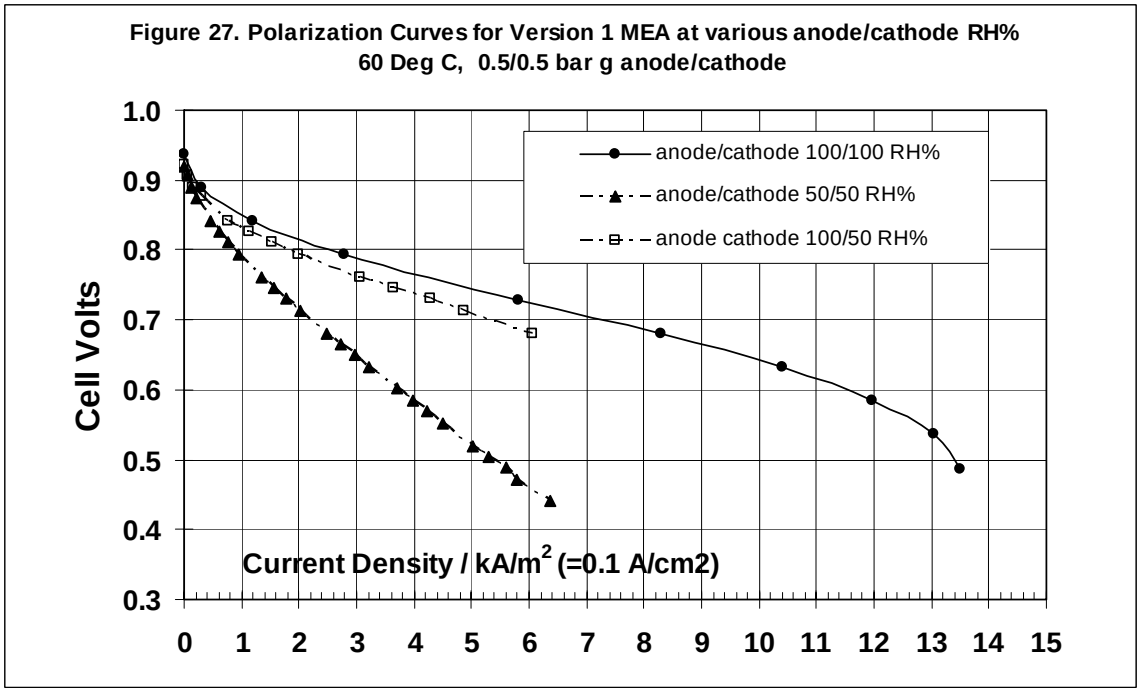

(2) Fine Tune Hydrophilicity

Based on the principle described above we further modified the electrode structures of anodes and cathodes. In 2nd quarter of 2006, we designed two new

electrodes with different hydrophilicity. Both of them were more hydrophilic than the electrode mentioned above that showed better performance at low RH, i.e., 50% RH cathode and anode, than the standard electrode. The hydrophilicity is in the following order:

most hydrophilic > moderately hydrophilic > mildly hydrophilic > standard

Here the standard is the version 1 in Figure 29. As Figure 30 shows at 100% RH, all MEAs showed similar performances except the electrodes with most hydrophilic anode and moderately hydrophilic cathode.
This again demonstrates the importance of fine tune of the relative hydrophilicity of cathode and anode. When anode is more hydrophilic, water management is facilitated very well. When the RH% of both H2 and air are decreased to 50%- Figure 31, the MEAs with “more hydrophilic” electrodes showed better performance than the MEAs with “moderately hydrophilic” electrodes. They both showed better performance than the MEA with mildly hydrophilic anode and cathode. This is easily explained by the water holding ability of more hydrophilic electrodes. Although the MEA with most hydrophilic anode and moderately hydrophilic cathode still showed the best overall performance, the performance of the MEA with most hydrophilic anode and cathode actually rose to top at lower current densities. The performance fell off at higher current density for this MEA points to the possibility of cathode water management problem even though the RH% is as low as 50%. We believe this is related to the aforementioned water imbalance problem: water is dragged by proton through osmotic force to the cathode side and in the mean time; water is generated at cathode side. If cathode and anode have the same hydrophilicity, the imbalance in water can cause drying at the anode and wetting (impede oxygen diffusion) at the cathode side.

Figure 30. Performance of MEAs with cathodes and anodes of various hydrophilicities. Condition: 70 deg C, H2/air: 0.5 bar g,

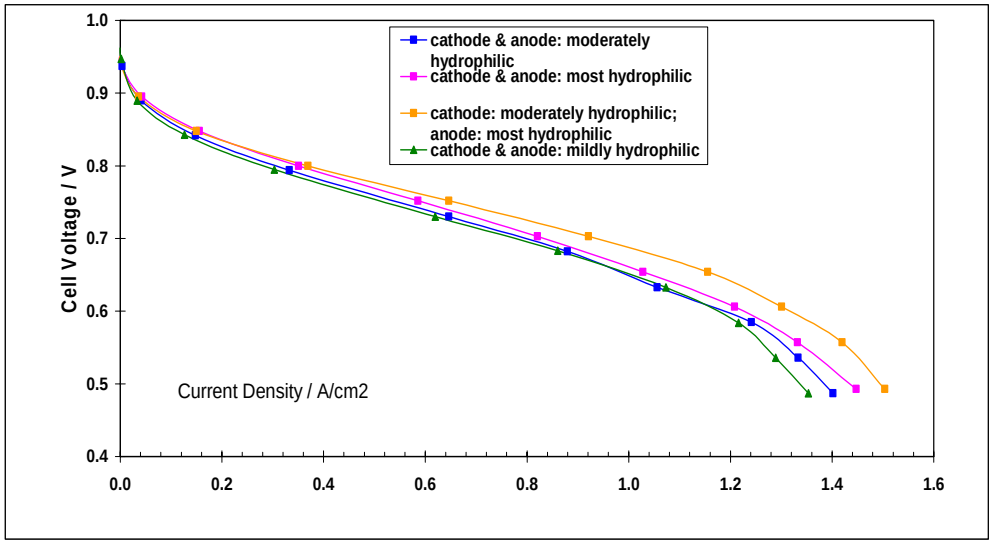

Figure 31. Performance of MEAs with cathodes and anodes of various hydrophilicities. Condition: Cell 70 deg C, H2/air, 2.5 psi g, 50% RH.

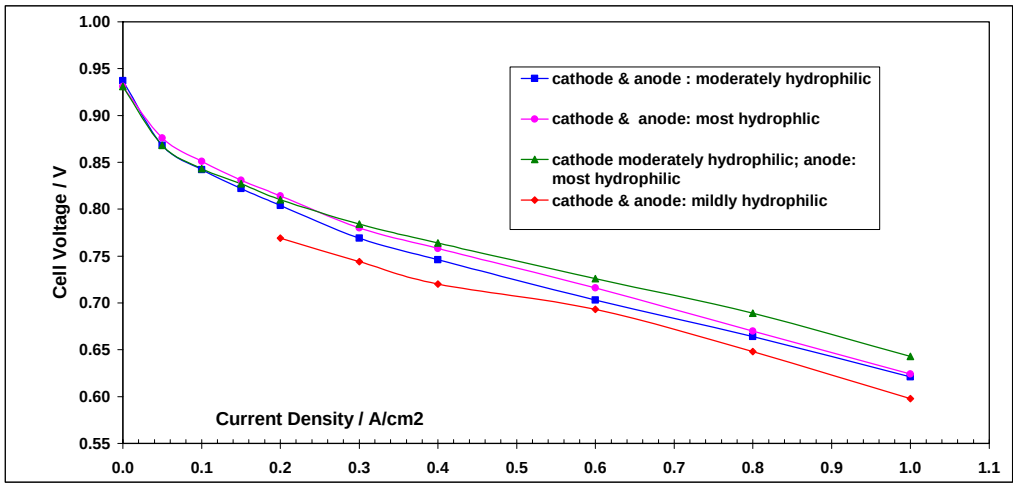

In conclusion, one can increase the hydrophilicity significantly by varying catalyst/binder in the electrode structure to build an MEA with very good performance in low RH% operation. However, excessive hydrophilicity of cathode can lead to water management problem at high current densities.

(3) High Power & Dry Hydrogen Operation

Many fuel cell applications require operating fuel cell under dry H2. For 60 deg C operation, feeding H2 at 25 deg C represents a RH% lower than 20%. E-TEK has developed fine-gradient MEAs on cloth and paper substrate to suit for this purpose. Moreover, there are applications willing to pay a premium for higher catalyst loading and higher power to use advanced MEAs to accomplish tasks such as telecom back-up and portable applications in remote areas. To this end one cloth and one paper MEA with standard catalyst loading have been developed. One high power cloth MEA was also developed to gain much higher power has also been developed. The performances in dry H2 and 75% air RH% are shown in Figure 32 and those for 50/50 RH% H2/air are shown in Figure 33.

Figure 32: Polarization Curves for 3 MEAs, dry H2

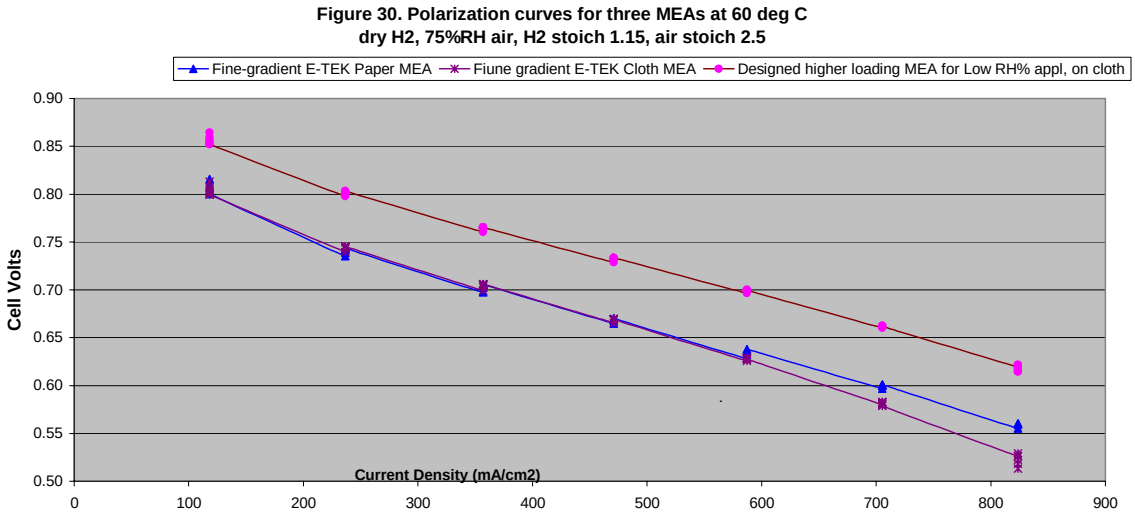

Figure 33 Polarization curves for 3 MEAs, 50% RH anode and cathode

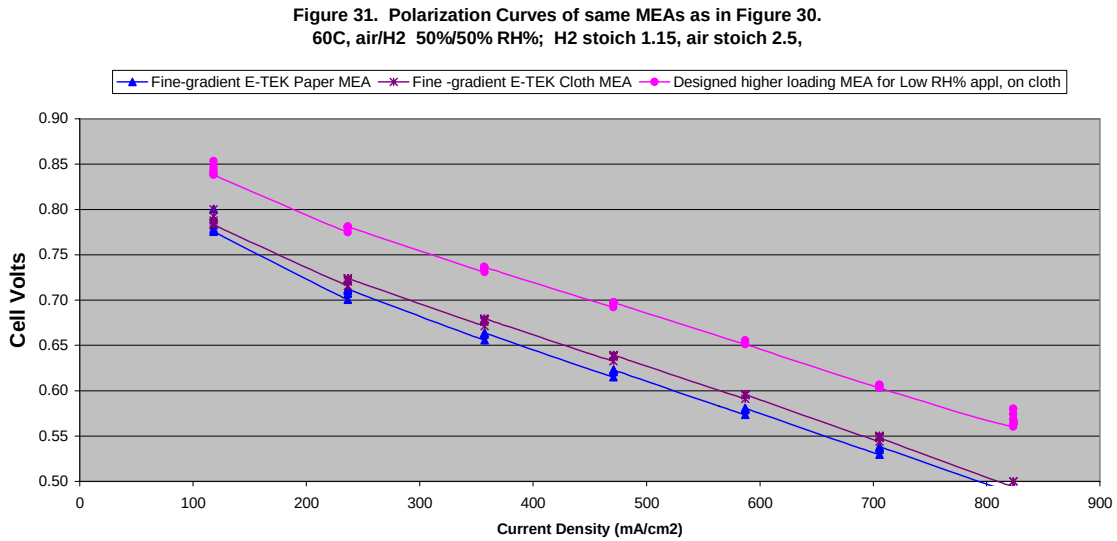

Overview of Stack Testing at Nuvera: Validation of MEA Technology

Before October, 2005, Nuvera used an old design with 225 cm2 active area. After wards, Nuvera adapted a new design with active area of either 250 or 500 cm2. The new design were fully developed in 2nd-3rd quarter of 2005 years for Nuvera commercial stacks and allow for elevated temperature and long term operation. Both stacks architectures utilize the concept of direct water injection to the cathode (CWI) developed and patented by Nuvera (M. Brambilla et al., Fuel Cell With Cooling System

Based On Direct Injection of Liquid Water, US Patent 6835477, issued Dec. 28, 2004)

Referring to Table 4, Stacks 1 through 8 were assembled using Nuvera Phase I cell architecture (225 cm2) with the conventional cooling cell separated from the electrochemical package of the fuel cell by the bipolar plates. Although fuel cells of Phase I architecture demonstrated high performance both on the commercially used by Nuvera MEAs and experimental MEAs by ETEK, the materials of the electrochemical package in these cells were not durable enough to perform long term fuel cell operation required by the market. These cells also were not designed to sustain elevated temperature operation required by the scope of this program and were not suitable for MEAs by DuPont/ETEK.

Based on the program requirements and provided availability of the commercial materials Nuvera decided to utilize its XDS, or Phase II cell architecture, to adjust to the experimental MEAs by ETEK and DuPont. Stacks 9-11 were assembled using XDS cells. XDS cells were developed in the past two years using patented CWI approach and have two alternative active areas: 250 and 500 cm2. Currently, Nuvera utilizes only 500 cm2 cells in the commercial applications and gained significant experience in long term operation of these cells at the conventional PEM cell temperatures. Recently at the Fuel Cell Seminar 2005, Nuvera demonstrated results of 10,000 hour operation of XDS cells in the short stacks with the minimal voltage decay.

There were two very successful stack runs for over 1000 hours - runs 7 and 10. After several attempts to operate ETEK MEAs for durability in Nuvera former Phase I (225 cm2) cells and analyzing results of 1000 hr run (run 7) of ETEK/Nuvera stack in Q2-Q3, 2005, there were some mutual efforts spent on developing protective sub-gaskets attached to ETEK MEAs and adjusting the new package inside Nuvera's 250 cm2 and 500 cm2 cells. These sub-gaskets target reinforcement of MEA sealing area under stack compression and smoothing transition of the compression load from the sealing area to the active area of the fuel cell.

(3) 1200 Hour Run
Run 10 in Table 4 was assembled in last quarter of 2005 and completed in 1st quarter of 2006. The total operation time was about 1200 hours. The result was very good. As shown in Figure 18 (excluding cell 1, the problem associated it was found to be associated with GDE/MEA fabrication) for cell 2-4 in this stack the observed degradation rates were in the range of 1-14 micro-volts /hour. These low degradation rates are in the very low range according to the standards in the present fuel cell industry, representing an outstanding achievement for both E-TEK's GDE/MEA technology and Nuvera's stack technology. The major reason for the success is the implementation of sub-gasket technology which reinforced the interface area between GDE edges and gasket. Run 10 used a four 250 cm2 cell stack. In the MEAs, the cathode has the fine-gradient Pt alloy cathode and the anode is E-TEK's special anode with low loading designed in this DOE program with total precious metal ~0.35 mg/cm2. In portion (1) of this section we have described the low loading anode was easily produced in large quantity on E-TEK's automated coating machine and its performance

was demonstrated in Nuvera 225 cm2 cell stack.. It showed essentially no performance loss compared with the standard anode in Nuvera 225 cm2 cells. A 7-cell stack of MEAs with this anode and standard cathodes also showed exceedingly well reproducibility. Since that time we have been engaged in intensive research on Pt alloy oxygen reduction catalysts, such as PtxCo and PtxCr as well as fine-gradient electrode structure. The technology reached a satisfactory and reproducible stage so the decision was made to make 250-500 cm2 MEAs with low loading anode and fine gradient cathode for stack testing in November, 2005.

Table 4. Summary of Stack Testing at Nuvera for This Program

Stack # in order of testing	**Production Date**	**E-TEK Materials**	**No.of stack cells**	**Total Test Hours**
1	April, 2003	Benchmark(control), new catalysts, improved cloth, preliminary FG structure	20	284
2	Oct. 2003	Control, new catalyst alloy, FG sub-build 1, FG sub-build 2	19	24
3	April, 2004	Control, FG for alloy 1, FG sub-build 3, low loaded anode	21	299
4	July, 2004	Standard MEAs, benchmark (evaluation of sealing methods)	4	10
5	July, 2004	Low loaded anode, stnd. cathode	7	40
6	July, 2004	Low loaded anode, stnd. cathode	7	34
7	Jan, 2005	FG for alloy 2	5	1116
8	Dec, 2004	FG sub-build 4	2	164
9	Oct, 2005	Low loaded anode, FG for alloy 2	4	0
10	Oct 2005	Low loaded anode, FG for alloy 2	4	1324
11	Nov, 2005	FG for alloy 3 (adjust water ejection in GDL)	4	40
12	Feb, 2006	Control, FG for alloy 4, IBAD anode (v. low Pt)	8	650

The four-cell Nuvera 250 cm2 stack equipped with fine-gradient Pt alloy cathode and special low loading anode as described above, showed essentially the same performance as E-TEK's standard MEAs with a total Pt loading in the range of 0.9-1.0 mg/cm2 Pt.

Diagnostic Studies

Besides performance evaluation, other electrochemical measurements were also conducted to monitor the mechanical/physical properties during the course of the durability test run time.

Shorting or Membrane Damage Monitoring – None is Found

Voltammogramms recorded in nitrogen/nitrogen (cathode/anode) was used to test shorting in MEA. Existence of shorts will manifest itself in a (sloping) titling curve. Voltammogramms recorded in hydrogen/nitrogen (anode/cathode) was used to monitor H2 cross-over due to hole

Figure 34 Durability Test of a 250cm2 Nuvera Stack with PtCr fine gradient Cathode and special low loading anode

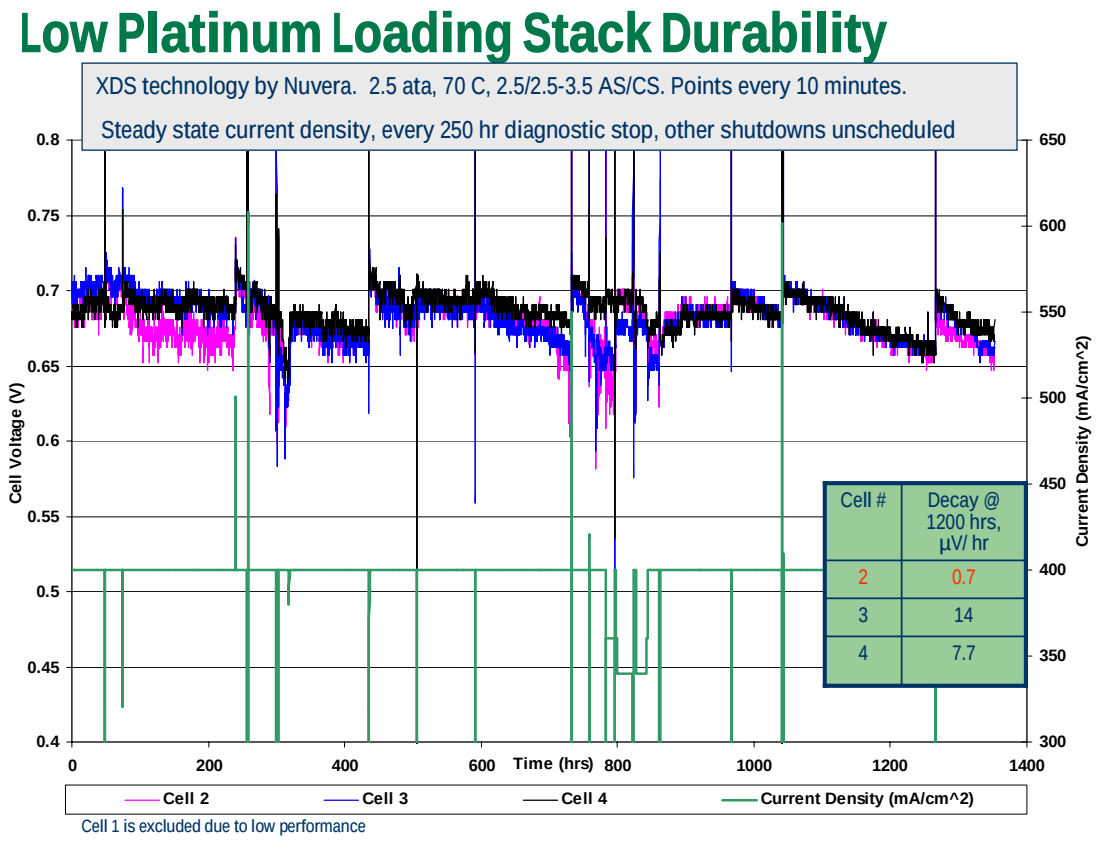

formation. There were no detectable shorts existing in any of the four MEAs as indicated in the measured “residual resistance” at the end of the test via nitrogen/nitrogen voltammetry, the data are summarized in Table 4. These values are in the range of well behaved cells.

Table 5. Summary of cell’s electrical conductance in stack LPT_250 at the end of durability test.

Cell Conductance, S	**cell 1**	**cell 2**	**cell 3**	**cell 4**
1000 hrs since BOL	.017	.043	.033	.083

Electrochemical diagnostics conducted at 250, 500, 750 and 1000 hour intervals concluded that resistive slope remained constant and no hydrogen crossover was detected throughout the entire test time.

(4) Nuvera 650 hour runs of eight-cell 500 cm2 Stack

(i) Outline

Although less successful as the 1200 hour operation of run10, 500 cm2 stack of run 12 of fuel cell stack HYD1-06-4 was the first of this size and the attack included some very important MEAs E-TEK decided to scale-up to this large size. It will be described below. This eight-cell stack was assembled with four different types of MEAs provided by ETEK. After initial conditioning it was decided to remove the last two cells because of damage caused during assembling, which also resulted in low performance. Afterwards the stack was reassembled into six-cell stack. Finally, the stack was tested for durability at the conditions specified by DOE for the program, steady state current and scheduled shut-downs for in-situ electrochemical diagnostics. After reassembly only four cells in the stack gained expected performance and showed progress in durability. Starting 400 hours of testing the cell voltage decay increased which was attributed the elevated hydrogen crossover. The test was stopped at 650 hours due to the high crossover in cell 2.

(ii) MEAs Descriptions
The characteristics of MEAs in this stack are summarized in Table 6.

Table 6. Summary of GDE characteristics in Nuvera 500 cm2 fuel cell stack HYD1-06-4

Cell Position	MEA ID	Description	Loading/Details	Comments
1	#1	standard	total C/A 0.9-1.0 mg/cm2 Pt	
2	#3	fine-gradient	total C/A 0.9-1.0 mg/cm2 Pt	could be improperly assembled
3	#5	PtxCo alloy cathode/low anode loading	cathode 0.29/anode 0.04 mg/cm2	
4	#7	IBAD anode/low cathode loading	IBAD 0.10/cathode 0.16 mg/cm2	
5	#2	standard	total C/A 0.9-1.0 mg/cm2 Pt	BOL inferior performance due to current colletor/gasket mismatch
6	#4	fine gradient	total C/A 0.9-1.0 mg/cm2 Pt	BOL inferior performance due to current colletor/gasket mismatch
7	#6	PtxCo alloy cathode/low anode loading	cathode 0.30/anode 0.04 mg/cm2	damaged in assembling
8	#8	IBAD anode/low cathode loading	IBAD 0.19/cathode 0.16 mg/cm2	damaged in assembling

There were two of each of the following: standard MEAs, fine-gradient MEAs (gradual change of porosity and hydrophobicity along membrane-GDL), two MEAs with PtxCo (0.29-0.3 mg/cm2) cathode and low loading anode (0.04 mg/cm2 Pt), and two MEAs with IBAD (ion beam assisted deposition) anode (0.1-0.19 mg/cm2) and low loading cathode.

(3) Assembling and BOL Performance

500 cm2 stack was a new development at Nuvera. Assembling of eight-cell stack was a exploratory work. Every effort was made to assemble the stack. However, it takes time and accumulated experience for success. The resulting stack showed an apparent unevenness in compression, resulting in poorer performance for cells 5-8. The BOL polarization curves are shown in Figure 35. For example, the replicates of MEA at position 3 and 7 in Figure 35 performed essentially the same in E-TEK lab fuel cells, but they performed differently in 500 cm2 cell stack (Figure 35). The same contrast can be made for cells 2 and 6, for cells 4 and 8, and for cells 1 and 5. At 0.4 A/cm2, a penalty due to cell position is in the range of 20 mv (cell 1 and 5) -60 mv (cell 4 and 8). Cells 5-8 were not only suffering from initial performance but also from mechanical damage. A H2/N2 hydrogen cross-over tests were conducted on all MEAs in the stack, the results are shown in Figure 20. In Figure 36, the voltammogramms were clearly separated into two groups- a group of 1-4 and another group of 5-8 cells. The later showed higher hydrogen permeation rates, indicating more cross-over. Another feature of the voltammogramms of cells 5-8 is the relatively smaller hydrogen desorption peak. This can be caused by insufficient compression (higher IR) and/or mis-alignment of MEAs with respect to cell stack. Even for cells 1-8, the performances were about 60-70 mv worse than what were observed in E-TEK lab cells. The origin of the difference has been described in 4th QTR 2005 report for this DOE program: it was a combined effects of the following three factors: (1) <100% RH, sometimes as low as 45-50% cathode RH%, about 30-40 mv; (2) insufficient compression and consequent high resistance- about 20 mv; (3) dead-end H2 supply, 10-20 mv. After these corrections (at least 60 mv) the performance in Figure 9 is rather good.

Figure 35. Polarization Curves for Individual MEAs Summarized in Table1. Condition Described on the Chart. AS and CS are anode stoich and cathode stoich.

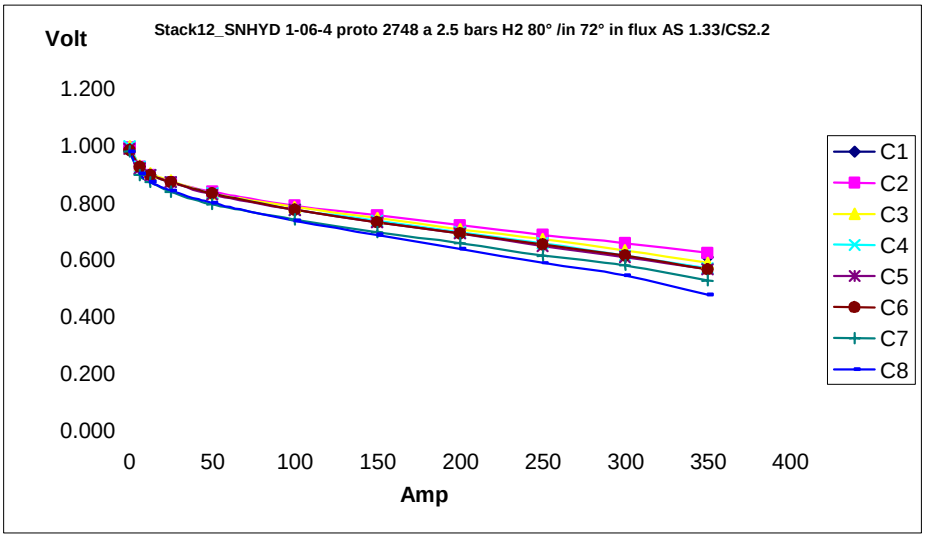

Within the group of cells 1-4, At 0.4 A/cm2, 85 C, the fine gradient MEAs (cell 2) showed about 10 mv advantage over the standard MEAs, cell1 (both had 0.9-1.0 mg/cm2 Pt). The fg PtxCo alloy MEA with much lower loading showed about the same performance as the standard. The IBAD MEA showed 10-15 mv worse performance

than the standard. It's very encouraging to observe an acceptable performance for MEAs containing GDEs made of fg-Pt alloy and IBAD technology at 500 cm2 scale.

Figure 36. Linear sweep (nitrogen/hydrogen) voltammogramms recorded for 500cm2 Nuvera Stack HYD1-06-4

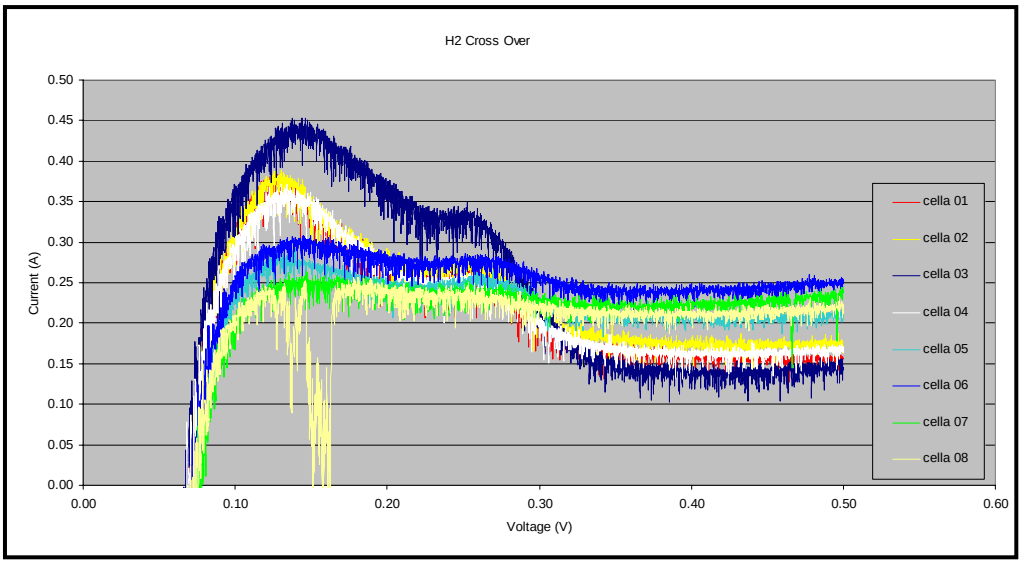

(4) Durability Test of 500 cm2 Nuvera Cell Stack HYD1-06-4

After initial break-in and H2-cross over testing, it was decided to take cells 7 and 8 out of the stack and reassemble a 6-cell stack. This stack was tested for durability at the conditions specified by DOE for the program, steady state current and scheduled shut-downs for in-situ electrochemical diagnostics. After reassembly only four cells in the stack gained expected performance and showed good progress in durability. Starting 400 hours of testing the cell voltage decay increased which was attributed the elevated hydrogen crossover. The test was stopped at 650 hours due to the high crossover in cell 2. It appeared that reassembling caused further damage of MEAs, so the originally well performing cell 1 and 2 developed mechanical problems that eventually caused failure of cell 2. The voltage at 0.1 A/cm2 and 0.4 A/cm2 for cells 1-6 for three selected time marks were shown in Figure 37a and 37b. The entire volts vs. time curves are shown in Figure 38. Cells 1 and 5 are both standard MEAs so the poor durability of cell 1 was most likely because of damage during re-assembling. Cells 3-5 showed very similar durability. Cell 6 also showed similar performances to cells 3-5 at 0.1 A/cm2, but its durability was worse at 0.4 A/cm2, probably due to water management issue at long-term.

Figure 37. Cell Voltages of Individual Cells of 500cm2 Nuvera Stack HYD1-06-4 at 150, 300, and 600 Hours of Testing

(a) 0.1 A/cm2

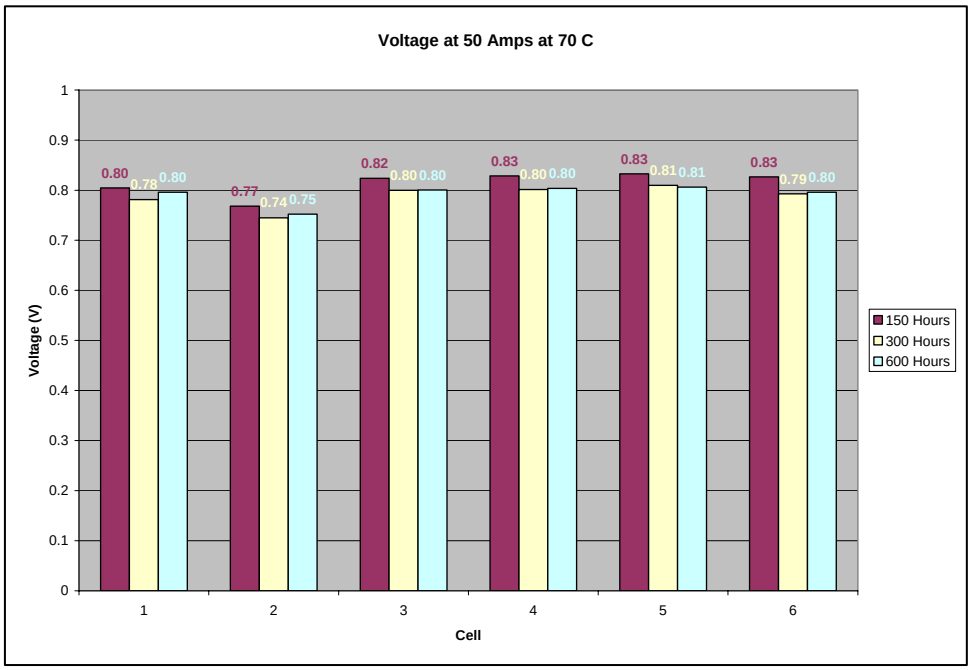

(b) 0.4 A/cm2

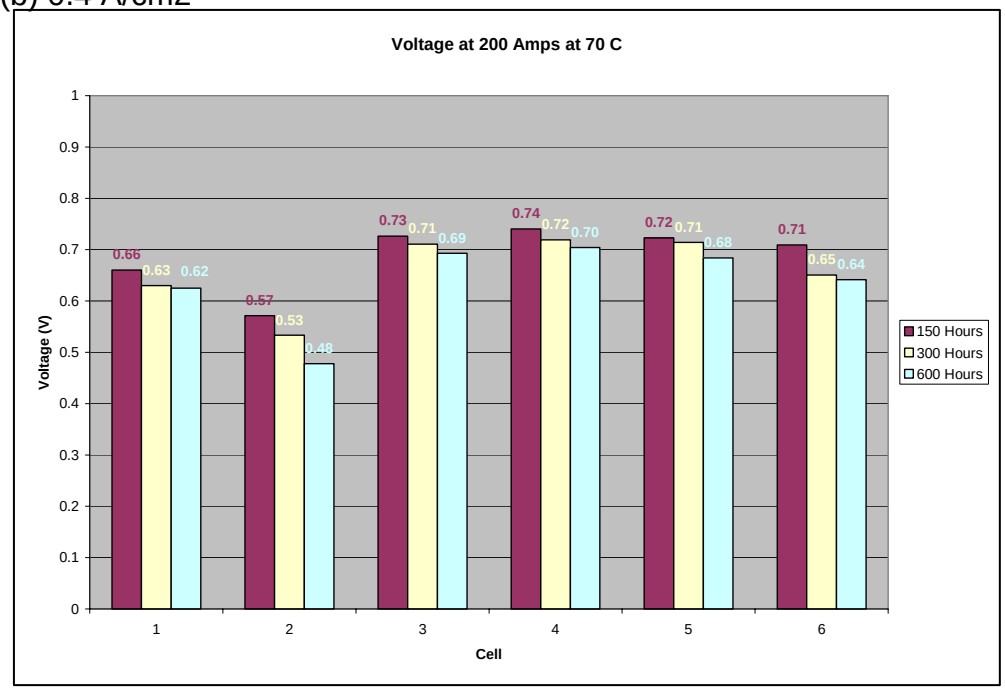

Figure 38. Continuous Cell Volts vs. Time Plots for 500cm2 Nuvera Stack HYD1-06-4

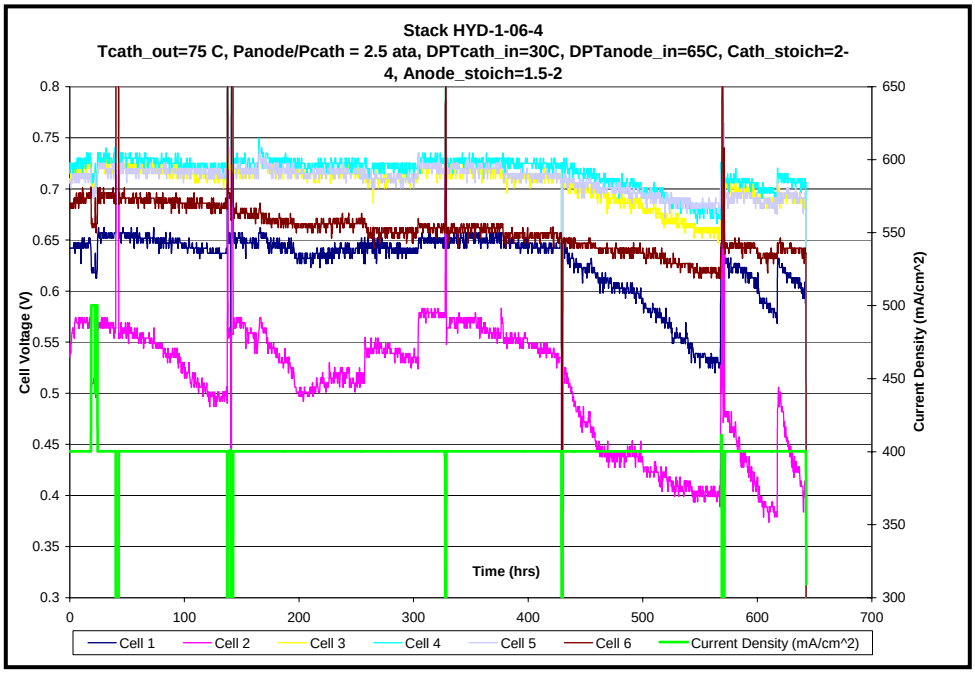

(5) Conclusions on 500cm2 Nuvera Stack HYD1-06-4 Testing

500cm2 Nuvera Stack HYD1-06-4 has been successfully tested for 650 hours at conditions close to DOE protocol. The lesson learned in assembling of stacks with MEAs of large active areas in this program will be very useful in the future for other or even commercial applications. For 500 cm2 MEA stacks four cell assembling might be a good choice. Improvement in current collector and gasket design might be desired.

The test results indicate that MEA containing fine gradient PtxCo alloy cathode at about ½ of precious loading and a very low anode loading (0.04 mg/cm2) can perform as well as an MEA with standard cathode/anode and with about the same durability. Current IBAD anode showed as good durability as E-TEK standard anode although its inferior gas permeation property precludes its usefulness as a cathode. E-TEK is working on improving the IBAD structure for higher porosity.

Stack Testing of MEA with Unsupported Catalysts

In DOE report last quarter we described the superior durability of Pt black GDEs under frequent shutdown or stop/start condition. 50 cm2 Pt black MEAs were tested under a very strenuous condition by operating at 0.05 A/cm^2 65 deg C for typically 8 hours then followed by shutdown and started up again on the next day. The Pt black MEAs were able to keep a stable performance under the above condition for 2000-2500 hours without much change in performance at 0.05 A/cm2 (less than 10 mv) except an initial drop. In this quarter several short stacks of ~300 cm2 Pt black MEA were tested under

the same strenuous condition and same superior durability for > 4000 hours was observed. Post analysis indicated that the Pt black cathode catalyst has very limited rate of particle size growth after 2000 hour start/stop operations, its size increased from 55-65 A to about 70-75 A.

Future improvement will be reducing the Pt loadings of cathode and anodes. Initial experiments with 300 cm2 MEAs indicated anode coating can be reduced to < 1 mg/cm2 level.

Accomplishments

Overview

Since this program's overall goal was to develop improved fuel cell components, the impact of the work that focused on catalysts and electrode/gdl structures led to numerous products, patents, and publications. There were several affiliated opportunities outside of PEMFC that also led to the application of the basic architecture "fine gradient" ELAT® to new platforms for direct methanol fuel cells. Similarly, the catalyst work also led to improved catalysts for DMFC

Products

Several new products were developed as a consequence of this work. The greatest contribution is the HP Catalyst line (High Performance). The extraordinary small crystallite size and lower cost of converting from platinum metal to platinum catalysts has allowed our customers to use lower levels of platinum in their assemblies. A spin off of this work (due, again, to the small crystallite size of the basic process) was the creation of highly active alloys of platinum-ruthenium, used both for reformed hydrogen systems and direct methanol systems. Finally, based on fine gradient concepts, we were able to release a new competitive MEA for direct methanol fuel cells.

Patents (applied, pending, or issued)

(Please also refer to appendix/DuPont high temperature membrane report)

1. Structures for gas diffusion materials and methods for their fabrication
2. Carbon supported metal alloy catalysts and method for the manufacturing thereof
3. Platinum catalysts from in-situ formed platinum dioxide
4. Gas Diffusion Electrodes, Membrane-Electrode Assemblies and Method For The Production Thereof
5. Platinum Alloy Carbon-Supported Catalysts
6. Gas Diffusion Electrodes, Membrane-Electrode Assemblies and Method For The Production Thereof
7. Methodology to prepare room temperature selected magnetic transition metal and transition metal alloys.

Publications

1. 'Oxygen Reduction Kinetics in Low and Medium Temperature Acid Environment: Correlation of Water Activation and Surface Properties in Supported Pt and Pt Alloy Electrocatalysts' V. Srininvasamurthi, R. C. Urian and S. Mukerjee, submitted to *J. Phys. Chem.,* (February, 2004) [Accepted]

2. ‘Oxygen Reduction and Transport Characteristics at a Platinum and alternative Proton Conducting Membrane Interface’ L. Zhang, C. Ma and S. Mukerjee, *J. Electroanalytical Chemistry* (In Press)
3. ‘In situ determination of O(H) adsorption sites on Pt based alloy electrodes using X-ray Absorption Spectroscopy’ M. Teliska, D. Ramaker, V. Srinivasamurthi and S. Mukerjee, submitted to *J. Phys. Chem.,* (submitted March 2004).
4. ‘Effect of Water Activation on the Activation Energy of Oxygen Reduction in a Polymer Electrolyte Interface’, J. Jerome, A. Anderson, V. Srinivasamurthi and S. Mukerjee, Manuscript under preparation for submission to *J. Phys. Chem.*
5. ‘Oxygen Reduction and Structure Related Parameters for Supported Catalysts’, S. Mukerjee and S, Srinivasan, *Handbook of Fuel Cells: Fundamentals, Technology and Applications, Vol. 2: Electrocatalysis*, Edited by W. Vielstich, H. A. Gasteiger and A. Lamm, John Wiley and Sons (2003).
6. ‘In situ X-Ray Absorption Spectroscopy of Carbon Supported Pt and Pt Alloy Electrocatalysts: Correlation of Electrocatalytic Activity with Particle Size and Alloying’, S. Mukerjee, *Advanced Nanoparticles for Fuel Cells and Electrocatalysis*, Edited by A. Weickowski, E. Savinova, and C. G. Vayenas, Marcel Dekker, (2003).
7. “Characterization of Transport Properties In Gas Diffusion Layers for PEMFCs”, M. Bluemle, V. Gurau, J. A. Mann, T. A. Zawodzinski Jr., E. S. De Castro, Y. M. Tsou:206th Meeting of Electrochem. Soc., Honolulu, Ha, October 2-8, 2004
8. “Permeability and Wettability Measurements for Gas Diffusion Layers for PEM Fuel Cells”, M. Bluemle, V. Gurau, J. A. Mann, T. A. Zawodzinski Jr., E. S. De Castro, Y. M. Tsou: 2004 Fuel Cell Seminar. San Antonio, TX, November 1-5, 2004
9. 'High Performance Electrode with very Low Pt Loading Prepared by Dual Ion Beam Assisted Deposition in PEM Fuel Cells' M. S. Saha, S. Mukerjee, A. F. Gulla and R. J. Allen' Extended Abstracts for the Meeting of the Electrochemical Society to be held in Quebec, Canada, May 2005.
10. 'Dual Ion Beam Assisted Deposition as a Method to Obtain Low Loading-High Performance Electrodes for Proton Exchange Membrane Fuel Cells', A. F. Gulla, M. S. Saha, R. J. Allen and S. Mukerjee, *Electrochemical and Solid State Letters,* (Submitted)
11. 'Oxygen Reduction and Transport Characteristics at a Platinum and Alternative Proton Conducting Membrane Interface' L. Zhang, C. Ma and S. Mukerjee, *J. Electroanalytical Chemistry* 58, 273 (2004).
12. Hua Deng, Qingzhi Guo; Maria Cayetano; Yu-Min Tsou; Emory Sayre De Castro, "An Investigation of Ionic Conductivity of the PEMFC by AC Impedance Spectroscopy", Meeting of Electrochem. Soc., Honolulu, Ha, October 2-8, 2004
13. “High Performance Oxygen Reduction Catalyst For PEM and DMFC Fuel Cells” Yu-Min Tsou, Lixin Cao, Emory De Castro Meeting of Electrochem. Soc., San Antonio, Tx May, 2004
14. “Approaches for low cost components and MEAs for PEFCs: current and future directions”, Fuel Cell Seminar, San Antonio, Emory S. De Castro, Yu-Min Tsou, Lixin Cao and Chien Hou Nov, 2004
15. , “New Nano-Catalysts and Reduction of Component Costs for Portable Fuel Cells”, Emory S. De Castro Small Fuel Cells, Arlington, Va., April 2004

16. "Characterization of Transport Properties In Gas Diffusion Layers for PEMFCs 1. Wettability (Internal Contact angle to water and surface energy of GDL fibers)", V. Gurau M. Bluemle,Jr., E. S. De Castro, Y. M. Tsou J. A. Mann T. A. Zawodzinski :Accepted in Journal of Power Sources, 2006
17. "High performance polymer electrolyte fuel cells with ultra-low Pt loading electrodes prepared by dual ion-beam assisted deposition." - M. Saha, A. Gullá, R. Allen, S. Mukerjee; *Electrochimica Acta*, 2006
18. "Towards Improving the Performance of PEM Fuel Cell by Using Mix Metals Electrodes Prepared by Dual IBAD." - A. Gullá, M. Saha, R. Allen, S. Mukerjee; *Journal of the Electrochemical Society*, 2006
19. "Dual Ion Beam Assisted Deposition as a Method to Obtain Low Loading-High Performance Electrodes for PEMFC's." – A. Gullá, M. Saha, R. Allen, S. Mukerjee; *Electrochemical and Solid-State Letters*, 2005
20. "Enhancing the Performance of Low Pt Loading Electrodes Prepared by Dual Ion Beam Assisted Deposition in PEM Fuel Cells." - A. Gullá, R. Allen, M. Saha, S. Mukerjee; presented at the 208th Symposium of the Electrochemical Society in Los Angeles, CA 2005
21. "Peroxide Yield on New Materials for Oxygen Reduction in Acid Media" - A. Gullá, R. Allen, C. Urgeghe, Y. Garsany, S. Mukerjee; presented at the 207th Symposium of the Electrochemical Society in Quebec City, Canada 2005
22. "High Performance of Electrode with Very Low Pt Loading Prepared by Dual Ion-Beam Assisted Deposition in PEM Fuel Cells" - A. Gullá, R. Allen, M. Saha, S. Mukerjee; presented at the 207th Symposium of the Electrochemical Society in Quebec City, Canada 2005
23. "New ELAT Interface Designs through Manufacturing Practices", Emory S. De Castro, Yu-Min Tsou, Lixin Cao and Chien Hou Fuel Cell Seminar, Palm Springs, Nov, 2005
24. "Factors Affecting Activities of Nano-sized Fuel Cell Catalysts and Diagnosis Methods", Y. Tsou, L. Cao, E. De Castro,208th ECS Meeting LA Oct , 2005, abstract# 907
25. "Impact of Machine Coating GDE/MEA on Commercialization of Fuel Cells or Electrolyzers, Y. Tsou, E. De Castro, Chien Hou, Zhiyong Zhu 208th ECS Meeting LA Oct , 2005, abstract#1025

Conclusions

We conclude that for low temperature MEAs, significant reduction in precious metal loading can be achieved through both the fine gradient ELAT and Ion Beam Deposition technology. Furthermore, the fine gradient approach enables both facilitated water ejection from the cathode, and improved structures for operation under dry conditions.

DuPont has identified several membrane materials that satisfy the three key criterion: thermal stability, conductivity at 120 deg C at low RH, and mechanical stability. DuPont will continue the development of one of these materials on their own with the objective of releasing a new product.

The role of Nuvera in validating our efforts to scale up low temperature MEAs with low precious metal content and high temperature MEAs in their stacks was deemed critical to the success of the program. However, in the course of the program, all groups underestimated the efforts it would take to incorporate high temperature MEAs in a stack, especially with regards to gaskets and sealing.

Recommendations

The use of Ion Beam Assisted deposition for creation of anode gas diffusion electrodes is close to being commercialized for use in standard MEAs due to the uniformity of low precious metal coatings, and absence of ionomer. Follow up R&D is needed for cathode constructions using IBAD.

Additional work on transitioning the carbon supported alloys developed in this program to either graphitic supports or carbon free supports is warranted to meet the durability goals of DOE.

See the DuPont appendix for recommendations on high temperature membranes.

Appendices

DuPont Subcontractor Final Report: High Temperature Membranes/MEAs

(SEE NEXT PAGE)

Final Technical Report

Project Title: **Integrated Manufacturing for Advanced Membrane Electrode Assemblies. Topics 1A1, 1A2, & 1A3.**

Note: Only the work within DuPont's sub-contract on Topic 1A2 High Temperature Polymeric Membranes is included in this report.

DOE Award Number: **DE-FC04-02AL67606**

Project Period: **Oct 2001 – Nov 2005**

Name, phone number and email address of Principal Investigator(s) – Author(s):

Dr. Mark G. Roelofs
302-695-2503
mark.g.roelofs@usa.dupont.com

Name and address of recipient organization

Sub-contractor:
E. I. du Pont de Nemours and Company
1007 Market Street
Wilmington, DE 19898

Names of other project team member organizations

Sub-sub-contractor:
Case Western Reserve University
Professor Morton H. Litt

Acknowledgment: This report is based upon work supported by the U.S. Department of Energy under Award No.DE-FC04-02AL67606.

Proprietary Data Notice:

This report contains Case Western Reserve University patentable material in Section 14.7 which starts on page 48.

This report does not contain DuPont proprietary data developed during the course of the program. DuPont proprietary data includes synthetic routes and chemical structural information for electrolytes. If the reader needs further clarification involving proprietary DuPont data, please contact Mark Roelofs.

Table of Contents

List of Figures

1. Executive Summary

During the course of this project, several novel chemistries for high temperature polymer electrolyte membranes for fuel cells were explored. The scope of work encompassed model compounds for new conductivity mechanisms, synthesis of 36 new polymer electrolytes, ionic conductivity measurements on 1100 samples, and when applicable membrane fabrication and characterization. Three polymer electrolytes were chosen for further invention and development in the latter half: V, AO-BA types, and AE-BP types. Accomplishments include the world record (we believe) for polymer electrolyte conductivity at low relative humidity (RH). While more progress will be needed to meet all functional requirements of a FC membrane for commercial applications, this research made substantial progress in inventing new, and narrowing the selection of, polymeric materials. DuPont is planning to continue further development of two of the classes, AO and AE, with the goal of eventual commercialization of one of them.

2. Introduction

There has been much discussion and controversy over the potential benefits and problems of a hydrogen economy. Some potential routes for hydrogen generation make it attractive as a domestically-produced, renewable energy carrier resulting in net zero CO_2 emissions, and these could advance societal desires for national security, sustainability, reduced global warming, and pollution reduction. The use of hydrogen in polymer electrolyte membrane (PEM) fuel cells (FC) has encountered barriers, documented in DOE's hydrogen multi-year plan[1]. These include low durability, high cost, and the need for increased energy efficiency.

The work within DuPont's subcontract centered on developing a new polymer electrolyte membrane for hydrogen/air fuel cells. The primary emphasis was on membranes for transportation applications with secondary emphasis on stationary applications. Commercialized benchmark membranes for PEM's use Per-Fluorinated polymers with pendant Sulfonic Acid groups (PFSA) to provide proton conductivity, with trade names Aciplex®, Flemion®, and Nafion®. Problems with existing PFSA membranes that need to be addressed with advanced membranes are:

1) **Durability** – PFSA membranes are subject to degradation in the fuel cell. Chemical degradation is observed through membrane thinning and fluoride ion release, and is believed to be caused by hydrogen and oxygen permeation through the membrane, formation of hydrogen peroxide, and its decomposition to generate hydroxyl or hydroperoxy radicals, which attack unstable groups of the membrane[2, 3]. There are also mechanical issues such as creep. Sufficient durability in automotive drive cycles and freeze-thaw cycles[4] has not been demonstrated.
2) **Thermal management** – Current PFSA's typically run at 80 – 90 °C maximum temperature. Two factors then require the radiators of PEMFC to be larger than those of internal combustion engines (ICE): First, the PEMFC has no equivalent of the hot exhaust of the ICE, so a larger fraction of the PEMFC waste heat must be dissipated through its radiator, and second, the low operating temperature of PEMFC gives a small difference between coolant temperature and ambient air temperature, which requires a further increase in heat transfer area[5]. To maintain the radiator at a reasonable size, there is a need to allow higher operating temperatures, e.g. peak 120 °C.
3) **Water and air management** – Current PFSA's are operated with a water vapor pressure near to saturation (100% RH), where they absorb 10-14 water molecules per sulfonic acid[6-8]. At lower relative humidities, they lose water and are not sufficiently conductive[9, 10]. However 100% RH at 120 °C requires 200 kPa of steam pressure, which must be added to the air pressure, and compressing the cathode air to high pressure requires too much parasitic energy loss. In addition, the hydrogen and air streams of traditional PFSA membranes may require humidification, with recovery of water in bulky/heavy condensers, further reducing system power density and specific power. Thus there is a need to completely eliminate or simplify humidification of the inlet gas streams. Both factors favor membranes that can conduct protons at low water vapor pressure (low RH).
4) **Hydrogen Purification/Carbon Monoxide Cleanup** – Hydrogen from reforming hydrocarbons is contaminated with various levels of carbon monoxide, it is difficult to remove (especially in small reformers), and the CO binds to anode platinum and lowers fuel cell voltage. The oxidation or desorption of the CO from platinum is faster at higher temperatures[11-13]. Thus raising the operating temperature to 120 °C brings modest tolerance to tens of ppm of CO impurity. With the decision to stop on-board reforming, this is a less important point for transportation applications. It is more of an issue for stationary applications with local reforming; however, the large CO tolerance desired comes only with much higher operating temperatures of 150 – 200 °C.

3. Background

Polymer electrolyte membranes for higher temperature operation have been well reviewed[14-17].

3.1. Objectives

The original goals that we and DOE set for us at the Oct-2001 kick-off meeting were:

- HT defined as operation above 100 °C.
- Conductivity of > ~50 mS/cm with water vapor pressure of < 7 psi
  RH < 25% at 120°C; RH < 11% at 150°C
  (*vs* Nafion®, which requires > 70% RH.)
- No leachable components – lifetime.
- Electrolyte/catalyst interaction must be favorable:
  – No deleterious adsorption on Pt
  – High oxygen permeability
  – Allows expected increase in cathode oxygen reduction kinetics to give > 800 mV cathode potential @ 1 A/cm2
- H_2 (or MeOH if DMFC) permeation < than Nafion®
- Ability to form 1 mil thick membrane
- Hydrolytic, oxidative, mechanical stability in FC, T > 120°C
- Cost ≤ Nafion®

DOE's technical targets for membranes for transportation applications are shown in Table 1 below:

Table 1. Membrane Targets from 2005 multi-year plan[1].

Table 3.4.12. Technical Targets: Membranes for Transportation Applications					
Characteristic	Units	2004 Status	2005	2010	2015
Membrane Conductivity at Operating Temperature Room temperature –20°C	 S/cm S/cm S/cm	 0.10 0.07 0.01	 0.10 0.07 0.01	 0.10 0.07 0.01	 0.10 0.07 0.01
Operating Temperature	°C	≤80	≤120	≤120	≤120
Inlet water vapor partial pressure	kPa (absolute)	50	25	1.5	1.5
Oxygen cross–over[a]	mA/cm²	5	5	2	2
Hydrogen cross–over[a]	mA/cm²	5	5	2	2
Cost	$/m²	65[b]	200	40	40
Durability with cycling At operating temp of ≤80°C At operating temp of >80°C	 hours hours	 ~1000[c] not available[e]	 2000	 5000[d] 2000	 5000[d] 5000[d]
Survivability	°C	–20	–30	–40	–40
Thermal cyclability in presence of condensed water		Yes	Yes	Yes	Yes

[a] Tested in MEA at 1 atm O_2 or H_2 at nominal stack operating temperature.
[b] Based on 2004 TIAX Study and will be periodically updated.
[c] Durability is being evaluated. Steady-state durability is 9,000 hours.
[d] Includes typical driving cycles.
[e] High-temperature membranes are still in a development stage and durability data are not available.

Differences from our initial goals in 2001 include operation at near or below 120 °C, and introduction of low temperature performance requirements. The need for membrane conductivity at lower RH (a focus of this program) arises implicitly from Table 1 in requirements for lower inlet water vapor partial pressures. Of course, as the FC consumes hydrogen and creates water, the relationship between inlet P_{water} and RH at the membrane is somewhat complicated, depending on temperature, stoichiometry, total pressure, hardware configuration, etc. – still the overall requirement for lower water vapor pressure is clear.

3.2. Approach

Work on higher temperature membranes was begun with an exploration of a wide variety of organic functional groups in small molecule electrolytes for their ability to conduct protons at low RH. The model electrolytes were examined for their ability to

conduct protons at low RH, by dint of either “holding on” to more water than Nafion® can, or by requiring less water in the electrolyte for the same level of conductivity. We also sought alternative conduction mechanisms, e.g. employing Brønstead bases as an alternative to water or electrolytes that conduct protons by the Grotthus mechanism. The scope at this point included some seven different types of acid groups with aromatic or fluorinated substrates.

After identifying promising small-molecule electrolytes, the next step was to prepare polymeric electrolytes, which “tie-down” the molecules, a necessity to reach the goal of no leachable components. At this point, the thermal stability of the new polymers was evaluated using a thermo-gravimetric method. The next steps involved learning to fabricate membranes from the new polymer electrolytes. Cross-linking and/or composite membrane approaches were chosen to improve their mechanical properties, and control water swelling and hydrogen crossover. Finally, MEA’s using the most promising candidate electrolyte were fabricated and tested in single cells. In parallel with these efforts on new electrolytes were smaller ones to benchmark the fuel cell performance of Nafion® and Nafion® inorganic composites at 120 °C.

3.3. Case Western – Uncollapsible Domains

Case Western Reserve University, under a sub-sub-contract from DuPont, worked to create polymer electrolytes having additional fixed internal free volume within hydrophilic domains bearing sulfonic acids. This program was carried out by Professor Morton Litt and graduate student Casey Check.

Motivation Previous work at Case centered on rigid-rod liquid crystalline polymers with sulfonic acid groups for use as proton exchange membranes (PEMs) for fuel cells. Initial studies conducted on polyimide sulfonic acid materials proved to be very promising with respect to both proton conductivity and water retention at lower relative humidities and temperatures[18]. Applying the molecular design criteria depicted in Figure 1, a series of materials were synthesized and tested.

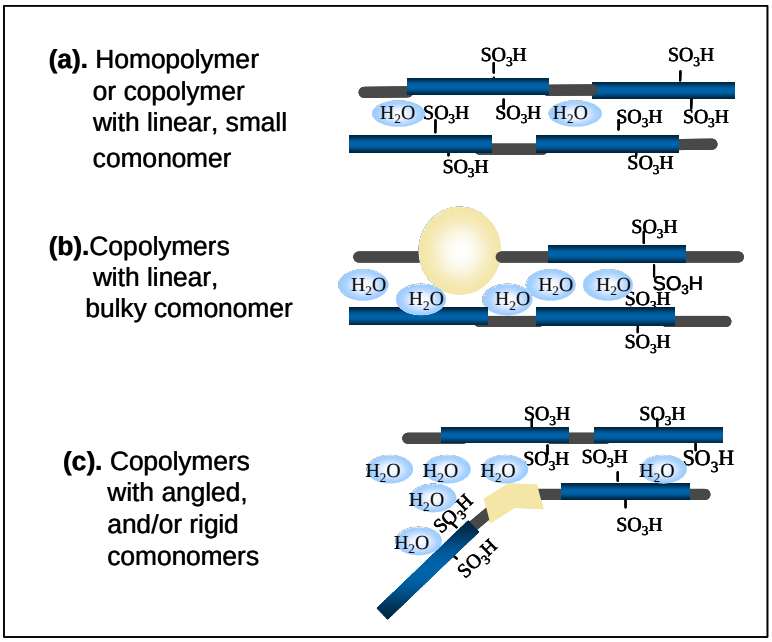

Figure 1. Molecular design approach of polyimide copolymers

Addition of a small percentage of bulky or angled comonomer improved proton conductivity and water retention characteristics even further. These materials were found to have properties that were significantly better than PFSA membranes. The major disadvantage of the sulfonated polyimide polymers is their tendency to slowly hydrolyze in acidic environments.

Using the knowledge gained from the study of rigid-rod polyimides, the emphasis of the new work focused on the design of materials containing hydrolytically, chemically and thermally stable rigid-rod backbones. The next generation of rigid-rod polyelectrolytes was developed based on poly(p-phenylene sulfonic acid)[19]. Polyphenylene materials do not contain any hydrolytically susceptible bonds on the backbone, and are chemically inert and thermally stable.

Using a design approach similar to that developed for the polyimides, a series of copolymers were synthesized based on a polyphenylene sulfonic acid homopolymer. Emphasis was placed on creating copolymers containing bulky or crosslinkable groups that could separate and/or fix chains to prevent volume loss on the molecular level. It was found that these materials had superior conductivity between 15-100% relative humidity and temperatures ranging from -20°C to 120°C.

There are two important factors that affect water retention in polyelectrolytes. The first is heat of solvation of the hydronium ion and the second is decrease in volume as water is removed. Heat of solvation is a fixed property that depends on the specific acid and on the number of water molecules per acid group. Volume loss can be

controlled by design of structures that are rigidly fixed and resistant to contraction as water content decreases. If there is a molecular-scale barrier to volume loss, water is held very strongly. Silica gel and molecular sieves are two materials that are known to hold water very strongly due to incompressible nanoscale pores. Combining knowledge of the structure of these inorganic desiccants with Case Western technology for the synthesis of rigid polyphenylene polymers, we designed an approach to the next generation of polyelectrolytes for PEMs and developed the synthesis of the electrolytes.

4. Results and Discussion

4.1. Experimental Methods

4.1.1. Liquid conductivity

Prior to monomer and then polymer synthesis, different electrolyte types were often evaluated for their ability to conduct at elevated temperatures. Small-molecule model compounds were purchased or synthesized and their conductivity measured in liquid form. As no commercially available cells could be found that would allow measurement of small volumes of highly acidic liquids at elevated temperatures, a cell was constructed as follows: Coil electrodes were formed by wrapping 0.38 mm dia Pt wire five times around a 5.14 mm dia machinable ceramic rod (Corning Macor) and insulating the remainder of the wire leads with heat-shrink PTFE tubing. Two electrodes were located 25 mm apart near the end of the rod, and held in place by threading the wires through small holes drilled in the rod. The liquid and then the rod with electrodes were inserted into a 9 mm OD X 6.8 mm ID X 178 mm glass tube. The tube was then placed into a GC oven for heating in the range of 25 °C to 225 °C. The real part of the impedance at 10 kHz was measured using a potentiostat/frequency response analyzer (Gamry Instruments PC4/750™ with EIS software). Phase angles were typically less than 2 degrees, indicating that the measured real part of the impedance was unaffected by capacitive contributions of electrode interfaces. The cell constant was determined using a 0.103 S/cm KCl standard and was typically in the range of 12 cm^{-1}, and the cell required only 800 μl of liquid.

It would be desirable to equilibrate the liquid with a controlled-RH atmosphere to assess the effects of temperature and RH independently. Though implemented for membranes (see section 4.1.4), RH was not explicitly controlled in this liquid cell. Yet, the effect of RH could still be crudely determined. A common procedure was to add an “excess” of water to the electrolyte, and then heat and cool in steps, making

measurements at 25, 50, 75, 100, 125, 150, 125, 100, 75, 50, and 25 °C. As the sample was heated in the open tube and the vapor pressure of water exceeded 1 atm, this "excess" water would volatilize out of the tube. The saturated vapor pressure of water at 125 °C is 2.3 atm, so if the vapor in the tube became essentially steam at 1 atm, the liquid would be equilibrating with water vapor of close to 1/2.3 = ~40% RH. Likewise, on heating the RH is approximately 100% at 100°C, ~40% at 125 °C, and ~20% at 150 °C. As the volume of the water vapor is much larger than that of the water in the liquid electrolyte, much of the vaporized water was lost permanently from the tube. On cool down from 150 °C, one measures the conductivity of the electrolyte that was exposed previously to ~20% RH at 150 °C. So this test roughly measured the ability of the electrolyte to "hold" onto water at low RH. Of course, if the amount of water was not excess, and little was lost at 150 °C, then this was indicated by a heating and cooling curve with similar conductivities.

4.1.2. Membrane pre-treatment

Membranes were usually pre-treated prior to conductivity measurements by acidifying at 80 °C for 30 min in 14% nitric acid, followed by 3X boiling in water for 15 min ea, with a change to fresh water (Barnstead Nanopure Filter System) after the 1st and 2nd 15-min periods. The choice of three 15 minute boils was decided after measuring the pH of the rinse water for a 38 cm^2 N117 membrane on successive boils in 75 mL of water, those pH's being 2.3, 4.3, 4.5, 4.6, 4.6, 4.6 – little additional acid was extracted after the 3rd rinse, and most membranes in this study were thinner than N117. In cases where we knew the membrane was already acidified, only one boiling step would be performed.

4.1.3. Conductivity by in-plane 2-point-probe (Los Alamos fixture)

A fixture developed at Los Alamos[20] has been used for a number of years at DuPont for measuring the conductivity of fuel cell membranes (see Figure 2). Two strips of Pt metal are used as electrodes, while the membrane and the electrodes are clamped between two blocks of Tefzel®. The centers of the blocks have been machined out to allow water access to the center of the membrane, and indeed the entire fixture is immersed in de-ionized water to insure full membrane hydration. AC current and voltage are supplied and measured by a frequency response analyzer (e.g. Solatron or Gamry). The fixture is a so-called "2-point-probe" because the voltage is measured across the same two electrodes through which the current flows. The resistance of the sample is usually determined by plotting Z'' *vs* Z', considering the higher frequencies above 2 kHz where the minimum imaginary part is obtained, and extrapolating the curve to an intercept with the real axis.

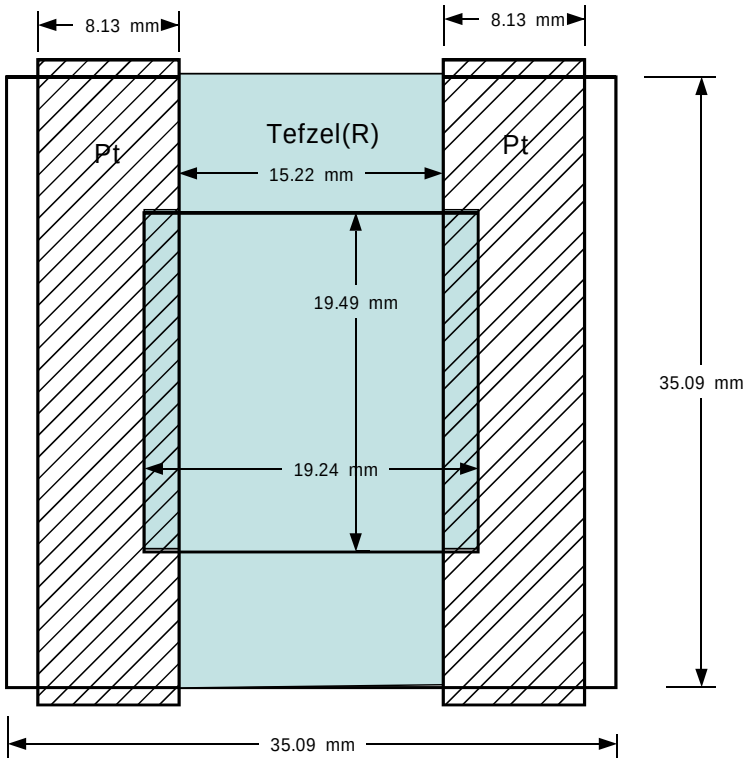

Figure 2. Schematic of the Los Alamos 2-probe conductivity fixture

The accuracy and repeatability of this conductivity measurement technique ("gage") were considered. The derivation of the conductivity from the resistance requires knowledge of a cell constant, which is dependent for each cell on the geometric details of the current distribution in the sample. The DuPont accepted value for the cell constant was 208.35 mil/cm, however, no documentation for this number could be found, it is not disclosed in the Los Alamos paper[20], nor did the Los Alamos personnel contacted have an available record. A "first principles" calculation of the cell constant was made for comparison to the accepted value. With reference to the drawing of the cell in Figure 2 , we made the following assumptions:

1) Current is injected into the membrane only in those areas where the membrane is clamped to the electrodes by the Tefzel®. Within the cutout in the center, there is no force holding the electrode to the membrane, even though the membrane overlaps the electrodes there.
2) Being covered by Tefzel® does not stop the membrane from conducting. All of the membrane between clamped electrodes conducts, including the parts that are between the two Tefzel® "bridges". To the extent that the Pt electrodes are

thick, the Tefzel® pieces are held apart, even allowing water to penetrate between the “bridges”. Thus the parts of the membrane that have current flowing in them are shaded.

3) The membrane punch is 34.91 mm X 34.87 mm *vs* design of 1.375” = 34.93 mm. Assume 34.93 mm for membrane width.
4) Approximately, the average length, or distance ions must travel through the membrane, is:

   Inner part (19.49/34.93) or 55.8% of 19.24 mm + 2 outer parts of 44.2% of 15.22 mm = 17.46 mm.

   Cell constant = 1.746 cm / (0.00254 cm/mil X 3.493 cm) = 196.8 mil/cm

Comparing with historical value of 208.35 mil/cm from LANL, this “first principles” approach gives a value that is really quite close by being within 6%. The cell constant is used, for example, with a 7.95 mil thick N117 membrane giving 212 ohm resistance at 5000 Hz:

Conductivity = 196.8 mil/cm / 7.95 mil X 212 ohm = 117 mS/cm.

The repeatability of the technique was examined by making repeated measurements on four samples (parts), being thick and thin Nafion® of standard 1100 EW (N1135 and N117), and thick and thin 1550 EW Nafion® . As the replicate samples were small pieces cut out near each other from a large piece of membrane, which came from a commercial production extruder, we assumed that there was no variation in the replicate parts themselves. The samples were boiled in water prior to measurement, and immersed in water. The result was that the standard deviation of conductivity was 3.7 mS/cm, which is 3% of the value for N117 of 117 mS/cm (Figure 3 and Table 2). Note however that the conductivity of N1135 was lower than that of N117, while the 4.7 mil 1542 EW sample had higher conductivity than the thicker 8 mil 1542 EW sample. If the membranes were truly made from the same batches of polymer, and if the conductivity were an intrinsic property independent of membrane thickness, then the same EW would have given the same values.

Table 2. Conductivity Gage Repeatability, 2-point-probe

Sample	Operator	Thick-ness (mil)	Resist-ance (ohm)	Cond-uctivity (S/cm)
N117	Norton	7.95	208.35	0.1220
N117	Norton	8.00	212.65	0.1188
N117	Norton	7.70	225.87	0.1162
N117	Norton	7.65	220.81	0.1196
N117	Norton	7.85	234.03	0.1100
Thick1542	Norton	8.00	871.76	0.0290
Thick1542	Norton	8.30	815.78	0.0298
Thick1542	Norton	8.05	905.62	0.0277
Thick1542	Norton	8.00	824.10	0.0307
Thick1542	Norton	8.10	781.94	0.0319
Thin1542	Norton	4.75	1131.20	0.0376
Thin1542	Norton	4.85	1207.60	0.0345
Thin1542	Norton	4.65	1195.90	0.0363
Thin1542	Norton	4.55	1132.90	0.0392
Thin1542	Norton	4.75	1062.90	0.0400
N1135	Norton	4.05	488.62	0.1021
N1135	Norton	4.20	488.66	0.0985
N1135	Norton	4.10	465.82	0.1058
N1135	Norton	3.95	459.30	0.1114
N1135	Norton	3.90	515.22	0.1006

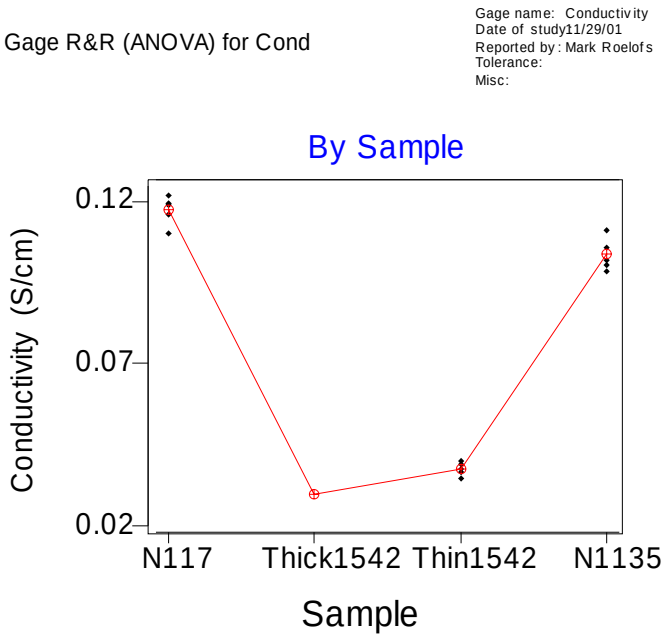

Figure 3. Gage repeatability of conductivity by Los Alamos 2-point probe

One observation made in this experiment was that the same de-ionized water was used for several of the samples without changing to fresh de-ionized water after each measurement. At the end of the measurements, a measurement was made of the resistance of the empty fixture (without membrane) immersed in the "used" de-ionized water. While it was still a high resistance, it was not negligible and would account for several percent error. It was confirmed that replacement of the water with fresh de-ionized water did result in a very high resistance value for the fixture without membrane. The standard procedure was, and continues to be, use of fresh de-ionized water with each sample.

4.1.4. Conductivity *vs* T and RH by in-plane 4-point-probe

The first apparatus assembled is sketched in Figure 4.

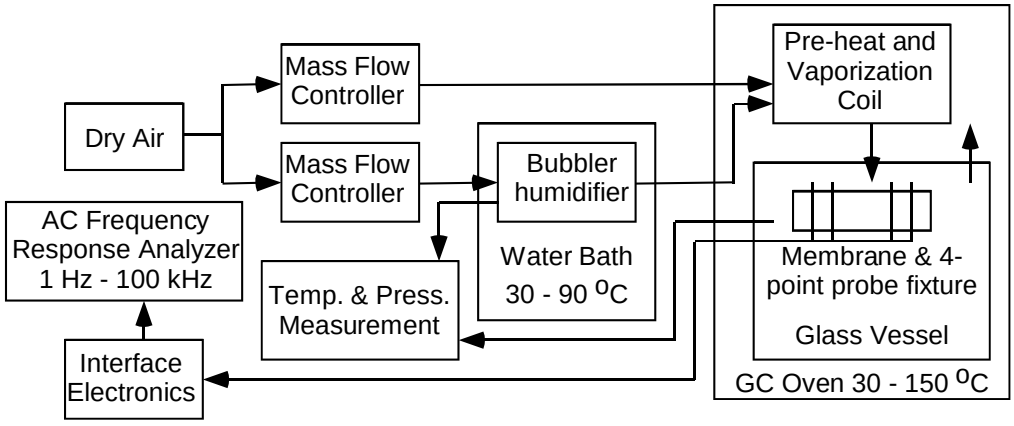

Figure 4. First apparatus for measuring in-plane conductivity under variable temperature and RH.

The membrane was exposed to air mixed with a variable and calibrated water vapor partial pressure between 0.004 and 0.7 bar at temperatures from 30 to 150 °C. Difficulties with this apparatus were that 1) the 4-point probe used stainless steel electrodes. which would corrode after many hours of contact with the membrane, 2) the vessel was not pressure rated, which limited the maximum attainable RH at elevated temperatures. To address the second problem, the bubbler was converted to a pressurizable Hoke cylinder immersed in an oil bath for uniform heating and the 4-point probe fixture was placed in a pressure vessel. The bubbler approach was abandoned when it was belatedly realized that upon changing the system pressure there would be significant time delays in attaining a stabilized output flow from the bubbler due to the dissolution or effervescence of the air from the bubbler water after a pressure change, which resulted in long measurement times.

These issues were addressed in the second apparatus, sketched in Figure 5, which was used for the measurements in this report.

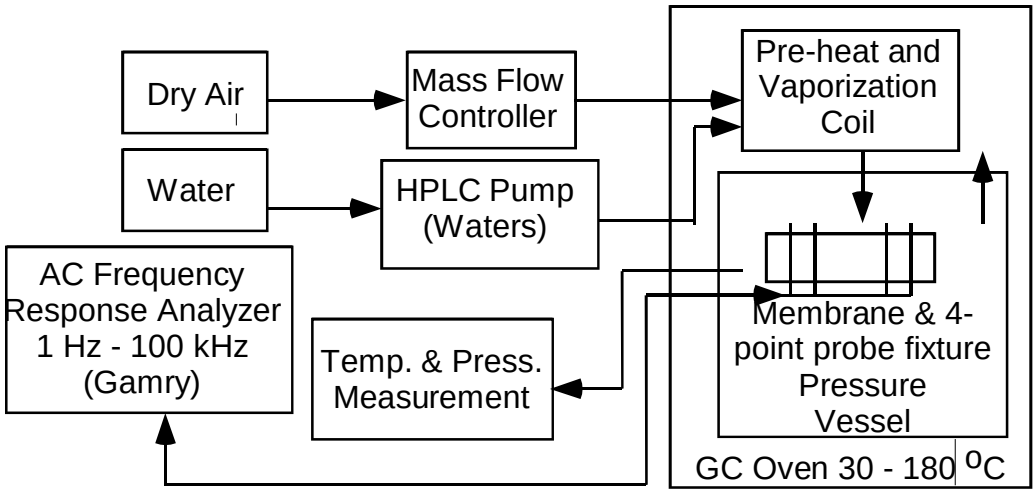

Figure 5. Second apparatus for measuring in-plane conductivity with variable temperature and RH.

Conductivity was measured under conditions of controlled relative humidity and temperature with the use of current that flowed in-plane (parallel to the plane of the membrane). A four-point probe technique was used, similar to that described in an article entitled "Proton Conductivity of Nafion® 117 As Measured by a Four-Electrode AC Impedance Method" by Y. Sone et al. [21]. Referring to Figure 6, a lower fixture **1** was machined from annealed glass-fiber reinforced PEEK, having four parallel ridges **2** that supported and held four 0.25 mm dia. Pt wire electrodes. The distance between the two outer electrodes was 25 mm, while the distance between the two inner electrodes was 10.0 mm. A strip of membrane was cut to a width between 10 and 15 mm, a length sufficient to cover and extend slightly beyond the outer electrodes, and placed on top of the Pt electrodes. An upper fixture (not shown), which had ridges corresponding in position to those of the bottom fixture, was placed on top and the two clamped together so as to push the membrane into contact with the Pt electrodes. The fixture with membrane was placed in a small pressure vessel (pressure filter housing), which was in turn placed in a GC oven (25 to 180 °C) and the temperature within the vessel measured by a thermocouple. Water was fed from a calibrated pump (Waters

HPLC model 515) and combined with dry air fed from a calibrated mass flow controller (200 sccm max). The water evaporated within a coil of 1.6 mm dia tubing within the oven, and the resulting humidified air was fed into the vessel. The total pressure within the vessel (100 to 345 kPa) was adjusted by means of a pressure-control let-down valve and measured using a capacitance manometer (Setra). The relative humidity was calculated assuming ideal gas behavior, tables of the vapor pressure of liquid water as a function of temperature, the gas composition from the two flow rates, the vessel temperature, and the total pressure. Slots **3** in the lower and upper parts of the fixture allowed access of gas to the membrane for rapid equilibration with water vapor. Current was applied between the outer two electrodes while the resultant voltage was measured between the inner two electrodes. The real part of the AC impedance (resistance) between the inner two electrodes at 1 kHz, R, was measured using a potentiostat/frequency response analyzer (Gamry Instruments PC4/750™ with EIS software). The ionic conductivity was calculated as

$$\kappa = 1.00 \text{ cm} / (R \times t \times w),$$

where t was the thickness of the film and w was its width (both in cm).

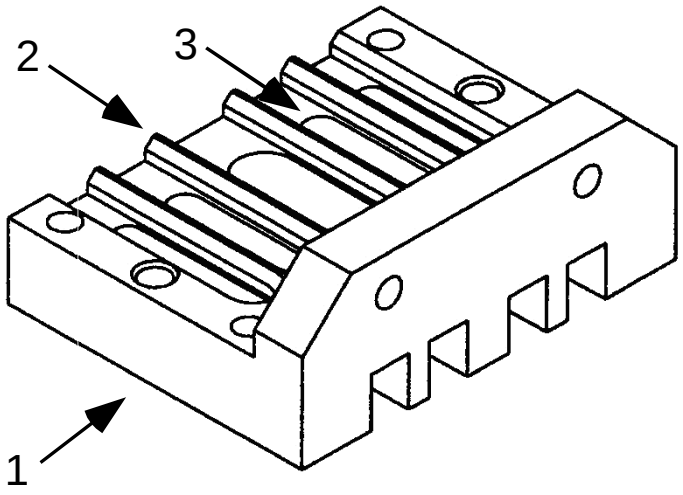

Figure 6. Base of in-plane 4-point-probe fixture based on PEEK and Pt wires.

A common protocol used early in the program was to measure at temperature/RH combinations of 80/95, 80/23, 120/25, and 80/95. This allowed some estimation of the sensitivity to both temperature and RH, and also allowed evaluation of the extent to which the loss of conductivity at 120 °C/23% RH is reversed by returning to high RH at 80 °C. The particular value of 23% RH and 80 °C was chosen for historical

reasons – air passed through a bubbler and humidified to 100% RH at 80 °C and 1 atm, if further heated to 120°C, has 23% RH. A faster protocol used later was to measure at RH's of 25, 50, and 95%, but at a single fixed temperature of 120 °C.

For N117 membrane, the substitution of nitrogen for air gave no change in conductivity as measured at 120 °C and 23% RH.

An issue arises in measuring the membrane thickness and width for use in the above expression. As these dimensions change with the swelling state of the membrane, they should ideally be measured at the same temperature and RH at which the resistance is measured. Lacking an *in situ* thickness probe, the thickness and width were measured *after* the membrane sample was removed from the fixture. This final thickness and width were shrunken relative to those of a freshly boiled membrane. Note, however, that the final condition the membrane was subjected to in the protocol was typically 95% RH, after which the thickness was measured. It would be difficult to argue that the membrane was actually thicker at the time its resistance was measured at lower RH's of 25-50%.

4.1.5. Response time of conductivity with RH change

Using the apparatus of Figure 5 and Figure 6, a Nafion® N117 membrane was exposed to a series of RH changes with results shown in Figure 7 and Table 3. For this experiment, the temperature was 120 °C, the air flow was 194 sccm (standard cubic centimeters per minute), the calibrated water flows were calculated from the pump setting by multiplying the setting by 1.006 and then subtracting an offset of 0.0023 mL/min, the thickness of the membrane was 209 μm, and the width of the membrane was 1.497 cm.

The volume of the pressure vessel was 225 mL and the 1/e time for changing the gas composition (time for 63% completion of change) inside the vessel was only 1.1 minutes. The membrane equilibrated with the new water vapor pressure more slowly, but after 40 to 60 minutes the conductivity values stabilized. The RH was changed in the sequence of 23, 50, 95, and 23%. The initial conductivity at 23% RH was 9.0-9.2, and after the high-RH conditions it returned to 10.3-10.4 mS/cm – not exactly the same as the starting values, but similar. Most of the membranes studied here have been thinner than N117 and have equilibrated in a shorter time. Samples were typically held at a given condition until the conductivity stabilized and successive measurements were within 10% of each other.

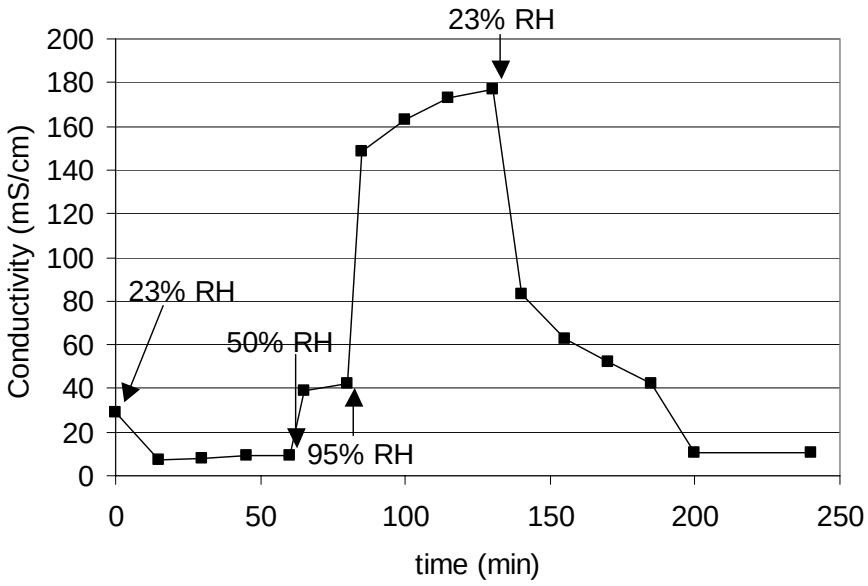

Figure 7. Conductivity for N117 at 120 °C *vs* time after changes to the water flow rate indicated by arrows.

Table 3. Response of conductivity measurement for N117 to change in RH. The columns are the time, pressure, set point of the Waters pump, AC resistance at 1kHz, calculated RH in %, calculated conductivity, and calculated water flow rate in mol of water/min.

Time	Vessel Press (psia)	Waters set ml/min	Resistance (ohm)	RH	Cond. (mS/cm)	Calc mol H2O/min
8:50	34.76	0.039	1,112	23.2	28.7	0.00205
9:05	35.30	0.038	4,378	23.0	7.3	0.00200
9:20	35.44	0.038	3,889	23.1	8.2	0.00200
9:35	35.45	0.038	3,482	23.1	9.2	0.00200
9:50	35.55	0.038	3,554	23.2	9.0	0.00200
9:55	35.00	0.110	815	49.9	39.2	0.00602
10:10	35.15	0.110	761	50.1	42.0	0.00602
10:15	35.11	0.550	215	95.1	148.5	0.03058
10:30	35.01	0.550	196	94.8	162.7	0.03058
10:45	35.16	0.550	185	95.2	173.2	0.03058
11:00	35.00	0.550	181	94.8	176.9	0.03058
11:10	35.70	0.038	384	23.3	83.2	0.00200
11:25	35.13	0.038	512	22.9	62.5	0.00200
11:40	35.10	0.038	613	22.9	52.1	0.00200
11:55	35.28	0.038	754	23.0	42.4	0.00200
12:10	35.04	0.038	3,100	22.8	10.3	0.00200
12:50	35.17	0.038	3,073	22.9	10.4	0.00200

4.1.6. Conductivity of Nafion® *vs* RH

Several samples of Nafion® membranes were measured at various temperatures and RH's using the in-plane 4-point-probe technique with the results summarized in Figure 8. Two conductivity apparatuses, located in different buildings, produced similar values at high RH, but at 25% RH the second instrument gave systematically lower conductivities than the first. Despite repeated calibrations, the reason for the difference was not understood. Data from both instruments is included in Figure 8.

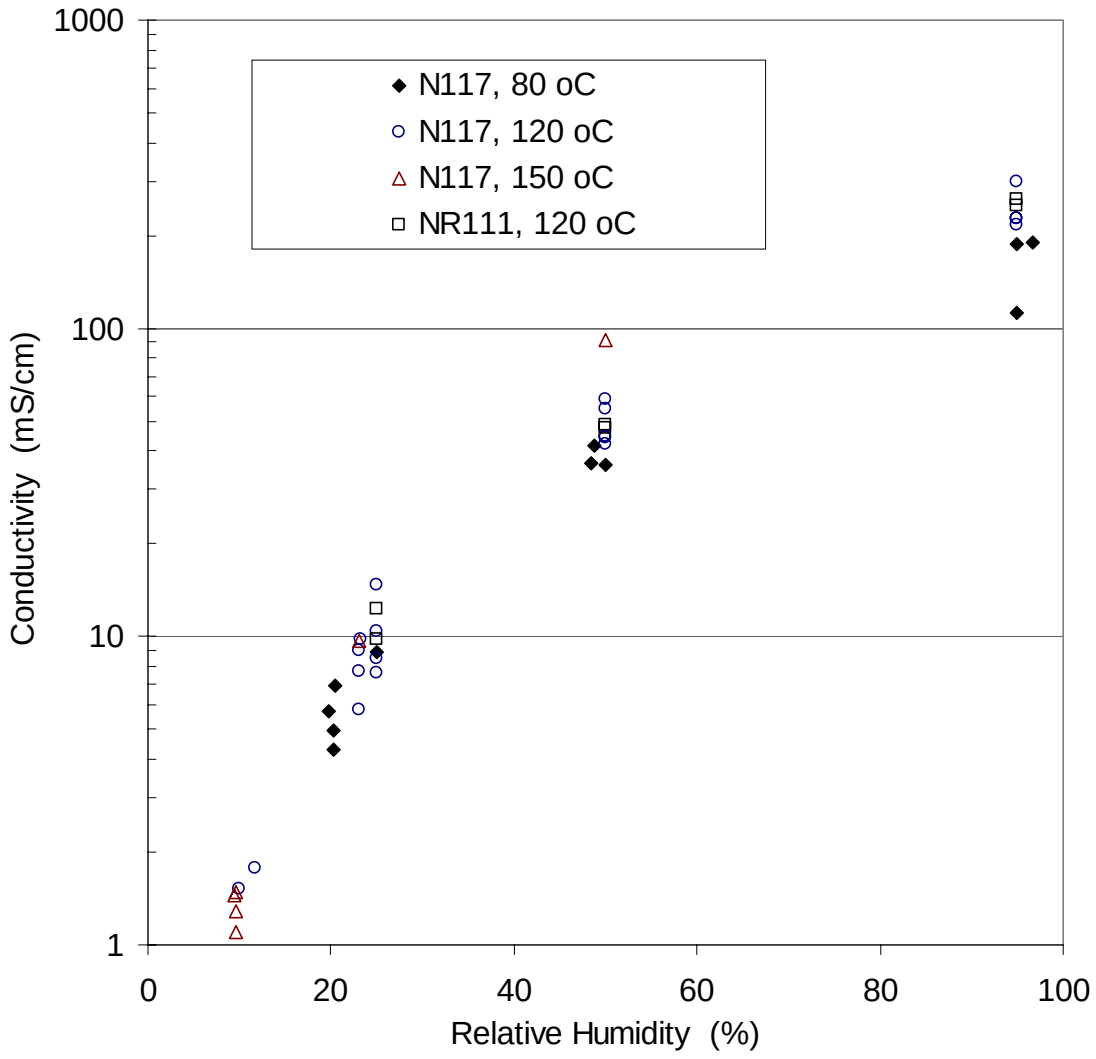

Figure 8. Conductivities of N117 and NR111 *vs* RH for several temperatures.

RH is the largest factor in determining the conductivity of Nafion®, while temperature plays a smaller role. The extruded thick membrane N117 is close in

conductivity to the dispersion-cast thin membrane NR111 (though there is other data, not shown, suggesting that NR111 may have slightly higher conductivity than N117). These DuPont results are somewhat higher than Alberti's [10] values for N117 at 120 °C, where they obtained 12 mS/cm @ 37% RH and 140 mS/cm at 91% RH. However, The DuPont results are somewhat lower than those obtained at Case Western([9].

4.1.7. Thermal stability

New polymer electrolytes were screened for thermal stability using an adaptation of a known TGA kinetic method[22]. A few mg of polymer sample were heated in air, which was humidified at 22 °C, using heating rates of 1, 3, 5, and 10 degree/min. The weight loss associated with the first stage of decomposition was determined, and then an Arrhenius-type analysis was made by plotting the log of the heating rate *vs* 1/T, where T is the temperature required to complete a certain fraction of the first stage of decomposition. The energy of activation, E_a, and the pre-exponential factor, A, for the decomposition were thus determined. These parameters were used to extrapolate back to 120 °C and determine how many hours would be required at 120 °C to have 10% of the first stage of decomposition completed.

For the more stable electrolytes, and with heating rates of 1 – 10 degree/min, most of the decomposition occurs well above 250 °C, so one may question the accuracy of an extrapolation back to a much lower intended use temperature. A simpler procedure was to simply hold the sample overnight at a constant temperature (isothermal), typically 150 °C, and compare, for various samples, the rate of weight loss obtained in the last several hours of the test. In some cases, the results of isothermal and kinetic TGA were combined, using the measured decay rate in the isothermal experiment at 150 °C along with the activation energy from the kinetic analysis, to extrapolate over an narrow range of only 30 °C back to decay rates at 120 °C

Caveats are that these TGA methods do not address electrochemical stability, nor stability under Fenton-type conditions, nor do they detect degradation that does not result in weight loss (e.g. backbone scission), and the effect of the very low RH used was not determined. Acceptable thermal stability by TGA was viewed as a necessary, but certainly not sufficient, condition for a new polymer electrolyte to displace Nafion®.

4.1.8. Fenton test

A membrane sample was dried, weighed (typically 1 g), immersed in 50 mL of 30% H_2O_2 with 20 ppm Fe derived from $FeSO_4.7H_2O$ for 18 hr at 80 °C, re-dried, weighed for weight loss, and the solution analyzed for fluoride release using an ion-

selective electrode. The 18 hr exposure was repeated three times and the cumulative weight loss and fluoride release were calculated.

4.1.9. Fuel cell test protocols & N112 evaluation

The fuel cell measurements made under the program at DuPont used single cells of 25 cm^2 active area with single serpentine channels in graphite blocks (Fuel Cell Technologies, Albuquerque, NM). Dry gas flows from mass flow controllers were combined with water flows from HPLC pumps, the water vaporized, and then the humidified gas fed to the fuel cell. Membranes were placed between two gas diffusion electrodes (ELAT® provided by De Nora) and assembled in the cell.

The protocols used to evaluate the cell usually included a cell conditioning step, followed by IV characterization, followed by a durability test. Two protocols, HT5 and HT6, are further described in Table 5 and Table 6 below. After IV curves, HT5 ran a durability test at 120 °C in which the cell was held for 10 min at OCV, then 0.5 V for ~5 h with RH of anode/cathode feed gases at 100%/70%, then 5 h at 40%/40%. These three steps were repeated in a 10 hr cycle. HT6 and HT7 were similar to HT5, except that the pressures were lowered to 7 or 21 psig, and the RH cycling went from 70%/70% RH down to 25%/25% RH:

Table 4. RH cycle for HT6 and HT7

Step	Time	Feed RH (%)	Condition
1	10 min	70%	OCV
2	5 h	25%	0.5 V
3	5 h	70%	0.5 V

The intent of the RH cycling was to mechanically stress the membrane by repeatedly changing its swelling state. These changes to lower pressure were made to make HT6 and HT7 more relevant to the DOE High Temperature test matrix from Oct. 2003. HT7 included additional characterization of the hydrogen permeation using H_2/N_2 feeds and linear sweep voltammetry.

To establish baseline performance in these protocols, commercially available Nafion® N112 membranes were examined with typical results for HT7 shown in Figure 9 to Figure 11. The IV performance at low RH feeds was quite poor (Figure 10) and the MEA suffered a rapid decline in OCV after 90 hr in the cycling test at 120 °C (Figure 11). A second N112 membrane failed after 18 h.

Table 5. HT5 protocol

Step	Temp (C)	Nom. Current (A)	Active Area (cm2)	Press. (psig)	Anode RH%	Anode Stoich	Cath RH%	Cath Stoich	Anode H2 (sccm)	Anode H2O (mL/min)	Cathode Air (sccm)	Cathode H2O (mL/min)
Cell conditioning Customer qual2	65	50	25	0	131	1.5	100	2	560	0.200	1786	0.436
ECA before cell goes on.												
two IV curves, to 0.3V, 20s/50mV	80	30	25	15	100	2	100	2	450	0.101	1072	0.241
two IV curves, to 0.3V, 20s/50mV	80	30	25	15	50	2	50	2	450	0.044	1072	0.105
two IV curves, to 0.3V, 20s/50mV	120	30	25	30	100	2	70	2	450	0.610	1072	0.658
two IV curves, to 0.3V, 20s/50mV	120	30	25	30	70	2	70	2	450	0.276	1072	0.658
two IV curves, to 0.3V, 20s/50mV	120	30	25	30	40	2	40	2	450	0.117	1072	0.278
TimeplotA OCV for 10 min, 1min/point	120	30	25	30	70	2	70	2	450	0.276	1072	0.658
TImeplotB 0.5V 4hr 50min, 10min/point	120	30	25	30	100	2	70	2	450	0.610	1072	0.658
TimeplotC 0.5V 5 hr, 10min/point, repeat cycle of A,B,C	120	30	25	30	40	2	40	2	450	0.117	1072	0.278
ECA when cell comes off												

Table 6. HT6 protocol. HT7 is identical, but adds LSV characterization steps.

Step	Temp (C)	Nom. Current (A)	Active Area (cm2)	Press. (psig)	Anode RH%	Anode Stoich	Cath RH%	Cath Stoich	Anode H2 (sccm)	Anode H2O (mL/min)	Cathode Air (sccm)	Cathode H2O (mL/min)
Cell conditioning Customer qual2	65	50	25	0	131	1.5	100	2	560	0.200	1786	0.436
ECA before cell goes on.												
two IV curves, to 0.3V, 20s/50mV	50	30	25	7	100	2	100	2	450	0.030	1072	0.072
two IV curves, to 0.3V, 20s/50mV	80	30	25	7	100	2	100	2	450	0.156	1072	0.371
two IV curves, to 0.3V, 20s/50mV	80	30	25	21	100	2	100	2	450	0.080	1072	0.191
two IV curves, to 0.3V, 20s/50mV	120	30	25	21	70	2	70	2	450	0.436	1072	1.039
two IV curves, to 0.3V, 20s/50mV	120	30	25	21	25	2	25	2	450	0.085	1072	0.202
two IV curves, to 0.3V, 20s/50mV	120	30	25	7	25	2	25	2	450	0.167	1072	0.397
TimeplotA OCV for 10 min, 1min/point	120	30	25	21	70	2	70	2	450	0.436	1072	1.039
TImeplotB 0.5V 4hr 50min, 10min/point	120	30	25	21	25	2	25	2	450	0.085	1072	0.202
TimeplotC 0.5V 5 hr, 10min/point, repeat cycle of A,B,C	120	30	25	21	70	2	70	2	450	0.436	1072	1.039
ECA when cell comes off												

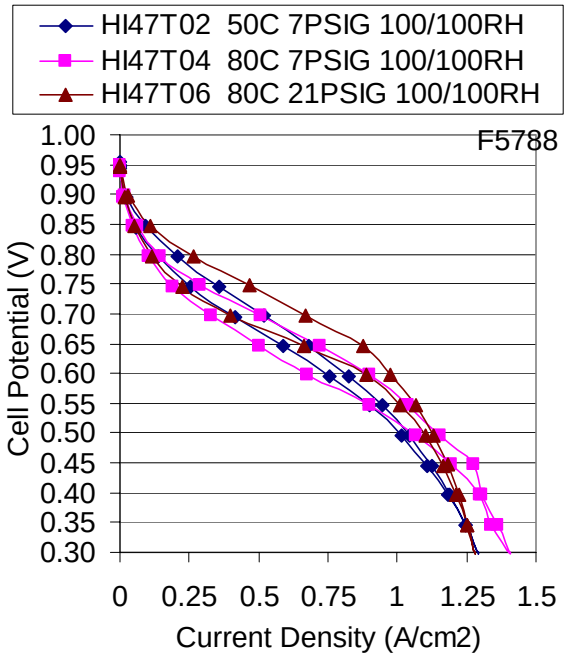

Figure 9. IV curves for N112 at 50 and 80 °C

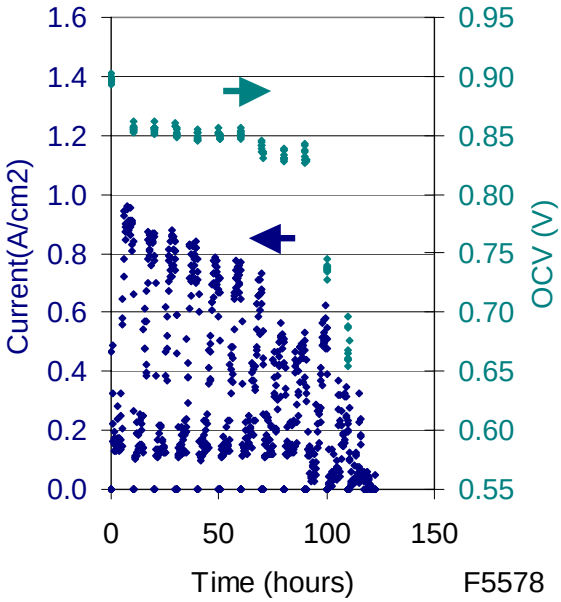

Figure 11. Durability test for N112 at 120 °C.

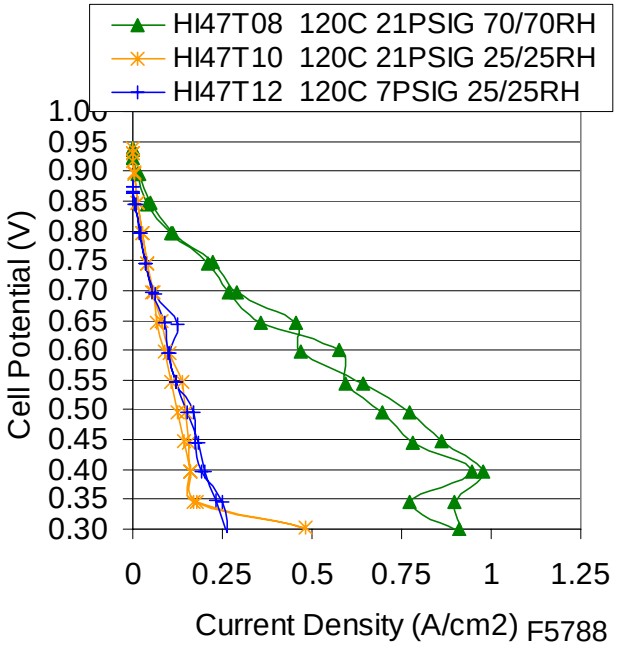

Figure 10. IV curves for N112 at 120 °C.

4.2. Liquid Conductivities

One of the hypotheses for high-temperature membranes was that low-EW was needed to obtain conductivity at low RH. To see if there is experimental support for such a claim, the conductivities of 73 samples of model electrolytes and monomers in liquid form were plotted *vs* their equivalent weight (Figure 12).

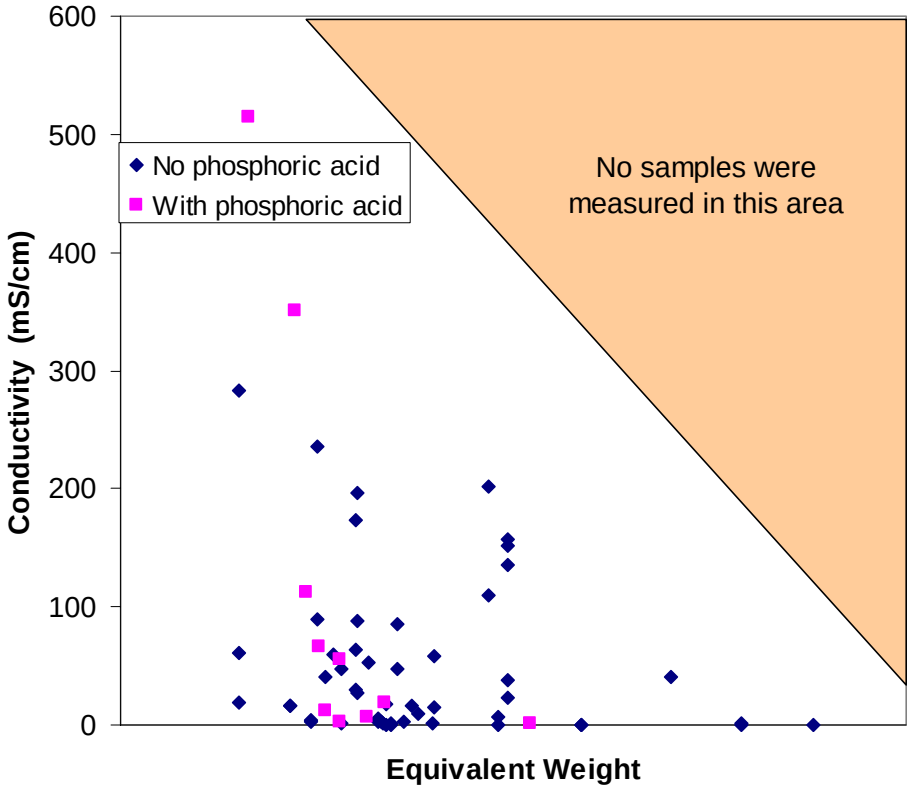

Figure 12. Conductivities of liquid electrolytes at 150 °C and atmospheric pressure, either containing no (diamonds) or some (squares) phosphoric acid.

Most of these measurements were made with water present (giving approximately 20% RH), while a few were for anhydrous electrolytes. No electrolytes were found that were both highly conductive and high EW, while many were also found with low-EW and low conductivity. The observations are consistent with the claim that low-EW is necessary, but not sufficient, for high conductivity at low RH. This study identified several different organic acid functionalities that were investigated further in polymeric form. The samples with phosphoric acid were attempts to find compounds that were synergistic with phosphoric acid in a way superior to the well-known PBI/phosphoric acid system.

The results of several experiments where the temperature was varied are shown in Figure 13. The water contents indicated were the starting compositions and were chosen to correspond to significantly lower water contents (acid:water, mole:mole) than is required by Nafion®. Though the water vapor pressure was not explicitly controlled, the cell was not pressurized and the water vapor partial pressure was less than 1 atm. A few samples attained 50 to 200 mS/cm at 150 – 180 °C. The maximum, which was followed by a decrease in conductivity at higher temperatures, observed for some samples is believed to be due to evaporation of water. Compound U was one of the very few electrolytes in which the neat liquid without added water generated appreciable conductivity.

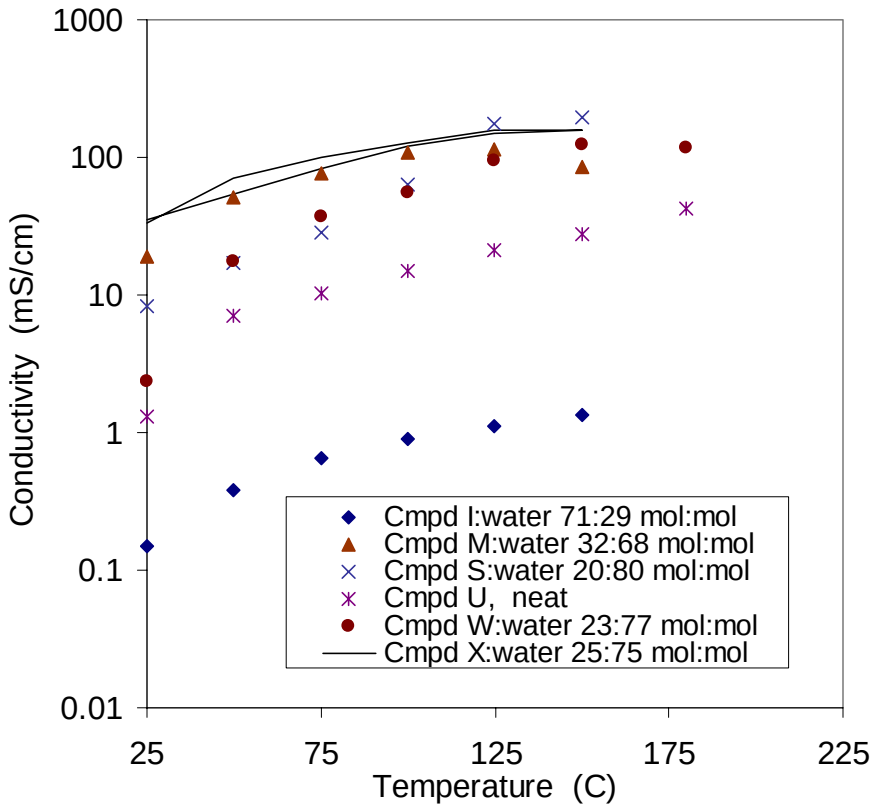

Figure 13. Conductivities of liquid electrolytes at various temperatures.

The electrolytes investigated covered a range of aliphatic and aromatic compounds, fluorinated and non-fluorinated, with sulfonic and non-sulfonic acid ionic groups. These small molecules studies were used to guide monomer and polymer synthesis. For example, the types of organic functionality present in

small molecules M, U, W, and X of Figure 13 were ultimately incorporated into novel polymer electrolytes AU, AN, and AK. Of these, only AK upheld the promise of its model compound and gave very high conductivity (see below).

4.3. Composite membranes V and AV

Another potential method for achieving a high temperature membrane utilizes composites of ionomers with hydrophilic inorganic compounds. The desire is for the inorganic compounds to alter the microstructure of the ionomer, perhaps by holding open the ionic pores or by increasing the attractive force with which the water is held in the membrane. A further function of the filler is to decrease the creep of the ionomer and prolong membrane life. Several Nafion®-inorganic composite membranes were prepared and evaluated, including candidates Q, V, W, AT, and AV.

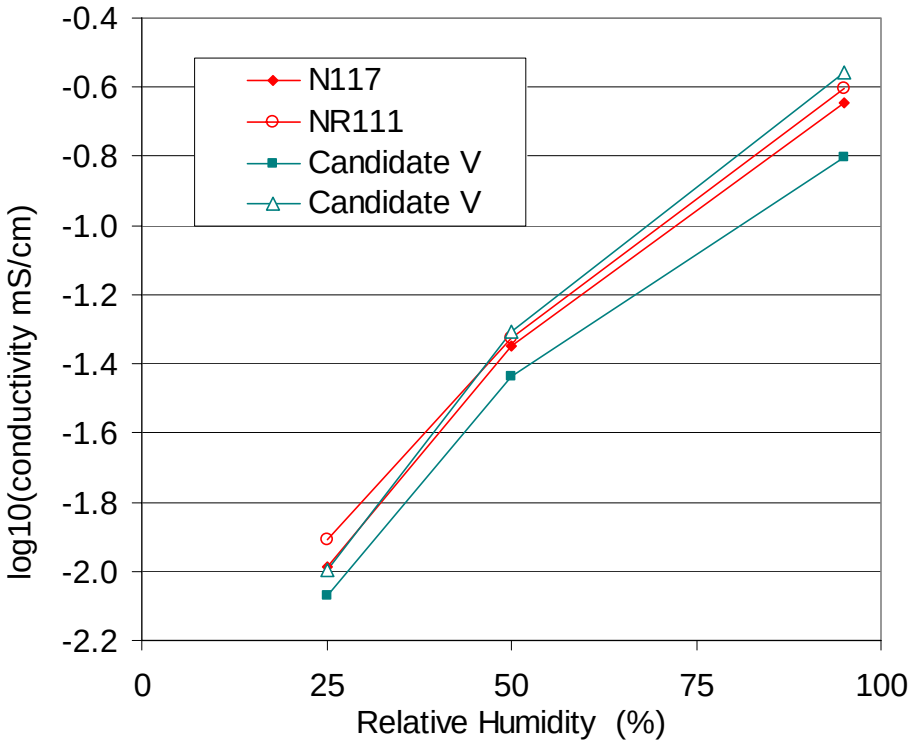

Figure 14. In-plane conductivity *vs* RH at 120 °C for two Nafion® membranes and two samples of candidate V membrane optimized for high conductivity.

In 2002, we had reported that candidate V showed higher conductivity at low RH *vs* a Nafion® N117 control. Unfortunately, this conclusion, which was based on two samples of V and two of N117, could not be reproduced with more

intensive studies. In part, further candidate V samples did not show such high conductivity, but mostly further studies of control Nafion® membranes showed increased conductivity. The thermal and acidic treatments that occur during the fabrication of V do alter the conductivity considerably. The final conclusion is that many fabrication conditions result in V membranes with reduced conductivity *vs* Nafion® controls, while some conditions were found that gave V membranes with conductivity slightly reduced or similar to Nafion® (see Figure 14). None of the other Nafion®/inorganic composites examined gave significantly higher low-RH conductivity than Nafion® membrane controls.

Membrane durability at 120 °C was in some cases increased using the inorganic composite approach. Results using HT6 (see section 4.1.9) on two candidate V membranes are shown in Figure 15 and Figure 16.

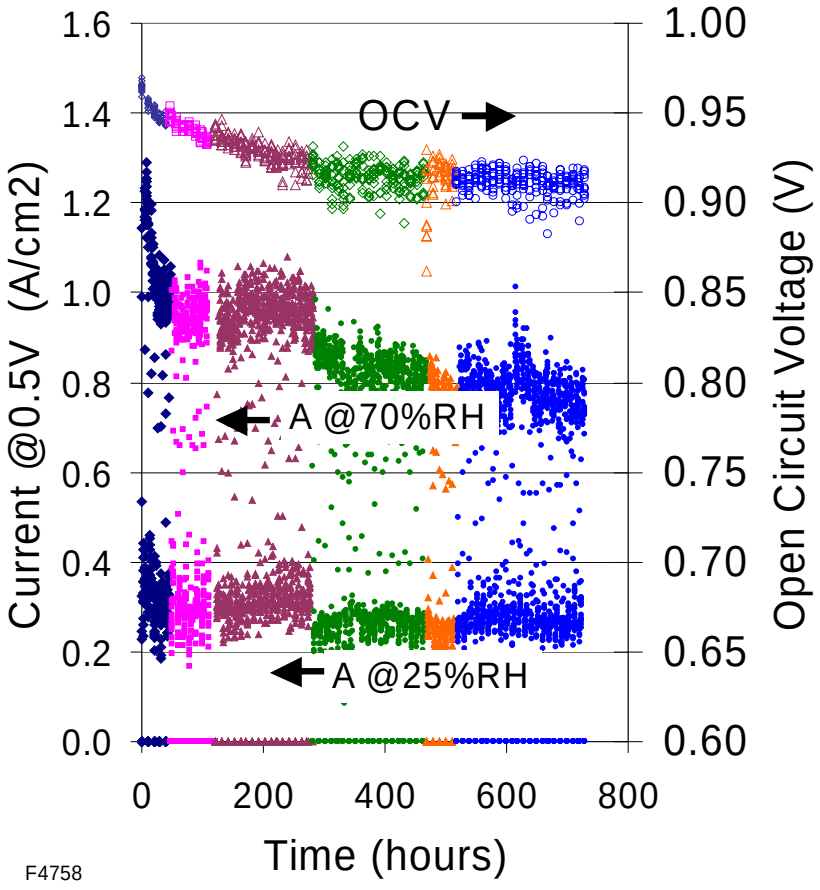

Figure 15. Durability for 33 μm candidate V in a 120 °C FC HT6 cycling protocol. Current in steps 1 and 2 and OCV in step 3 are shown *vs* time. The color change in symbols denotes test restart after power interruption, maintenance, etc.

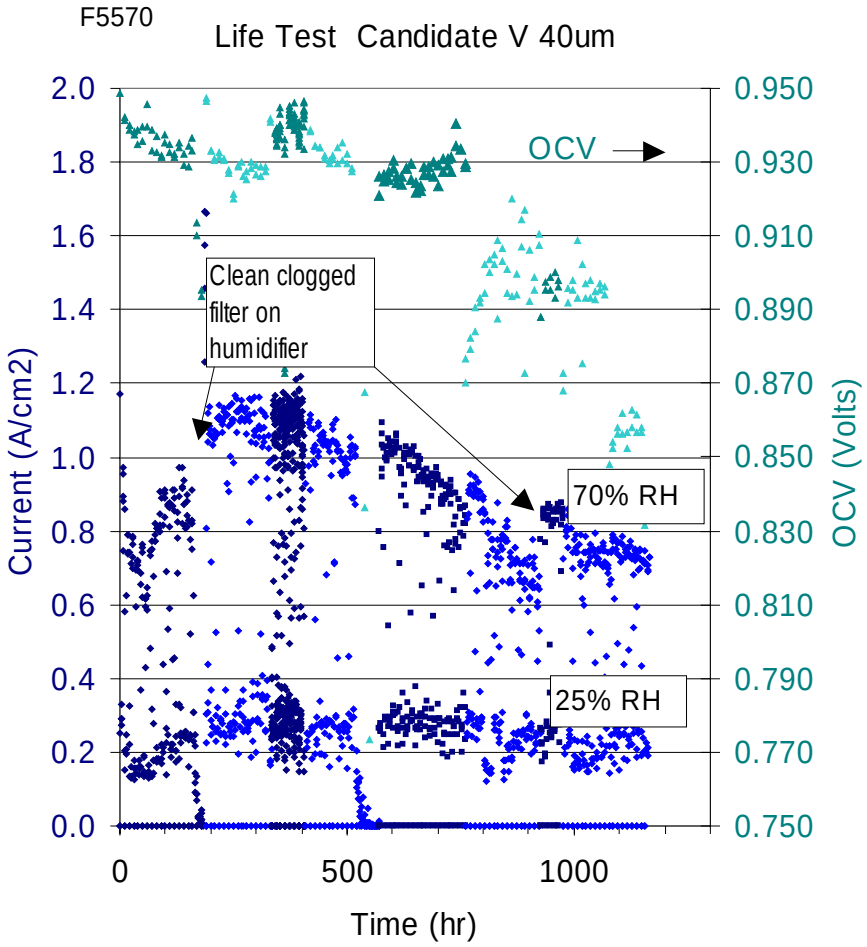

Figure 16. Durability for 40 μm candidate V in a 120 °C FC HT6 cycling protocol. Current in steps 1 and 2 and OCV in step 3 are shown *vs* time. The color change in symbols denotes test restart after power interruption, maintenance, etc.

The test of Figure 15 was stopped before membrane failure, while the membrane of Figure 16 suffered damage after the restart at 720 hours, and OCV dropped below 870 mV at 1000 hr. Membranes that had large drops in OCV were found to have high hydrogen crossover (electrochemical test with N_2/H_2 flows), confirming that under these conditions the major drop in OCV was due to membrane failure and not catalyst degradation. Cycling to a lower RH value of 25% was found in general to damage membranes faster than the earlier protocol (HT5) which cycled between 70% and 40% RH. Nafion® membranes without the inorganic component, e.g. N112, which is thicker than these V membranes, failed within 100 hr using HT7 protocol (Figure 11).

Candidate AV is a multi-component composite Nafion® membrane containing the same inorganic compound as candidate V, but in addition it contains a fluorinated polymeric reinforcement. A candidate AV membrane was also demonstrated to have increased durability at 120 °C (Figure 17). This test used HT5 protocol, which was similar to HT6 described above, except the pressure was 300 kPa and the RH cycling was between 40% and 70%. The membrane had not failed yet at 1490 hr when the test was stopped, while under the same test conditions, a control membrane with reinforcement, but no inorganic compound, developed shorts near 150 hr.

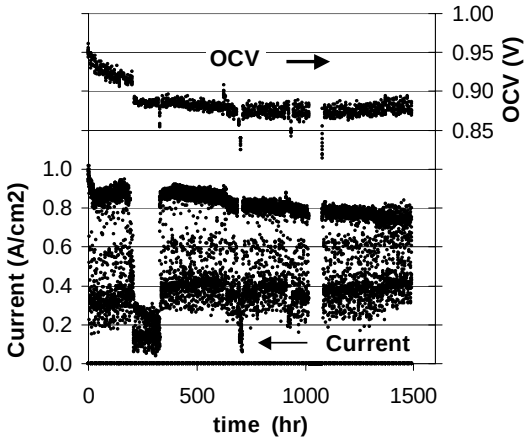

Figure 17. Durability of candidate AV in a 120 °C FC HT5 cycling protocol. Membrane resistance was 350 mohm cm^2 @ 40% RH feeds.

The Fenton test, which subjects membranes to free radical attack arising from the iron-catalyzed decomposition of hydrogen peroxide, has historically been used to chemically test membrane durability[3]. Two types of Nafion®, which differ in their resistance to Fenton reagent, were fabricated into composite V membranes. In Figure 18, the values are an average of two to four samples of each type. Significant reductions were observed in fluoride release rates with incorporation of the inorganic compound.

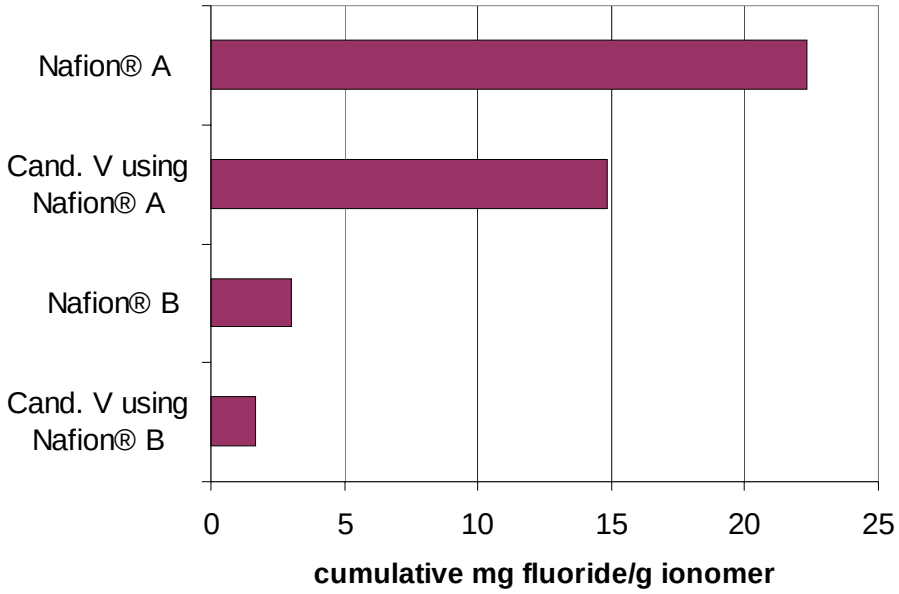

Figure 18. Fenton results for Nafion® and candidate V

Another accelerated test for membrane durability is the so-called OCV test (DD1 protocol) Here the MEA's are subjected to hydrogen on one side and oxygen on the other, held at open circuit voltage (zero current) at 90 °C, 0.1 MPa total pressure (0 psig), and with 30% RH in the feed gases. The test is terminated when the OCV drops below 850 mV, or exceeds 6 days. Results for two Nafion® NR111 control membranes and two candidate V membranes are shown in Figure 19 with the candidate V membranes demonstrating a longer life in this accelerated test. A second metric provided by the DD1 test is the quantity of fluoride ion emitted per unit of MEA area per unit time. Again, the candidate V membrane was fabricated using different types of Nafion® (A, B, C, D). The fluoride emission for the composite membrane V with the inorganic compound was also significantly lower in this measurement (see Figure 20).

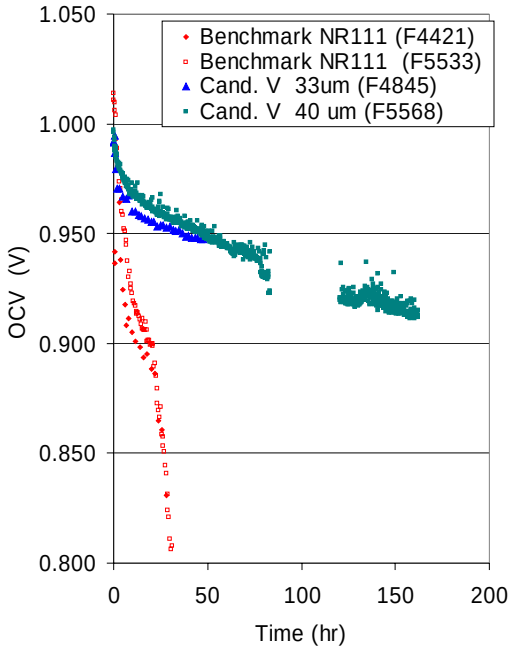

Figure 19. OCV test on NR111 and Candidate V membranes.

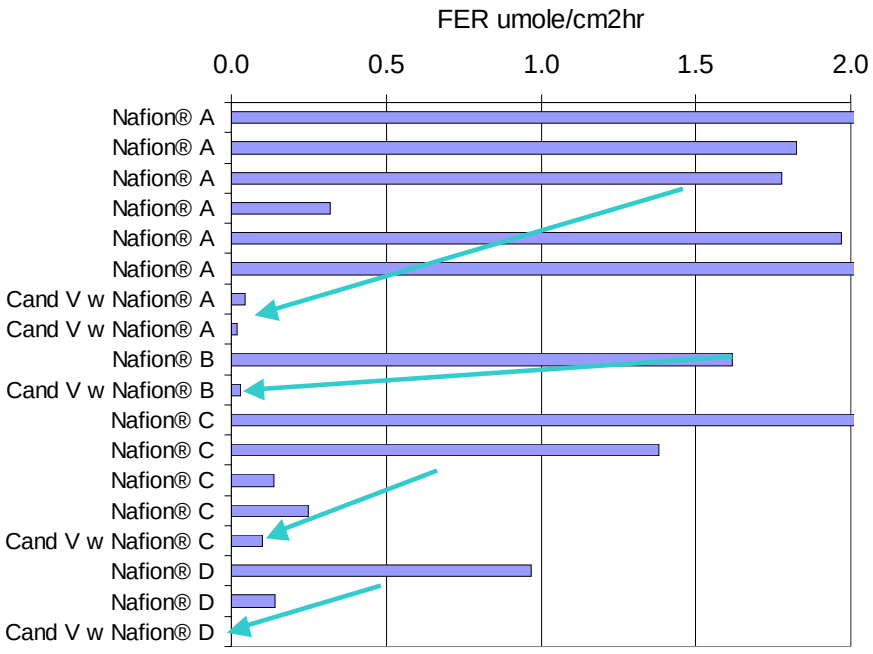

Figure 20. Fluoride emission in DD1 for Nafion® and candidate V MEA's.

As discussed in Section 3, our original 2001 goals and the multi-year plan targeted reduced levels of hydrogen crossover. Permeation was measured on

membrane electrode assemblies based on Nafion® or candidate V membranes using an electrochemical technique. Fuel cells with 25 cm^2 active area were fed hydrogen on one side and a slow flow of ultra-pure nitrogen on the other. A voltage of 0.15 to 0.35V was applied, which is sufficient to oxidize the hydrogen that crosses the membrane to the nitrogen side. By varying the voltage in this range, the contribution from electrical shorts could be separated from that arising from hydrogen permeation. The permeation in Nafion® increased strongly with both temperature and RH, which is consistent with prior studies[23]. For a dispersion-cast Nafion® NR111 (31 um thick) at 120 °C and 100% RH, and 1 atm bar partial pressure of H_2, the permeation coefficient from Figure 21 can be converted back to an equivalent crossover current as
51 X 10^{-9} scc cm cm^{-2} s^{-1} $cmHg^{-1}$ X 1 atm H_2 X [2 equiv/molH_2 X 96,500 C/equiv X 76 cmHg/atm]/[22,415 scc/mol X 0.0031 cm] = 11 mA/cm^2 crossover, which is much higher than the target of 5 mA/cm^2 or 2 mA/cm^2 in 2010. Of course, the goal is to operate at much lower vapor pressures of water. At 20% RH and 120 °C, the crossover current for NR111 was 2.5 mA/cm^2, which is much closer to the target. Although one might desire the presence of an inorganic compound to lower the permeation of Nafion®, this was unfortunately not found in this case and candidate V has very similar hydrogen permeation to Nafion® membranes without inorganic compounds (Figure 21).

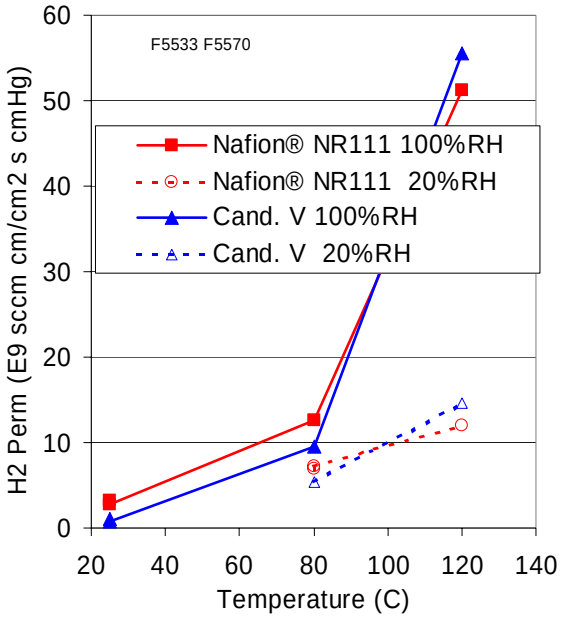

Figure 21. Hydrogen permeation for Nafion® and candidate V membranes

One of the difficulties with candidate V membranes is that their fabrication increases the number of processing steps beyond standard Nafion®, which would result in a higher cost.

4.4. AE, AK, BP polymer electrolytes and membranes

As mentioned in 4.2, a model compound electrolyte (candidate X) had been synthesized that provided good conductivity at 150 °C with steam pressure less than 1 atm. This inspired work that led, over the last 3 years of the project, to the synthesis of fluorinated polymer electrolytes AE, AK, BL, BN, and BP.

AE might be considered the progenitor of this class of polymer electrolytes as it has the simplest structure. The first two of these polymer electrolytes were measured in this program to have much higher conductivity at low RH than Nafion®, as shown in Figure 22, where AE is 7X and AK is 15X more conductive than Nafion®. AK is a new polymer electrolyte that incorporated all the features of the model compound X. Its conductivity is the highest of all the polymer electrolyte measured in this program, and is in a range that might allow operation below 20% RH.

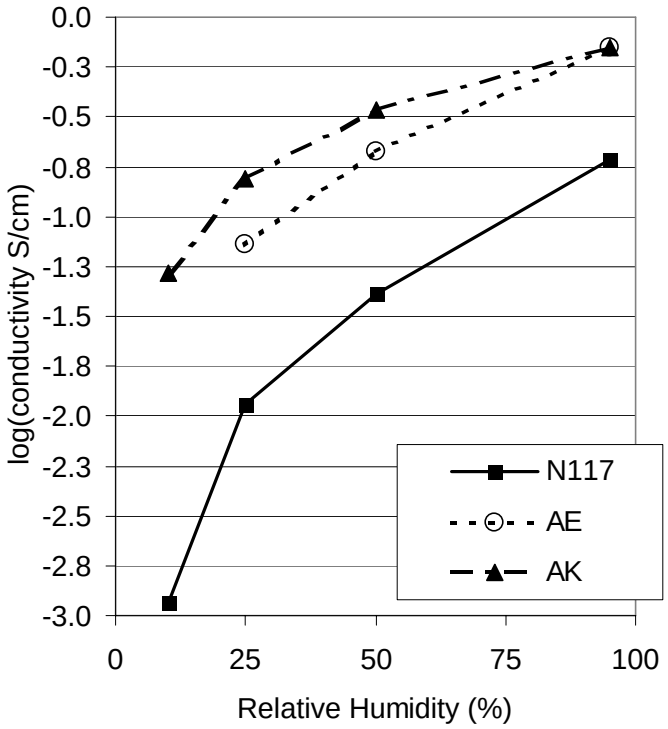

Figure 22. AE, AK, and N117 conductivity *vs* RH at 120 °C.

Unfortunately, AK was found to have very low thermal stability with its upper lifetime at 120 °C being estimated by kinetic TGA as only 5 hr. In contrast, AE had a very high activation energy of 250 kJ/mol *vs* 150 kJ/mol for N112, which implied a very high thermal lifetime at 120 °C. The isothermal weigh loss rate for AE was later measured to be –0.00042 %/min after 23 hr at 150 °C. Although not as high as predicted by kinetic TGA, this still compared favorably with Nafion® N112's decay rate of –0.00012 %/min at 150 °C. When combined with the higher activation energy, this decay rate implied that AE would still have higher thermal stability than Nafion® at 120 °C. A further very attractive attribute of AE polymer electrolyte was its high stability in the Fenton test, where it produced only 0.17 to 0.9 mg F^-/g polymer *vs* 3.5 to 30 mg F^-/g polymer for various types of Nafion®.

A problem with both AE and AK polymer electrolytes is that they are water soluble. A similar issue with PBI/phosphoric acid PEM's occurs because the electrolyte H_3PO_4 is water soluble. At steady-state operation at high temperature, only water vapor is present in the FC, so the water solubility of H_3PO_4 is not a large issue. However, under start-up, shut-down, or idle conditions, the stack temperature would be expected to drop below 100 °C, such that condensed water could form, and water soluble electrolytes would be expected to be lost. Unlike small-molecule H_3PO_4, AE and AK are polymers for which alternate strategies for insolubilization might be pursued. A further problem with AE and AK was that the polymerization chemistry was not sufficiently high in yield, such that their molecular weights were low (up to ~8,000), which led to membranes with low strength. The choice was made to work to improve the mechanical and swelling (solubility) properties of AE, and if successful, then return with these learnings to work further on the thermal stability problems of AK to also capture its higher conductivity in a membrane with all required properties.

Significant effort was made in 2003 to 2004 to improve AE molecular weight and lower solubility, through modification of the polymerizing functional groups and/or crosslinking, but without success. In 2005, the monomers were redesigned to include certain aromatic functional groups that were intended to give greater versatility in the polymerization chemistry and reduce the water swelling. This led to new polymer electrolytes BL, BN, and BP, which differ in the manner by which the hydrophilic and hydrophobic moieties are distributed in the

polymer chain. Measurements of some of the properties of the resulting polymers are shown in Table 7.

Table 7. M_w, swelling, TGA, and conductivity of AE-type polymer electrolytes.

Candidate	M_w	Solubility	TGA wt. loss, 150 °C (%/hr)	Conductivity at 120 °C (*denotes at 80 °C)			
				in-plane		through-plane	
				95%RH	25%RH	95%RH	25%RH
AE	est 8,000	Soluble 22 °C	-0.025			700	73
BL	100,000	Insoluble 22 °C Soluble 100 °C	-0.47	440-460*	0.2*	360-400*	17* 16
BN	62,000	Soluble 22 °C	-4.1	390	0.2		
BP	84,000	Insoluble 22 °C Soluble 100 °C	-0.0084	450	5*	405	16* 5

The new approaches did indeed give higher conversion in the polymerization, which resulted in considerable increases in molecular weight *vs* AE, and tough films in the case of BL and BP. Higher thermal stability was expected for BL and BN, but only realized with BP, which shows a lower rate of weight loss in isothermal TGA at 150 °C than does Nafion®. BL shows a low degree of crystallinity by DSC, which likely provides the modest decrease in solubility *vs* AE. The high acidity of the fluorinated electrolyte groups, in combination with their aromatic groups, likely gives rise to excessive thermal decomposition at elevated temperatures for BL and BN. Conductivity, while excellent at high RH, dropped precipitously at low RH for in-plane measurements. However, conductivities measured in the fuel-cell-relevant through-plane direction at low RH were higher than Nafion® for BL and BP. Based on these results, we do not recommend the combination of the fluorinated polymer electrolyte of AE with simple aromatic systems. However, the results for BP with its more complicated and stable aromatic system, obtained in the final months of the project, have given us sufficient encouragement to continue work on the AE-type electrolytes in the current form of candidate BP.

4.5. AO & BA Membranes

Four related partially-fluorinated ionomers were developed in this program, and each was combined with a structural non-conducting polymer to give composite membranes AO, BG, AZ, and BA. The first of these, AO, was made in 3Q 2003. Its low-RH conductivity, while not as high as some of the other electrolytes, was still significantly higher than that of Nafion® N117 (see Figure 23)[1]. However, unlike candidates AE or AK, AO had less swelling and could be boiled in water without loss of material from the membrane.

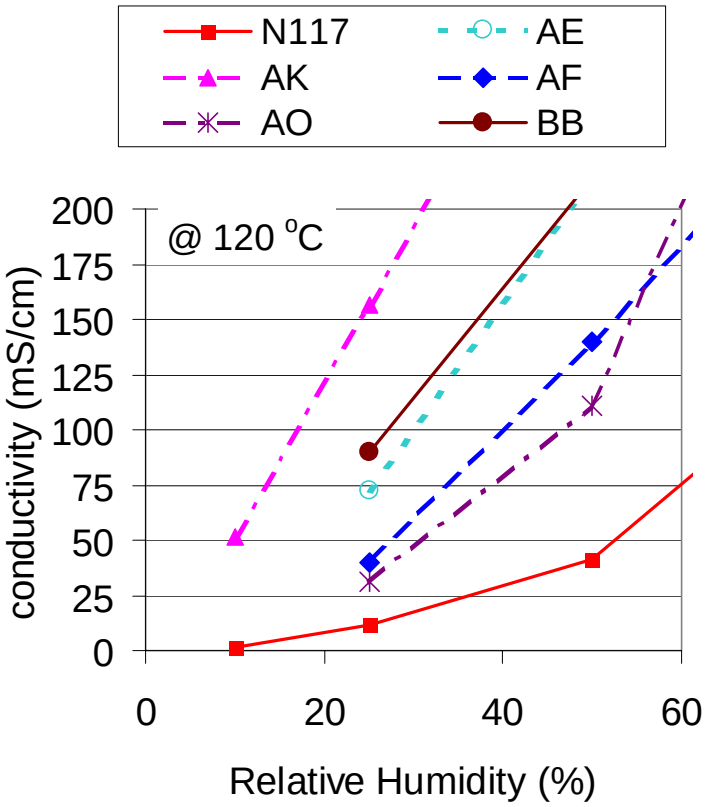

Figure 23. Conductivity for N117, AE, AK, AO, AF, BB *vs* RH, measured in-plane.

[1] BB is a polymer electrolyte that was not developed or synthesized under this program. AF was a polymer electrolyte previously developed at DuPont, but additional samples were synthesized under this program. Both had their conductivity evaluated under this program. While very attractive based on their conductivity, neither electrolyte proved to be thermally stable and were not investigated further.

Unfortunately, the thermal stability of AO was very low and the kinetic TGA method estimated an upper limit to lifetime of only 5 hr at 120 °C. Thermal degradation of the AO polymer was studied further in an attempt to understand the mechanism. It was concluded that degradation was initiated by an acid-catalyzed loss of fluoride ion from a CF_2 group (see Figure 24). The intermediate carbonium ion is believed to be stabilized by the presence of an electron donating group (EDG). Attack of water and further loss of HF would result in a carbonyl-containing compound, the presence of which was identified using ^{19}F NMR of the thermal decomposition products of a model compound for AO.

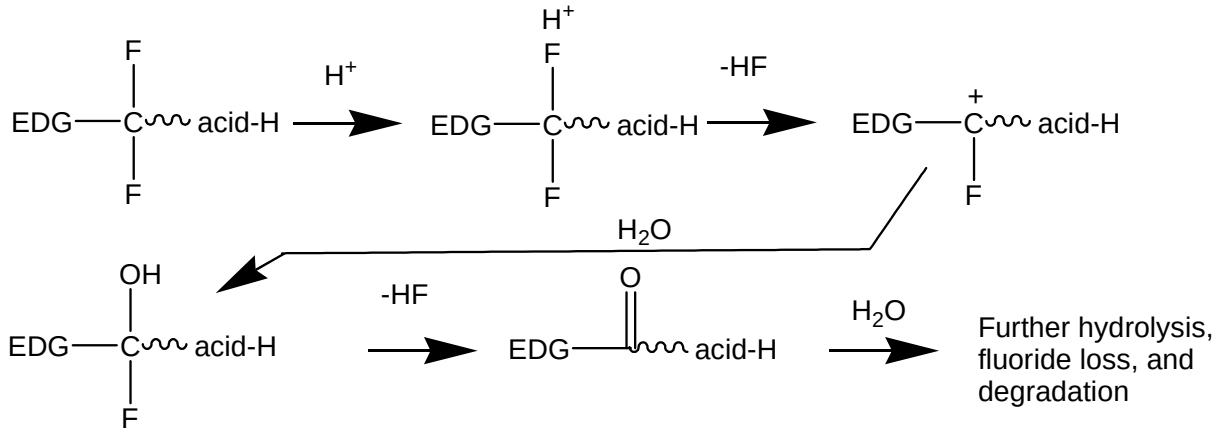

Figure 24. Schematic thermal degradation of AO.

The subsequent ionomers in this class, BG, AZ, and BA, were designed to alter the nature of the EDG to minimize thermal degradation. The results met with mixed success; upper limits to lifetime at 120 °C as estimated from kinetic TGA were 60,000, 200, and >100,000 hr for BG, AZ, and BA, respectively. All three of these could be boiled in water without weight loss. The low-RH conductivities (120 °C/25% RH) of these three membranes were 0.4, 10-14, and 14-30 mS/cm, respectively. Of the four candidates, AO, BG, AZ, and BA, only BA had a good combination of conductivity higher than Nafion® and thermal stability similar to Nafion®, so further work was focused on BA.

The relative ratios of the ionomer and the structural polymer may be varied in the BA membrane. The highest conductivities are obtained with increasing content of the ionomer portion as indicated in Figure 25. A trade off occurs with swelling and mechanical properties, which are poor for BA membranes with IEC above 1.7 meq/g. For the current fabrication process, the best compromise is in the range of 1.3 to 1.6

meq/g for which conductivity is 2X to 2.5X that of N117. Swelling by weight increase from vacuum-dried to boiling water is 62 %, which is higher than desired. One might view the results of Figure 25 as indicating that BA is a simple extension of Nafion®, however, note that straight-forward extension of PFSA membranes would result in solubility in boiling water at such high IEC's.

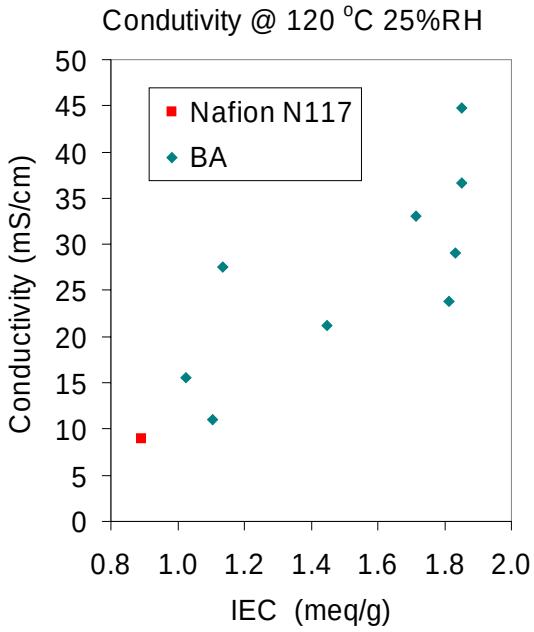

Figure 25. Conductivity for N117 and BA membranes fabricated with varying IEC.

During the fabrication of BA membranes, there is a step in which a reduced functional group is oxidized. If the oxidation is not complete, the residual reduced functional group acts as an impurity that limits thermal stability. In samples for which the amount of impurity was significantly reduced, the thermal stability of BA becomes very similar to that of Nafion®, as shown for isothermal TGA at 150 °C in Figure 26.

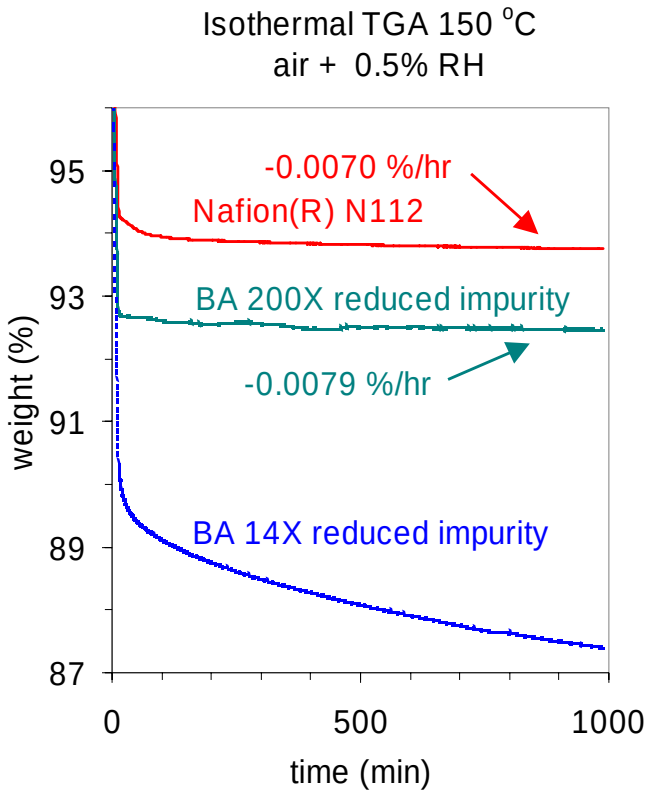

Figure 26. TGA weight loss for N112 and BA membranes.

In May 2005, five BA membranes, which had been oxidized using reagent A, were delivered to De Nora for fabrication of MEA's, then returned to DuPont for FC tests. All of these MEA's developed leaks during conditioning or shortly after initiation of testing, so that the membrane was failing for mechanical reasons. In the last half of 2005, it was realized that the oxidant used was likely damaging other parts of the membrane, which led to the MEA failures, such that some oxidized membranes had lower strength than expected, and that oxidation in some cases resulted in membrane thinning. Further work was done to identify reagents for the oxidation that were more active and selective. An alternative oxidant D was identified that gave membrane strength of 2.5 to 3.5 kPSI when the residual impurity had been reduced to below 1% (Figure 27). Four BA membranes oxidized using reagent D were sent in December 2005 to De Nora for single cell testing.

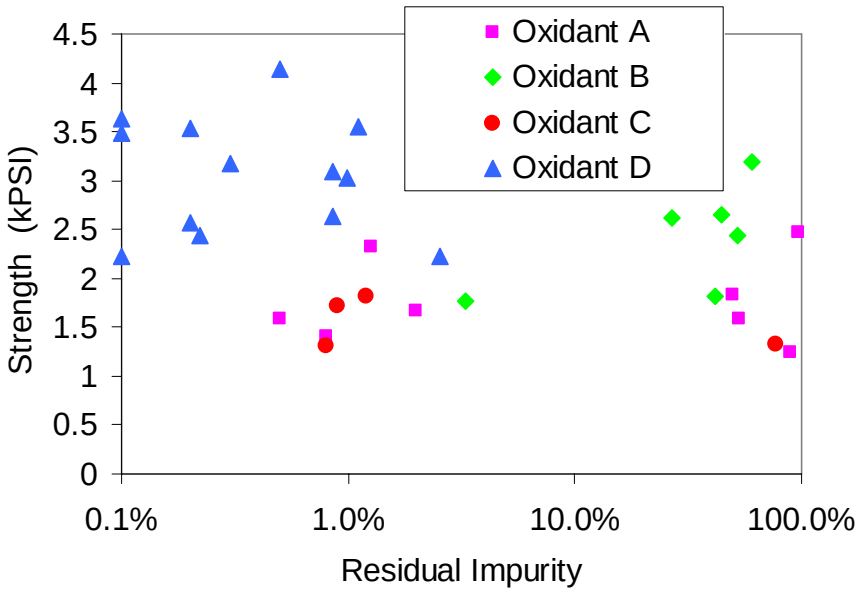

Figure 27. Strength *vs* residual impurity for BA membrane using alternative oxidants

MEA's were made using non-optimized GDE's with PFSA-containing electrodes. BA was tested in 25 cm^2 cells at 120 °C using a constant gas flow, which gave stoichiometry on both anode and cathode of 2 @ 1.2 A/cm^2; the RH reported is the RH at the inlet of the gas feeds. Generally, thinner membranes give higher performance, but have lower durability. The BA membrane tested was 53 um thick, which is similar to the thickness of the N112 comparison membrane. BA gave similar performance as N112 at high RH, but the BA MEA suffered a much smaller drop in performance on reducing RH to 25% @ 250 kPa than did N112 (Figure 28).

The current density and OCV for a durability cycling test of a BA membrane (oxidized using oxidant A) are shown in Figure 29 and Figure 30. At 161 hr, there was a test station failure followed by a restart (symbols change from blue to magenta). At 217 hr, the current peaked for an unknown reason, but possibly due to a drop in dry gas feed rate. This was followed by a sudden cell death. Another BA membrane (data not shown) suffered a more gradual drop in both current density and OCV (880 mV down to 750 mV at 230 hr), followed by rapid decline in 25% RH current to 100 mA/cm^2 and OCV below 660 mV at 270 hr. Thus the durability of the BA membrane in these first steps is similar to, or slightly better, than that of N112 (Figure 11). Nafion® has unstable end-groups, which are removed to obtain increased durability. Further work is needed to establish whether this also holds for BA membranes.

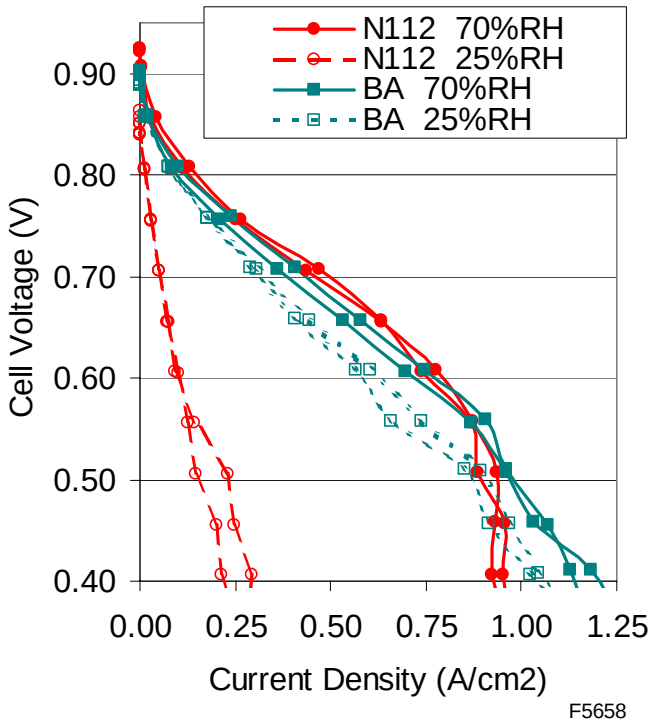

Figure 28. Polarization curve for N112 and BA MEA's with H_2/air at 250 kPa.

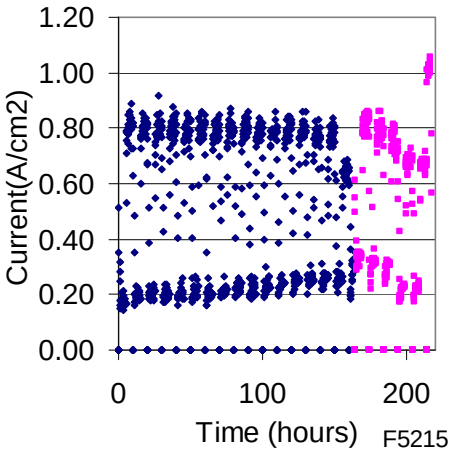

Figure 29. Current for BA in HT6

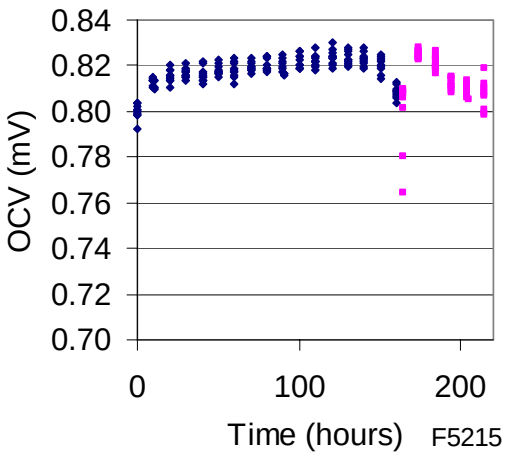

Figure 30. OCV for BA in HT6

4.6. Lower-Temperature Conductivity

Targets for membranes in 2010 include conductivity at –20 °C of 10 mS/cm and survivability to –40 °C (Table 1). Conductivity was measured at sub-ambient temperature as follows: A four-point probe fixture was made consisting of a Teflon® block with four gold wires embedded in it. The membrane strip (10 mm X 30 mm) was

laid on the block, covered with another Teflon® block, and the two blocks pushed together to force the membrane in contact with the strip electrodes. The geometry was similar to that of Figure 6, except there were no slots in the blocks that would allow equilibration with the surrounding air. However, one edge of the membrane was still exposed to the air within the glass bottle. The fixture was mounted in a glass jar that was immersed in a variable temperature chilled bath. The temperature within the jar near the sample was monitored with a thermocouple. Initial measurements were made on a Nafion® N117 membrane that had been acid washed, water washed, and boiled (fully swollen). On cooling from ambient to –10 °C, the conductivity dropped to 29 mS/cm. However, on heating back to 20 °C the conductivity recovered to only 59 mS/cm, not the original 92 mS/cm (Figure 31).

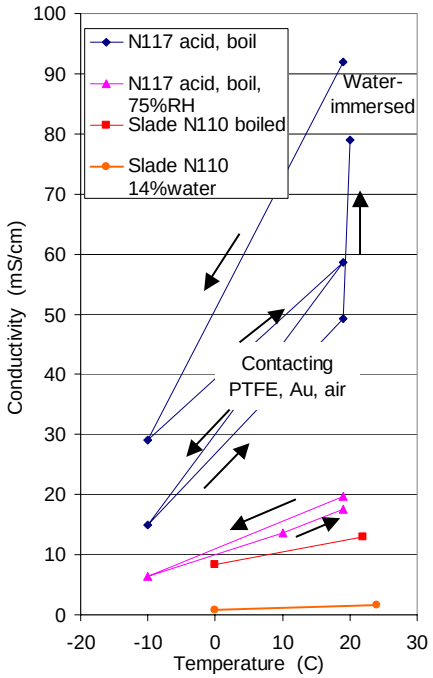

Figure 31. Low-T conductivity of N117.

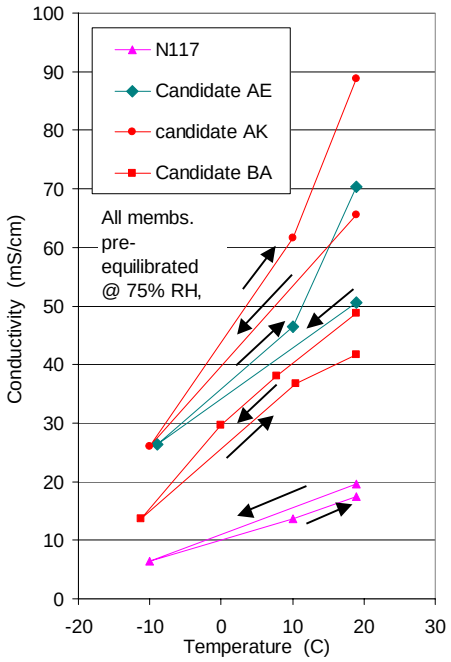

Figure 32. Low-T conductivity of AE, AK, BA.

On a second cycle, the conductivity dropped to 15 mS/cm at –10 °C, but it partially recovered to 79 mS/cm upon standing after rewarming to 20 °C. The non-reproducibility might be due to loss and regain of water in the membrane, or to changes in the membrane conductivity caused by the cooling that are independent of water content. A membrane with lower water content was prepared by equilibrating the acidified, water-washed N117 for more than 18 hr over a sodium chloride/water slush, which produces ~75% RH. For this partially-

dried membrane, the cooling/warming cycle gave a smaller hysterisis, though the conductivity levels were not as high. For comparison, measurements[24] on N1100 membranes of two different water contents are also shown. Note that the value of 13 mS/cm at 20 °C for a fully humidified Nafion® membrane (Slade et al.) is much lower than the currently accepted value[7]. Examining only the relative changes, the conductivity was lowered by 2.1 to 3.1X (–10 °C *vs* 20 °C), while it was lowered by 2.0X for the membrane containing 14% water.

The same technique was applied to measuring the conductivities of polymer electrolytes AE, AK, and BA, which had been pre-equilibrated with ~75% RH over $NaCl/H_2O$ slush. These electrolytes also lose conductivity at lower temperature, though the relative ranking obtained from 120 °C is still maintained with BA being intermediate between Nafion® and AK or AE.

In an attempt to gauge progress against the conductivity targets for below –10 °C, a different apparatus was employed. Water-wet membranes were loaded into the fixture of Figure 6 (in-plane conductivity), the fixture was sealed into a plastic bag, and the bag placed into a GC oven that was equipped with a liquid-nitrogen-cooled cryogenic temperature controller. The membrane was held at each temperature for 1 to 4 hours, typically 2 hours. The Nafion® membrane was a dispersion-cast film of ~50 μm thickness and nominal 0.97 meq/g IEC (NRE212). The BA membrane was found to have a significant conductivity advantage over the Nafion® membrane only down to ~–25 °C; both membranes gave the same conductivity at –40 °C. A single cycle gave little hysterisis between –40 and 0 °C, but for both membranes the conductivity was lower upon returning to 25 °C. Either of these *initially-fully-hydrated membranes* would meet the target of 10 mS/cm @ –20 °C. However, extrapolation to –20 °C of the measurements in the first apparatus with *partially dried membranes* would suggest that only AE or AK, but not Nafion® or BA, would meet the target.

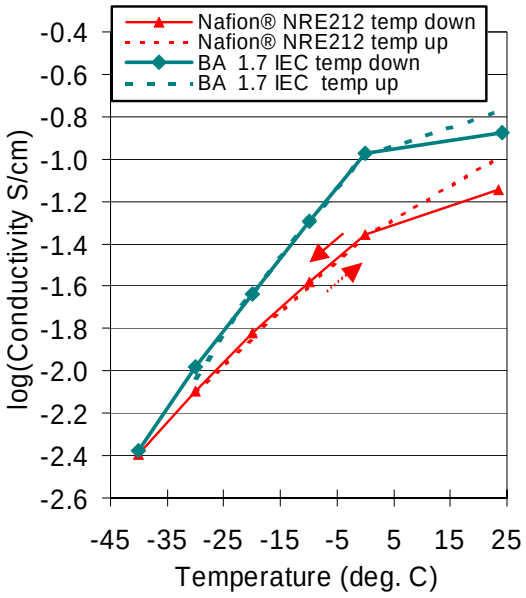

Figure 33. Low-T Conductivity of NRE212 and BA.

4.7. Case Western – Uncollapsible Domains

(Note: References for this section are numbered starting with 3 and collected at the end of this section.)

In order to expand the scope of the work on rigid-rod polyphenylene sulfonic acid materials and to understand how polymer architecture affects the water retention and conductivity, polymers were designed with even greater control over the architecture. With this in mind, an advanced molecular design strategy was proposed and developed (Figure 34).

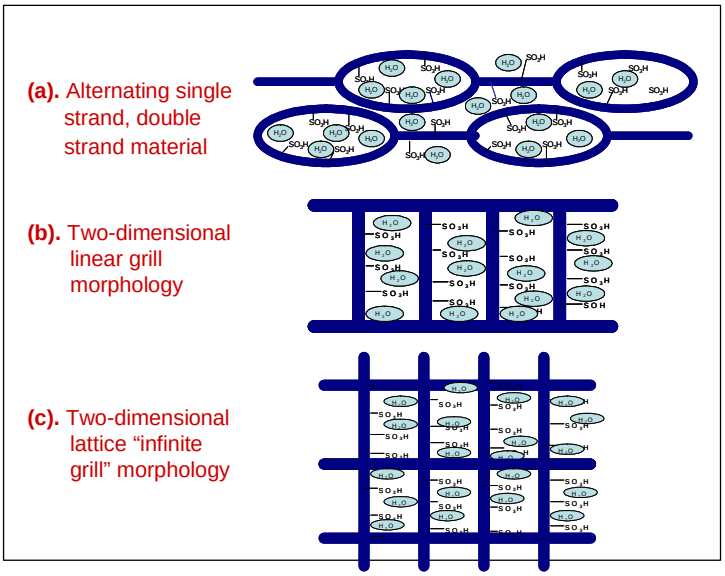

Figure 34. Some possible new sulfonated polymer architectures

Some possible new polyphenylene sulfonic acid architectures

Initial work was focused on the synthesis of the linear/double strand materials (Figure 34**a**). We felt that these materials would be the simplest to synthesize and characterize. Early synthesis attempts using sulfonic acid salts led to a number of problems purifying intermediates. It was found that the ionic products were difficult to separate from ionic impurities. The synthetic route was modified replacing sulfonic acid salts with sulfonate esters to simplify purification. More difficulties were encountered when applying boronic acid materials in excess to prevent polymerization. These problems combined with our trouble obtaining the sulfonate esters forced us to rethink our synthetic strategies.

Redesign of the sulfonate ester synthesis and application of protecting groups provided an alternate synthetic pathway to the linear/double strand polymers (Figure 34**a**). The revised synthesis method allowed us to obtain the sulfonate esters in high purity and acceptable yields from readily available starting materials. Use of sulfonate esters eliminated purification difficulties associated with ionic sulfonic acid salts. Incorporation of protecting groups provided an alternate route to half-cycle materials while preventing the need to apply boronic acid materials in excess. We synthesized the protected half-cycle materials, but opted to test protecting group conversion reactions on simpler compounds.

Starting with intermediates previously obtained in the synthesis of the linear/double strand materials, we developed a simplified synthetic pathway to reduce the number of intermediates needed to make the final polymer structure. We proposed a smaller version of the linear/double strand polymer that bypassed the need to synthesize oligomeric sulfonic acid intermediates. We chose to test the protecting group conversion reactions on these simplified materials. Although we were able to transform the protecting groups, we were unable to obtain the deprotected half-cycle in its pure form. This led us to develop an alternative method for synthesis of the cycle precursor materials. We designed a secondary synthetic pathway, but were unable to obtain the key intermediate for this route. Emphasis was shifted back to optimization of previous methods and purification of obtained materials.

Using previously synthesized intermediates, we developed a plan to produce two-dimensional “infinite” grill materials (Figure 34**c**). We chose to synthesize a protecting group containing precursor polymer that would be used as a framework to support the sulfonated biphenyl units. Purification and characterization was difficult due to its poor solubility in nearly all common solvents. Attempts were made to convert the protecting groups of the polymer to functional groups despite incomplete characterization. Because of these difficulties, we eventually concentrated work on an even simpler system that is based on small-molecule intermediates.

Our current work is concentrated on the simplest possible method to make the two-dimensional “infinite” grill architecture (Figure 34**c**). Only two synthesis steps are needed to get from previously synthesized materials to the final grill polymer. We will begin by highlighting our most recent progress on the various structures followed by a detailed account of all previous synthesis and design strategies since the beginning of the project.

Simplified "infinite" grill polymer (Figure 34***c,*** Figure 35***)***

In an effort to simplify and expedite the process of obtaining a final product with a two-dimensional structure, a simplified version of the "infinite" grill polymer was designed. This approach provides the least complex synthetic route to the final polymer. This structure is advantageous because each uniform hexagonal cycle contains only six non-sulfonated rings, giving the material a high degree of sulfonation. The cycle size is significantly wider than any of the previously proposed materials, which may allow more water to be stored in the polymer. The synthesis is shown in Figure 35.

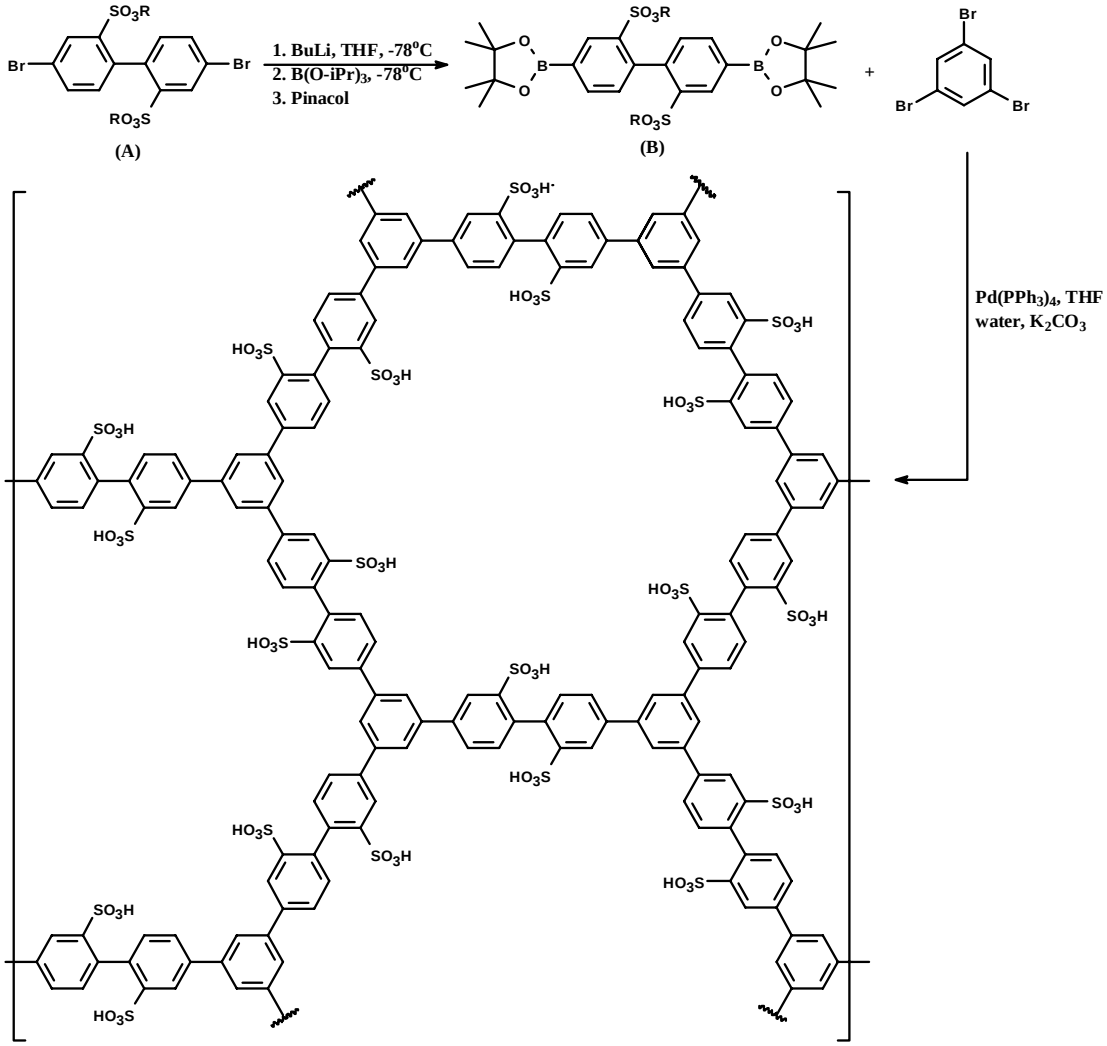

Final Polymer Structure

Figure 35. Simplified polymer

Simplified uniform hexagonal 2-D "infinite" grill polymer

The final polymeric structure can be synthesized in two steps from the 4,4'-dibromobiphenyl-2,2'-disulfonate ester (Figure 35, **A**). We have been able to successfully synthesize the 4,4'–biphenyldiboronic acid-2,2'disulfonate ester (Figure 35, **B**) and are currently in the process of purification and optimization of the reaction conditions. To the best of our knowledge, this is the first report of a sulfonated boronic acid compound. We hope to obtain the first polymeric materials and begin collecting data regarding water content and conductivity in the near term.

Small cycle linear/double strand polymer (Figure 34***a,*** Figure 36***,*** Figure 37***)***

Continuing work on linear/double strand materials described later, we designed a simplified structure with fewer intermediates and reaction steps needed to obtain the final polymer. We chose to use the 4,4'-dibromobiphenyl-2,2'-disulfonate ester (Figure 36, **A**) rather than the originally proposed pentaphenylenetetrasulfonic acid (Figure 43, **S**) or its ester to reduce the number of reaction steps. This results in a smaller cyclic material. Coupling of one equivalent of the 4,4'-dibromobiphenyl-2,2'-disulfonate ester (Figure 36, **A**) with two equivalents of 3-trimethylsilylbenzeneboronic acid (Figure 36, **C**) produced the ditrimethylsilyl-protected quaterphenyldisulfonate ester (Figure 36, **D**).

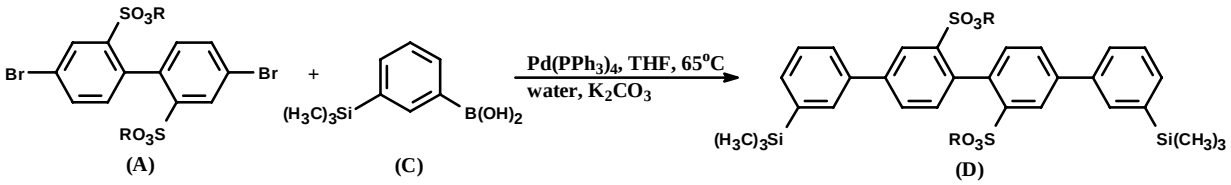

Figure 36. Synthesis of intermediate

Synthesis of small half-cycle ditrimethylsilylquaterphenyldisulfonate ester

This material was easily purified and obtained in high purity. It was found however that reaction to the quaterphenyldiboronic acid (Figure 37, **E**) was much more complicated than anticipated.

Initially, the product obtained from the reaction with boron tribromide was a mixture of partially and fully reacted materials as well as other byproducts. We attributed the partial conversion to old, impure boron tribromide/methylene chloride solution. After obtaining new, pure boron tribromide and modifying the reaction conditions, using a longer time and a larger excess of reagent, the trimethylsilyl substituents were completely replaced. Figure 37 depicts the synthesis of the smaller cycle (**F**) and linear-double strand polymer.

Purification of the crude quaterphenyldiboronic acid (Figure 37, **E**) proved very difficult despite many attempts to recrystallize, extract, and chromatograph the mixture. Efforts to reduce byproducts of the reaction by careful set up and purified reagents also proved ineffective in obtaining the quaterphenyldiboronic acid in purity that was acceptable to begin cyclization reactions. We therefore searched for alternative synthesis methods to obtain the quaterphenyldiboronic acid (Figure 37, **E**)

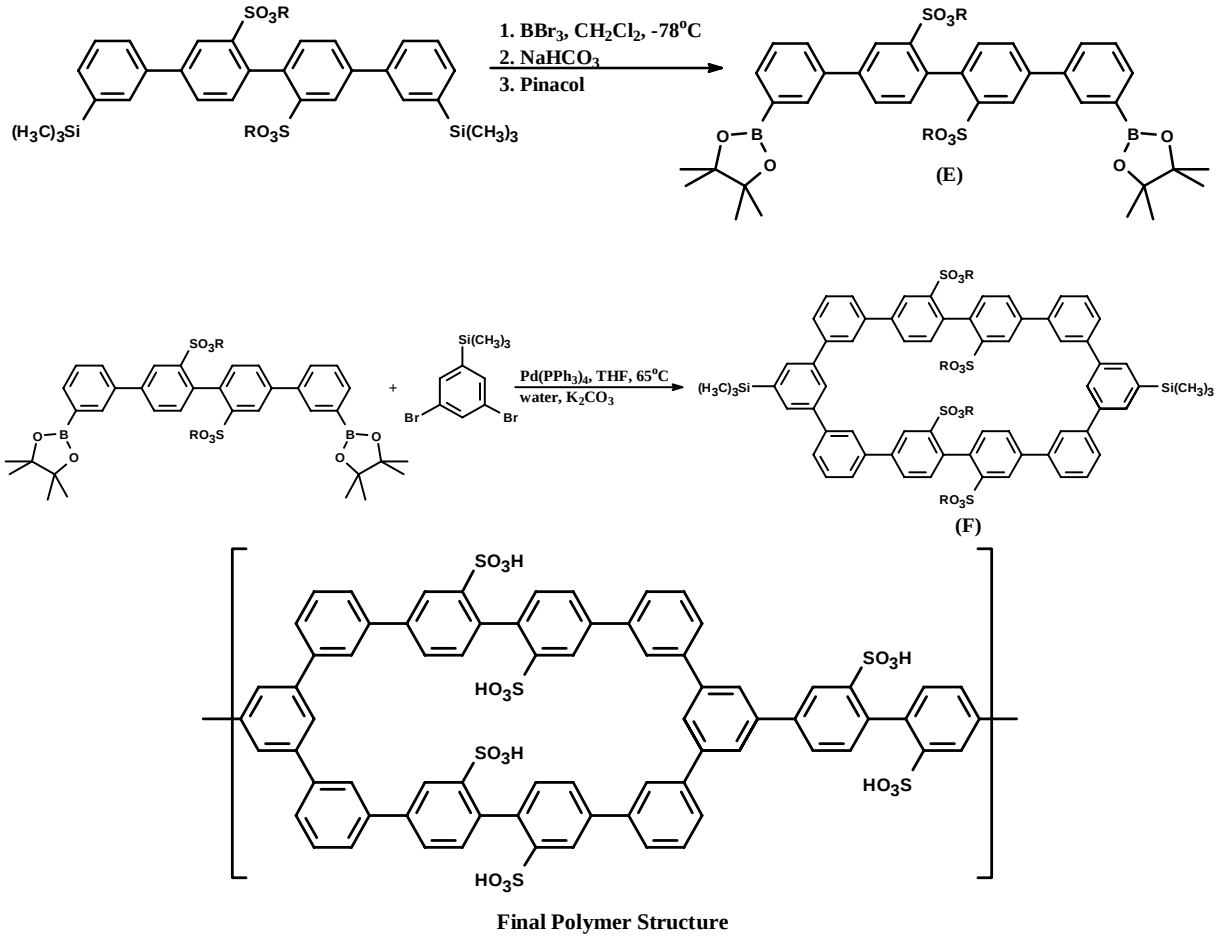

Figure 37. Synthesis of simplified polymer

Synthesis of simplified, small linear-double strand polymer

Alternate approach for small cyclic material

Difficulties in synthesis and purification of half-cycle compound (Figure 37, **E**), prompted us to explore alternate synthetic pathways. It has been well documented that alkyltin compounds undergo palladium-mediated coupling reactions commonly referred to as the Stille coupling[3]. Yamamoto and coworkers found that trialkyltin functionalities react preferentially to boronic acid ester functionalities when Stille

coupling conditions were applied[4]. This enabled the design of an alternate pathway to the desired half-cycle quaterphenyldiboronic acid (Figure 37, **E**) that would directly introduce the boronic ester functionality and was compatible with the sulfonate materials. The key intermediate in this synthetic scheme was 3-tributylstannylbenzeneboronic acid pinacol ester (Figure 38, **K**).

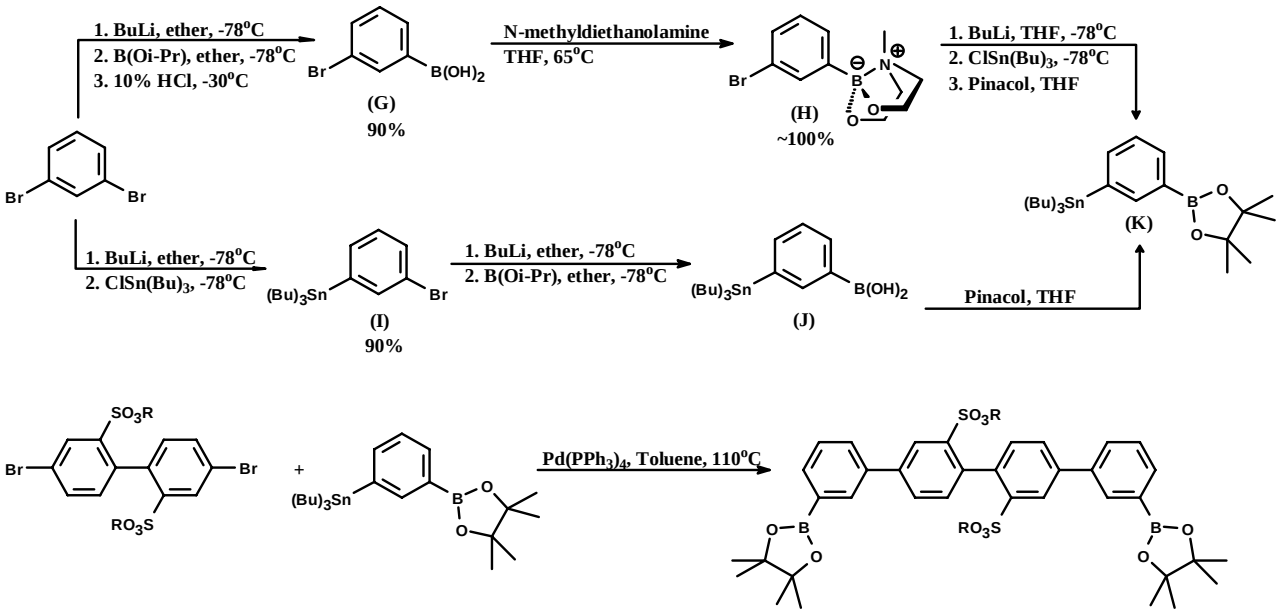

Figure 38. Synthesis of intermediates

Synthesis of intermediates through Stille coupling route

Both pathways illustrated in Figure 38 were attempted. We were able to introduce either the tributylstannyl or boronic acid functionalities on the dibromobenzene. Reaction conditions necessary for introduction of the boronic acid group on the 3-bromotributylstannyl benzene (Figure 38, **I**) seemed to displace or destroy the tributylstannyl group. Alternately, attempts to introduce the tributylstannyl group on the 3-bromobenzeneboronic acid N-methyldiethanolamine ester (Figure 38, **H**) led to complicated mixtures of materials that could not be separated or easily identified by conventional techniques. Unfortunately, neither path led to the final product in usable form. It was concluded that this method was not an effective means to obtain the final half-cycle quaterphenyldiboronic acid (Figure 37, **E**).

Efforts were shifted back to synthesis and purification of the quaterphenyldiboronic acid (Figure 37, **E**) by conversion of the trimethylsilyl groups to boronic acids using boron tribromide. We are currently working on the optimization of the trimethylsilyl-boronic acid exchange and purification of the obtained materials.

Alternate synthetic route to linear-double strand polymer (Figure 34***a)***

Much of the previously described work dealing with the small linear/double strand materials and the simplified "infinite" grill materials was based on ideas and materials developed during the redesign of the synthesis of the originally proposed linear/double strand materials. We will detail the development of this alternate approach to the linear/double strand materials and highlight key intermediates that are important to the synthesis of several of the polymeric structures.

Redesign of the monomer

Due to the difficulties we encountered in our early synthetic attempts in converting the 4,4'-diiodobiphenyl-2,2'-disulfonic acid (Figure 43, **S**) to the disulfonyl chloride and then to the sulfonate ester, an alternate synthesis scheme was designed that bypassed the diazotization reaction. Based on our group's experience with copper-mediated Ullmann coupling, a new synthetic plan was proposed (Figure 39).

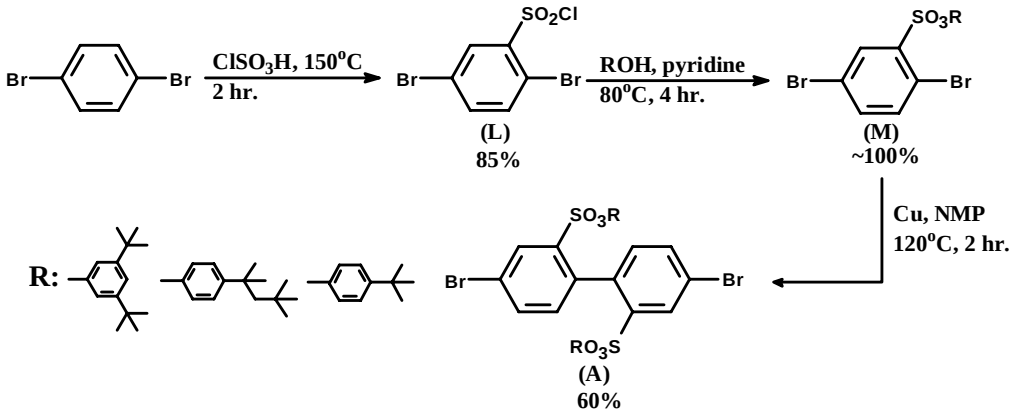

Figure 39. Direct synthesis of sulfonated intermediates

Direct synthesis of 4,4'-dibromobiphenyl-2,2'-disulfonate esters

The literature documents that the Ullmann reaction is accelerated by electron-withdrawing groups *ortho* to the halogen atom[5]. Electron-withdrawing groups in the *meta* or *para* position do not promote the coupling of the compound. It was therefore concluded that the coupling of a dihalogenated aromatic ring with an electron-withdrawing group ortho to one halogen atom and meta to a second halogen atom will couple primarily to a biphenyl with both electron-withdrawing groups ortho to the newly formed bond (electron withdrawing groups become 2,2'-substituents in the biphenyl). Work done by both Yamato and coworkers[6], and Jian and coworkers[7] confirms that it is possible to couple 2,5-dibromo-nitrobenzene to make 4,4'-dibromo-

2,2'-dinitrobipheny in high yields. Both Kice and coworkers[8], and Armarego and coworkers[9] demonstrated that sulfonate esters can be coupled using the Ullmann reaction, 2-iodobenzene phenylsulfonate was coupled to make biphenyl-2,2'-di(phenylsulfonate). With this knowledge, we set out to develop an alternate synthetic method to the desired 4,4'-dibromobiphenyl-2,2'-disulfonate ester using readily available starting materials.

Conversion of 1,4-dibromobenzene directly to the sulfonyl chloride (Figure 39, **L**) was an extremely simple, high yield reaction, and was much simpler than our failed earlier approach. The disulfonyl chloride could be converted almost quantitatively to the alkyl-substituted phenol ester to yield a 2,5-dibromobenzene(alkylphenyl)sulfonate (Figure 39, **M**), which could be coupled using the copper-mediated Ullmann reaction to give the final 4,4'-dibromobiphenyl-2,2'-disulfonate ester (Figure 39, **A**).

Ullmann coupling of the 2,5-dibromobenzenesulfonate ester (Figure 39, **M**) gave acceptable yields of the final 4,4'-dibromobiphenyl-2,2'-disulfonate ester monomer (Figure 39, **A**). The product was easily isolated from the reaction mixture and readily purified by a combination of column chromatography and recrystallization.

Preventing boronic acid wastage

In our early studies, we found that there was significant wastage of boronic acid materials when used as an excess reagent. We sought to overcome this problem by the use of a protecting group on a mono-boronic acid compound. 3-trimethylsilylbenzenenboronic acid was easily synthesized from 1,3-dibromobenzene to give good yields of protected boronic acid. The synthesis is shown in Figure 40.

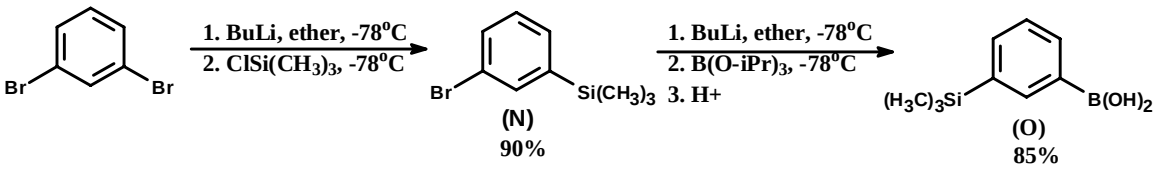

Figure 40. Synthesis of monofunctional intermediate

Synthesis of monofunctional protected boronic acid

Reaction of a large excess of 4,4'-dibromobiphenyl-2,2'-disulfonate ester (Figure 39, **A**) with 3-trimethylsilylbenzeneboronic acid (Figure 40, **O**) gave the mono-reacted, trimethylsilyl-protected terphenyl (Figure 41, **P**). The product was easily separated from the excess (**A**) by extraction and purified by column chromatography.

This method allowed complete recovery of unused (**A**) after the reaction was complete. The revised synthetic scheme is shown in Figure 41.

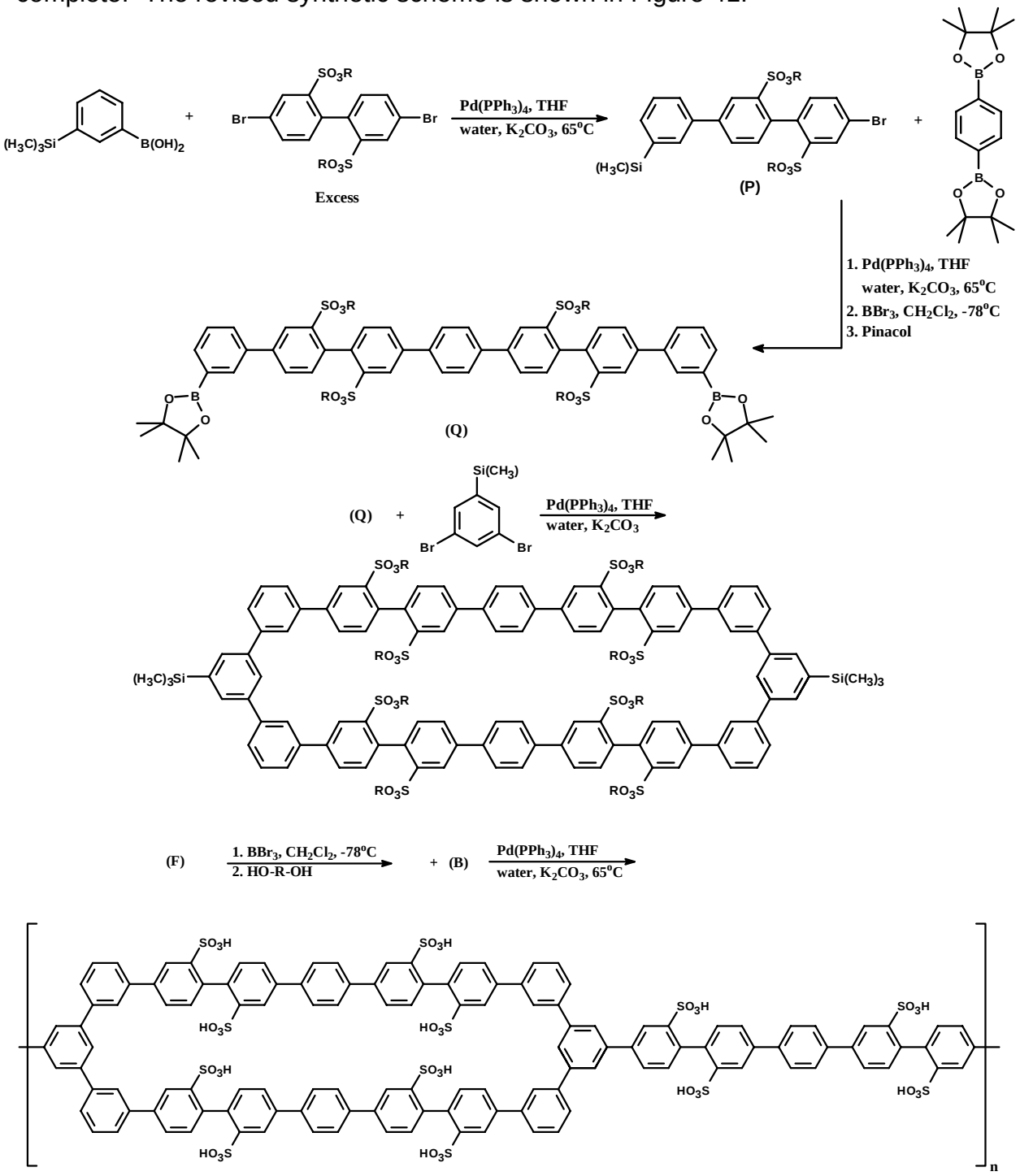

Figure 41. Alternate approach to polymers

Alternate approach to the synthesis of linear-double strand polymers

Two equivalents of terphenyl (Figure 41, **P**) were coupled with one equivalent 1,4-phenylenebisboronic acid to make a trimethylsilyl-protected heptaphenyltetrasulfonate ester half-cycle (Figure 41, **Q**). This circumvented the need to use an excess of boronic acid to obtain high yields of intermediates for the cyclic material (Figure 41, **F**). We succeeded in synthesizing the heptaphenyltetrasulfonate ester, but chose to work with the previously described smaller half-cycle precursor to test the trimethylsilyl to boronic acid conversion reactions.

Modified polymer-based "infinite" grill structure (Figure 34***c,*** Figure 42***)***

Initial work on the two-dimensional structures focused efforts on a "infinite" grill polymer that was modified from the initially proposed structure. We sought to use intermediates that were already obtained from previous work. Having both 3,5-dibromotrimethylsilyl benzene (Figure 43, **V**) and 1,4-phenylenebisboronic acid pinacol ester in high purity, work was started on a precursor polymer to the infinite grill morphology. We chose to use 4,4'-dibromobiphenyl-2,2'-disulfonate ester (Figure 35, **A**) rather than originally proposed pentaphenylene tetrasulfonic acid (Figure 43, **T**) to simplify test reactions for synthesizing the grill polymers. The final structure would have a more hexagonal, less elongated cycle size than the previously described linear-double strand, ladder-type, or "infinite" grill polymers. Figure 42 illustrates the synthetic scheme designed and applied to make these grill polymers.

Initial polymerization reactions to make the precursor trimethylsilyl-substituted polymer were setup using equivalent conditions to those used for previous Suzuki coupling reactions. The use of tetrahydrofuran as the solvent resulted in precipitation of the coupled material after several hours, thus limiting the molecular weight attainable. A switch to toluene as the solvent allowed the polymer to grow until the solution gelled. The final product of the reaction was a *meta-para* linked polyphenylene with trimethylsilyl substitution on every other ring.

Purification and characterization of the polymer was difficult due to poor solubility of the final product. After gelation, the polymer was insoluble or poorly soluble in all common organic solvents. Although the polymer is flexible due to *meta*-linkages, it is likely that *para*-linked terphenyl units between each *meta*-linkage are large enough to allow some aggregation of polymer chains, thereby reducing solubility. If the polymer was rendered more flexible or if a greater number of longer-chain trialkylsilyl groups were introduced, the solubility would be likely be increased.

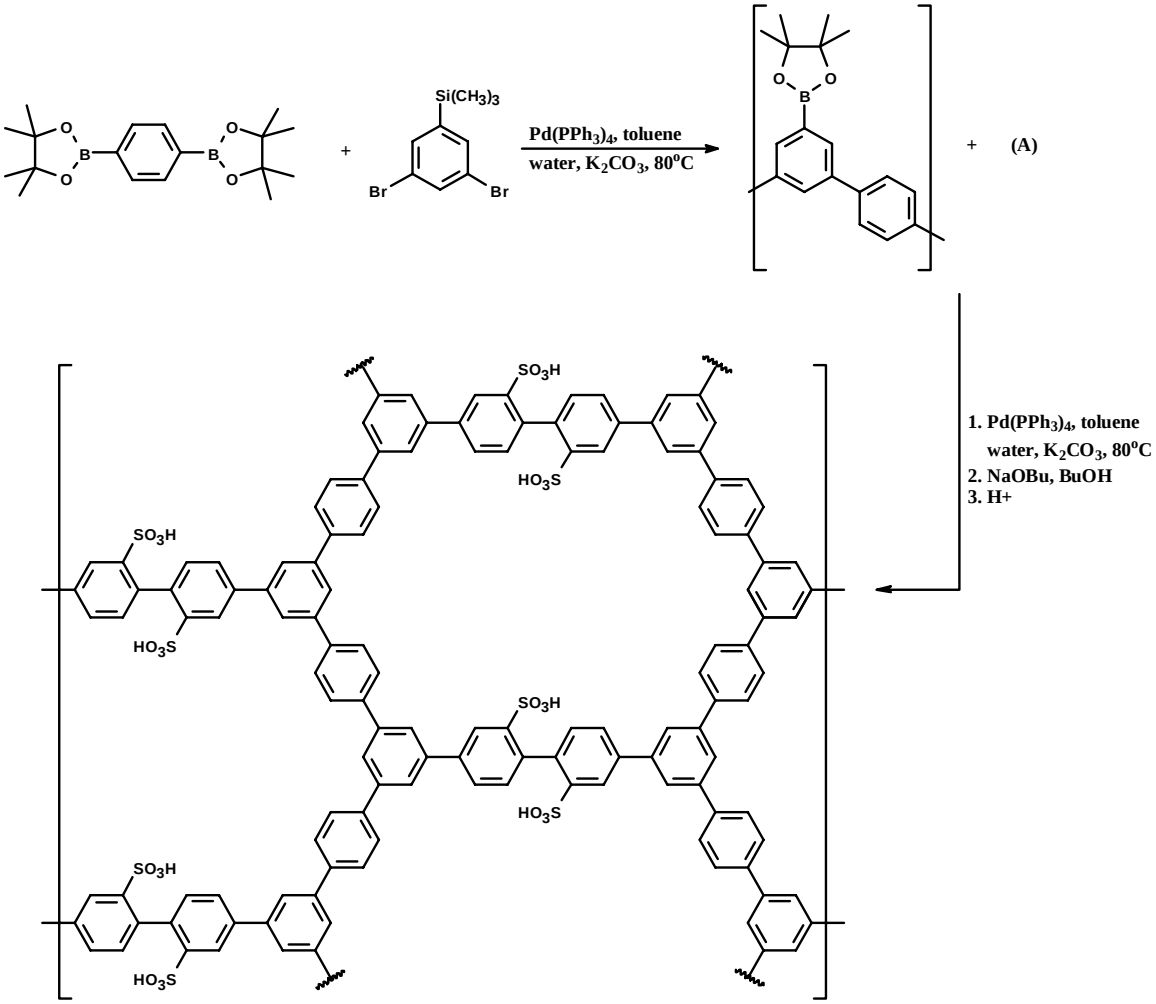

Figure 42. Applied synthesis scheme for alternate polymer

Applied synthesis scheme for alternate "infinite" grill polymer

Reactions to convert the trimethylsilyl groups to boronic acids were conducted even though characterization of the precursor polymer was difficult and incomplete. Initially, it was found that polymers contained a significant percentage of trimethylsilyl groups after reaction. After applying conditions similar to those used for the synthesis of the small linear-double strand quaterphenyldiboronic acid (Figure 37, **E**), the amount was reduced to minimal levels. Due to the difficulties with synthesis and characterization, we eventually shifted focus from polymer based infinite grill materials to the simplified infinite grill system previously described.

Development of early synthetic methods

Palladium-mediated Suzuki coupling of aryl boronic acids with aryl halides was chosen as the primary route to the synthesis of all the proposed polymeric materials

and many of the intermediates. This synthetic method has the advantage of working well in the presence of many functional groups and solvents.

4,4'-diiodobiphenyl-2,2'disulfonic acid (Figure 43, **S**) was chosen as the initial monomer since it can be made in a single step from commercially available 4,4'-diaminobiphenyl-2,2'-disulfonic acid (benzidine-2,2'-disulfonic acid). It is desirable to have the sulfonic acids in the 2,2' positions of the biphenyl since all proposed polymeric structures and many of the intermediates have non-sulfonated rings next to the sulfonic acid containing rings. A sulfonation level of 66% is the highest percentage that can be attained using the proposed Suzuki polycondensation method; there have been no reports of sulfonated boronic acids to the best of our knowledge.

4,4'-Dibromobiphenyl-3,3'-disulfonic acid has been synthesized in our lab, however use of this compound would place a sulfonic acid *ortho* to an electron rich non-sulfonated benzene ring. This would allow side-reactions, forming a cyclic sulfone by attack of the sulfonic acid on the neighboring ring at high temperatures and dry conditions.

Initial synthesis was performed using the potassium salt of 4,4'-diiodobiphenyl-2,2'-disulfonic acid (Figure 43, **S**). This salt was chosen to prevent cation exchange with the Suzuki coupling base, potassium carbonate. Previous work by Novak and coworkers suggested that the lithium salts of carboxylic acids[10] could be coupled in the Suzuki reaction.

Several test reactions were run in order to determine if it was possible to couple sulfonic acid salts using palladium catalyzed Suzuki coupling. A test polymerization of the potassium salt of 4,4'-diiodobiphenyl-2,2'-disulfonic acid (Figure 43, **S**) and 1,4-phenylenebisboronic acid was performed to determine if linear, high molecular weight polymer could be attained. Coupling was found to take place; however no high molecular weight polymer was isolated. The main problem in the formation of polymer was the difficulty in obtaining extremely pure 4,4'-diiodo-2,2'-biphenyldisulfonic acid (Figure 43, **S**) from the diazotization reaction, thus offsetting stoichiometry. The 1,4-phenylene bisboronic acid was easily purified by conversion to the pinacol ester followed by column chromatography and recrystallization. Ionic materials such as sulfonic acid salts cannot be purified using conventional chromatographic techniques due to strong interactions with the adsorbent. It was therefore difficult to attain the level of purity necessary for a polycondensation reaction.

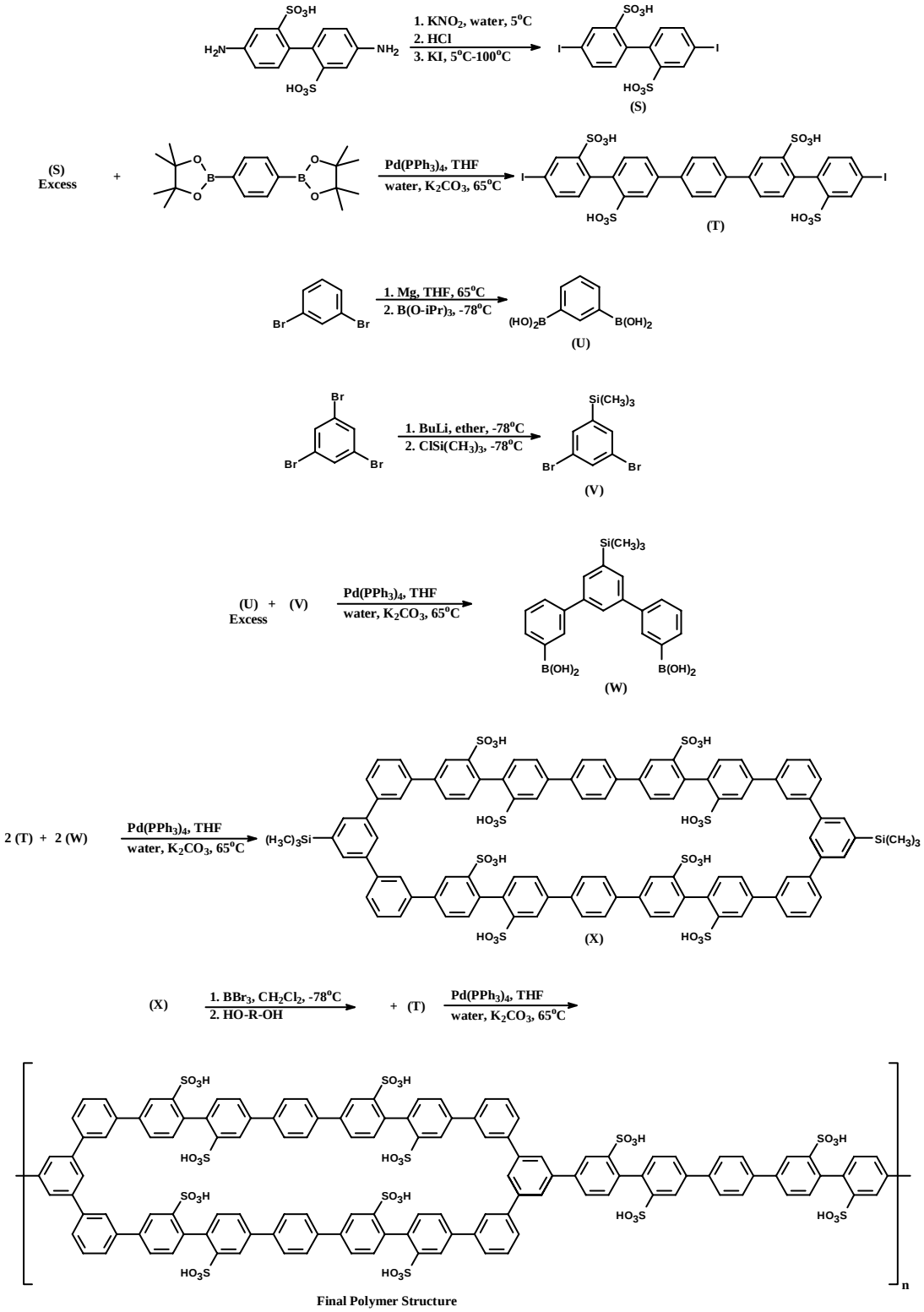

Figure 43. Initially proposed synthesis route for polymer

Initially proposed synthesis route for linear/double strand polymer

Early synthesis of alternating single/double strand polymer (Figure 34***a,*** Figure 43***)***

Initially, synthesis of pentaphenylenetetrasulfonic acid (Figure 43, **T**) was attempted, using a large excess of 4,4'-diiodobiphenyl-2,2'-disulfonic acid (Figure 43, **S**) relative to 1,4-phenylene bisboronic acid. Polymerization was discouraged by using 4,4'-diiodobiphenyl-2,2'-disulfonic acid (Figure 43, **S**) in excess. It was therefore unnecessary to start with extremely high purity materials. However, the mixture of coupled product (Figure 43, **T**) and excess 4,4'-diiodobiphenyl-2,2'-disulfonic acid (Figure 43, **S**) was extremely difficult to separate. This prompted us to devise alternative methods for obtaining the pentaphenylene tetrasulfonic acid material (Figure 43, **T**).

After reevaluation of the literature regarding Suzuki coupling and Suzuki polycondensation, it was found that sulfonic acid containing materials could be made if they were reacted as sulfonate esters[11]. Conversion of the sulfonic acids to esters also had the advantage of rendering all intermediates soluble in organic solvents, allowing the use of conventional chromatographic techniques for purification.

Several later reactions need to be run in organic solvents, making conversion of sulfonic acids to esters even more desirable. Reactions involving the conversion of trimethylsilyl groups to boronic acids, needed to synthesize the cyclic compound (Figure 43, **X**), must be done in organic solvents to ensure all species are soluble in a homogeneous reaction medium. Subsequently, sulfonate esters can be hydrolyzed quantitatively to the corresponding acids by reaction with sodium butanolate in butanol, followed by acidification[8-9, 11].

In order to synthesize the sulfonate esters, it was necessary to convert the 4,4'-diiodobiphenyl-2,2'-disulfonic acid (Figure 43, **S**) to the disulfonyl chloride (Figure 44). The product from this method must be isolated very carefully and rapidly to prevent significant hydrolysis of the disulfonyl chloride. Despite many attempts, we were unable to obtain pure, unhydrolyzed acid chloride.

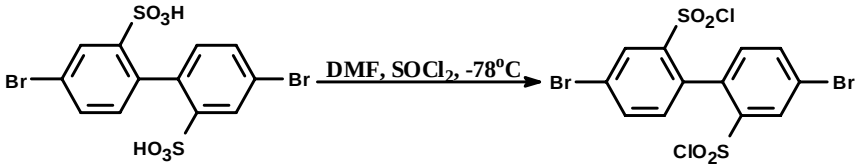

Figure 44. Synthesis of intermediates

Synthesis of sulfonyl chlorides from sulfonic acid materials

Another unanticipated problem occurred during the synthesis of the trimethylsilyl-protected *meta*-terphenyldiboronic acid (Figure 43, **W**). It was found that the use of excess diboronic acid under Suzuki coupling conditions caused significant wastage of unconsumed boronic acid due to deboronification reactions. In some cases, upwards of 20-30% could not be recovered after the reaction. This was unacceptable since the boronic acid recovery was necessary for use in future reactions. We remedied these problems with the use of protecting groups described in the alternate synthesis of the linear/double strand materials.

Early two-dimensional "infinite" grill polymer design

In order to maximize the void volume of the polyphenylene sulfonic acid polymers, two-dimensional "infinite" grill structures were designed. These graphite-like porous structures were intended to impart control over two-dimensional free-volume. The initially proposed two-dimensional structure is shown in Figure 45.

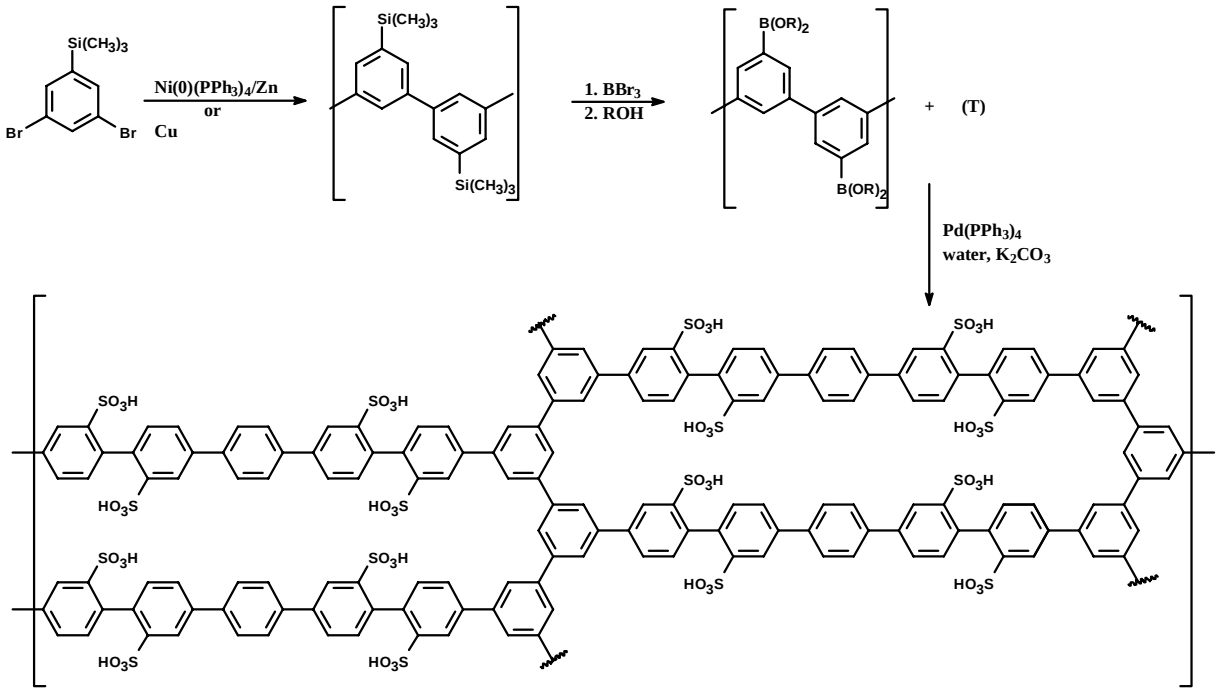

Figure 45. Initially proposed synthetic method for polymer

Initially proposed synthetic method for 2-D "infinite" grill polymer

We chose to work on the modified polymer-based variation of this approach as previously described rather than the explicitly proposed synthesis. A single reaction was attempted to determine if the 3,5-dibromotrimethylsilylbenzene (Figure 43, **V**) could be polymerized by copper-mediated Ullmann coupling. It was found that under

the applied reaction conditions, no coupling could be detected and no starting material was recovered.

Ladder-type polymer (1-D grill)

Initially, a linear one-dimensional ladder-type polymer was proposed as a variant of the linear-double strand materials that would maximize the free volume in a linear polymeric structure. Figure 46 depicts the synthetic approach applied to make an idealized structure.

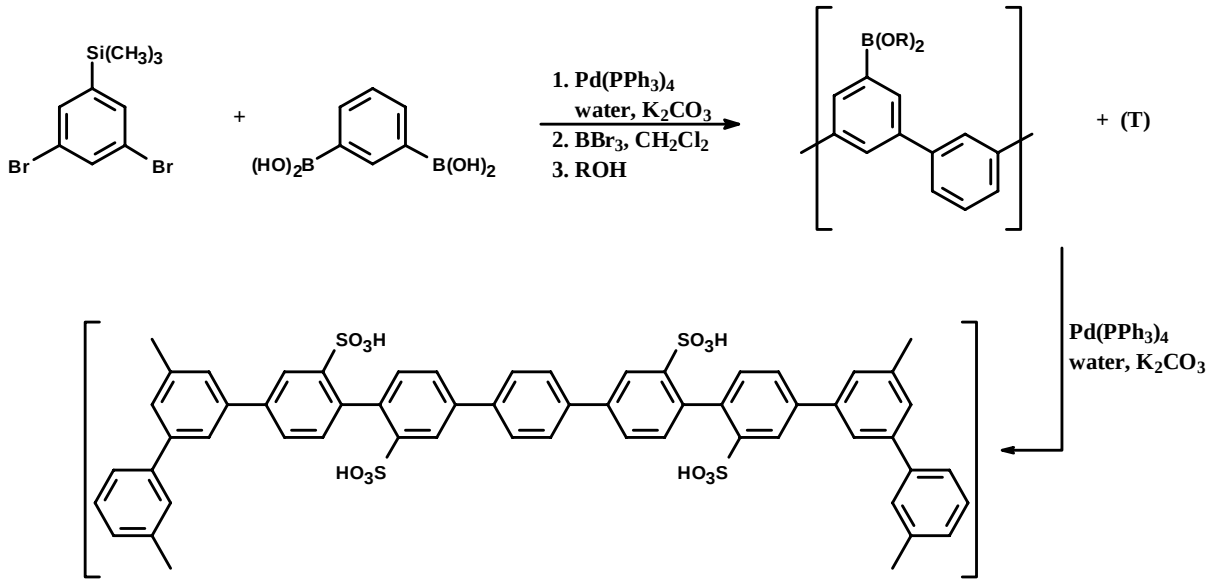

Figure 46. Synthetic scheme for polymer

Synthetic scheme for ladder-type polymer

We chose to concentrate our efforts on structures that could be made with readily available compounds rather than spend time synthesizing new intermediates. Focus was concentrated on the linear/double strand materials and the two-dimensional “infinite” grill materials as described previously.

The previous synthetic routes were not carried through to final polymeric material, requiring too many synthetic steps with insufficient yields, and unexpectedly difficult purifications of the intermediates. In the last quarter, simplified alternative routes were identified, e.g. reducing the final seven reactions to four steps. Insufficient time remains in the sub-contract to take these to polymer, though likely attempt will be made to continue the work to a conclusion.

References for Section 4.7 related to synthesis

3. Scott et al., *Journal of the American Chemical Society*, (1984) 106, 4630-4632
4. Yamamoto et al., *Journal of Organic Chemistry* (1989) 54, 4734-4736
5. Fanta, Chemical Reviews, (1964) 64(6), 613-632
6. Yamato et al., *Journal of Organic Chemistry* (1991) 56, 6248-6250
7. Jian et al., *Journal of Organic Chemistry* (2003) 68, 5091-5103
8. Armarego et al., *Journal of the Chemical Society* (1956), 3668
9. Kice et al., *Journal of Organic Chemistry* (1977) 42(20), 3265
10. Wallow et al., *Journal of the American Chemical Society* (1991) 113, 7411
11. Rulkens et al., *Macromolecules Rapid Communications* (1994) 15, 669

5. Accomplishments

In this program, some organic electrolyte functionalities were identified that provide moderate to high conductivity at low RH. Several polymer electrolytes were synthesized that have ionic conductivity at low RH at least 2X higher than Nafion®. Three of these, AE, BP, and BA, have thermal stability that is believed to be adequate for operation at 120 °C. One of these (BA) is also insoluble in boiling water, though its swelling is still higher than Nafion®. The increased conductivity of BA was demonstrated to provide higher MEA performance at low RH in a fuel cell *vs* N112. AE demonstrated conductivity 7X higher than Nafion®, although it was water soluble. Another AE-type polymer electrolyte, AX, demonstrated conductivity 15X higher than Nafion®, but it was thermally instable. Routes to immobilize AE-type polymer electrolytes were demonstrated, although at some sacrifice in conductivity. A PFSA/inorganic composite membrane (V) was produced that has durability much improved over traditional Nafion® membranes, and was demonstrated to have 1000-1500 hr life in a cycle test at 120 °C.

5.1. Patents

Several patent applications have resulted from this work, including CL-2179, CL-2203, CL-2247, FC-0014, FC-0015, FC-0016, FC-0028, FC-0030, CL-3000, CL-3037, CL-3367, CL-3033, CL-3034, CL-3035, and CL-3137.

6. Conclusions

It is difficult to identify novel electrolytes that do not require water for proton conduction and have conductivity higher than PFSA at 25% RH. There are several routes to polymer electrolytes that, though still requiring *some* water, require significantly lower water vapor pressures than traditional Nafion®. The multiple material requirements for a next generation membrane of high conductivity, thermal stability, oxidative stability and strength, along with low hydrogen permeation and water swelling, remain exceedingly challenging to achieve in novel membranes based on new polymer compositions that are quite different from that of Nafion®. Focusing on the improvement in any one attribute tends to require an increase in the complexity of the monomer and polymer

synthesis, and membrane fabrication, which in turn will lead to higher cost. A trade-off in these attributes most likely will be required to achieve acceptable performance in high-temperature fuel cells.

7. Recommendations

Future work should continue on three of the candidate membranes, V, AE/BP, and BA. For V, alternative fabrication method(s) need to be identified to simplify the process and bring down the cost of manufacture. For BP membranes, further work is needed to alter the polymer structure to further reduce the swelling of AE-type polymer electrolytes. For both BP/AE and BA, further work is needed to optimize their membrane fabrication and demonstrate durability in fuel cell tests. For example, membranes with higher proton conductivity and lower hydrogen permeation that currently demonstrated need to show that these attributes translate to significant improvement in durability compared to Nafion®.

8. References

1. **DOE, *Hydrogen, Fuel Cells & Infrastructure Technologies Program; Multi-Year Research, Development and Demonstration Plan*. 2005, http://www.eere.energy.gov/hydrogenandfuelcells/mypp/**
2. **Stucki, S., G.G. Scherer, S. Schlagowski and E. Fischer, *PEM water electrolysers: evidence for membrane failure in 100 kW demonstration plants.* Journal of Applied Electrochemistry, 1998. 28: p. 1040-1049.**
3. **LaConti, A.B., M. Hamdan and R.C. McDonald, *Mechanisms of Membrane Degradation*, in *Handbook of Fuel Cells, Fundamentals, Technology and Applications*, H. Gasteiger, Editor Vol. 3,edition, 2003, John Wiley and Sons. p. 647-662.**
4. **McDonald, R.C., C.K. Mittelsteadt and E.L. Thompson, *Effects of Deep Temperature Cycling on Nafion(R) 112 Membranes and Membrane Electrode Assemblies.* Fuel Cells, 2004. 4(3): p. 208-213.**
5. **Masten, D.A. and A.D. Bosco, *System Design for Vehicle Applications (GM/Opel)*, in *Handbook of Fuel Cells, Fundamentals, Technology and Applications*, W. Vielstich, A. Lamm, and H. Gasteiger, Editors, Vol. 3,edition, 2003, John Wiley and Sons.**
6. **Hinatsu, J.T., M. Mizuhata and H. Takenaka, *Water Uptake of Perfluorosulfonic Acid Membranes from Liquid Water and Water***

Vapor. **Journal of the Electrochemical Society, 1994. 141(6): p. 1493-1498.**

7. **Zawodzinski, T.A., C. Derouin*, et al.*, *Water Uptake by and Transport Through Nafion(R) 117 Membranes.* Journal of the Electrochemical Society, 1993. 140(4): p. 1041-1047.**
8. **Morris, D.R. and X. Sun, *Water-Sorption and Transport Properties of Nafion 117 H.* Journal of Applied Polymer Science, 1993. 50: p. 1445-1452.**
9. **Miyake, N., J.S. Wainright and R.F. Savinell, *Evaluation of a Sol-Gel Derived Nafion/Silica Hybrid Membrane for Proton Electrolyte Membrane Fuel Cell Application.* Journal of the Electrochemical Society, 2001. 148(8): p. A898-A904.**
10. **Alberti, G., M. Casciola, L. Massinelli and B. Bauer, *Polymeric proton conducting membranes for medium temperature fuel cells (110-160 ^{0}C).* Journal of Membrane Science, 2001. 185: p. 73-81.**
11. **Zawodzinski, T.A., C. Karuppaiah, F. Uribe and S. Gottesfeld. *Aspects of CO Tolerance in Polymer Electrolyte Fuel Cells: Some Experimental Findings*. in *Proc. Symp. on Electrode Materials and Processes for Energy Conversion and Storage IV*. 1997, The Electrochemical Society, p. 139-146.**
12. **Gottesfeld, S. and T.A. Zawodzinski, *Polymer Electrolyte Fuel Cells*, in *Advances in Electrochemical Science and Engineering*, R.C. Alkire*, et al.*, Editors, Vol. 5,edition, 1997, Wiley-VCH. p. 197-297.**
13. **Jiang, R., H.R. Kunz and J.M. Fenton, *Electrochemical Oxidation of H_2 and H_2/CO Mixtures in Higher Temperature (T_{cell} > 100 ^{o}C) Proton Exchange Membrane Fuel Cells: Electrochemical Impedance Spectroscopy.* Journal of the Electrochemical Society, 2005. 152(7): p. A1329-A1340.**
14. **Alberti, G. and M. Casciola, *Solid state protonic conductors, present main applications and future prospects.* Solid State Ionics, 2001. 145: p. 3-16.**
15. **Hogarth, M. and X. Glipa, *High Temperature Membranes for Solid Polymer Fuel Cells*, Johnson Matthey Technology Centre, 2001 Report No. ETSU F/02/00189/REP DTI/Pub URN 01/893,**
16. **Savadogo, O., *Emerging membranes for electrochemical systems Part II. High temperature composite membranes for polymer electrolyte fuel cell (PEFC) applications.* Journal of Power Sources, 2004. 127: p. 135-161.**
17. **Thampan, T.M., N.H. Jalani, P. Choi and R. Datta, *Systematic Approach to Design Higher Temperature Composite PEMs.* Journal of the Electrochemical Society, 2005. 152(2): p. A316-A325.**
18. **Zhang, Y., M. Litt, R.F. Savinell and J.S. Wainright, *Molecular design considerations in the synthesis of high conductivity PEMs for fuel cells.* ACS Polymer Preprints, 1999. 40(2): p. 480-481.**
19. **Granados.-Focil, S. and M.H. Litt, *Novel highly conductive poly(phenylene sulfonic acid)s and its evaluation as proton***

exchange membranes for fuel cells. **PMSE Preprints, 2003. 89: p. 438-439.**

20. **Zawodzinski, T.A., M. Neeman, L.O. Sillerud and S. Gottesfeld, *Determination of Water Diffusion Coefficients in Perfluorosulfonate Ionomeric Membranes.* J. Phys. Chem., 1991. 95(15): p. 6040-6044.**
21. **Sone, Y., P. Ekdunge and D. Simonsson, *Proton Conductivity of Nafion 117 as Measured by a Four-Electrode AC Impedance Method.* Journal of the Electrochemical Society, 1996. 143(4): p. 1254-1259.**
22. **Flynn, J.H. and L.A. Wall, *A Quick, Direct Method for the Determination of Activation Energy from Thermogravimetric Data.* Polymer Letters, 1966. 4: p. 323-328.**
23. **Broka, K. and P. Ekdunge, *Oxygen and hydrogen permeation properties and water uptake of Nafion(R) 117 membrane and recast film for PEM fuel cell.* Journal of Applied Electrochemistry, 1997. 27(2): p. 117-123.**
24. **Slade, R.C.T., A. Hardwick and P.G. Dickens, *Investigation of H+ Motion in Nafion Film by Pulsed 1H NMR and A.C. Conductivity Measurements.* Solid State Ionics, 1983. 9-10: p. 1093-1098.**

8.1. Acronyms

DMFC	Direct Methanol Fuel Cell
EDG	Electron Donating Group
EW	Equivalent Weight (mass of electrolyte contributing 1 mole of acidic protons)
FC	Fuel Cell
^{19}F NMR	Fluorine-19 Nuclear Magnetic Resonance
GDE	Gas Diffusion Electrode
HT	High(er) Temperature
ICE	Internal Combustion Engine
MW	Molecular Weight
PFSA	PerFluoro Sulfonic Acid
PTFE	PolyTetraFluoroEthylene
RH	Relative Humidity
SCCM	Standard Cubic Centimeters per Minute (standard being 273.15 ^{o}K, 1 atm)
TGA	Thermo Gravimetric Analysis